Helsinki University of Technology Control Engineering Laboratory

Espoo 2007 Report 152

RADIO RESOURCE MANAGEMENT IN WIRELESS COMMUNICATION: BEAMFORMING, TRANSMISSION POWER CONTROL, AND RATE ALLOCATION

Vesa Hasu

TEKNILLINEN KORKEAKOULU
TEKNISKA HÖGSKOLAN
HELSINKI UNIVERSITY OF TECHNOLOGY
TECHNISCHE UNIVERSITÄT HELSINKI
UNIVERSITE DE TECHNOLOGIE D´HELSINKI

Helsinki University of Technology Control Engineering Laboratory

Espoo June 2007 Report 152

RADIO RESOURCE MANAGEMENT IN WIRELESS COMMUNICATION: BEAMFORMING, TRANSMISSION POWER CONTROL, AND RATE ALLOCATION

Vesa Hasu

Dissertation for the degree of Doctor of Science in Technology to be presented with due permission of the Department of Automation and Systems Technology, for public examination and debate in Auditorium AS1 at Helsinki University of Technology (Espoo, Finland) on the 14th of June, 2007, at 12 noon.

Helsinki University of Technology

Department of Automation and Systems Technology

Control Engineering Laboratory

Distribution:
Helsinki University of Technology
Control Engineering Laboratory
P.O. Box 5500
FI-02015 HUT, Finland
Tel. +358-9-451 5201
Fax. +358-9-451 5208
E-mail: control.engineering@tkk.fi
http://www.control.tkk.fi/

ISBN 978-951-22- 8821-2 (printed)
ISBN 978-951-22- 8822-9 (pdf)
ISSN 0356-0872

Picaset Oy
Helsinki 2007

Available on net at http://lib.tkk.fi/Diss/2007/isbn9789512288229

ABSTRACT OF DOCTORAL DISSERTATION	HELSINKI UNIVERSITY OF TECHNOLOGY P.O. BOX 1000, FI-02015 TKK http://www.tkk.fi

Author Vesa Hasu

Name of the dissertation
Radio Resource Management in Wireless Communication: Beamforming, Transmission Power Control, and Rate Allocation

Manuscript submitted	11.12.2006	Manuscript revised	18.5.2007
Date of the defence	14.6.2007		

☐ Monograph ☒ Article dissertation (summary + original articles)

Department	Automation and Systems Technology
Laboratory	Control Engineering Laboratory
Field of research	Control engineering
Opponent(s)	Prof. Tapani Ristaniemi, D.Sc. (Tech.) Zekeriya Uykan
Supervisor	Prof. Heikki Koivo
Instructor	Prof. Heikki Koivo

Abstract

Effective sharing of the radio spectrum in current and future multi-user radio communication systems is important for the maximisation of communication capacity. Efficient sharing requires obtaining the target ratio between signal and interference powers defined by the requested services for every user with minimum use of resources. In this thesis, three radio resource management techniques – transmission power control, adaptive beamforming, and transmission rate management – are considered separately and jointly in attacking the problem of radio channel sharing. Transmission power control balances the signal-to-interference ratios of the connections, adaptive beamforming performs spatial filtering of signal in antenna arrays, and transmission rate management controls communication speeds of all connections in the system.

This thesis proposes an algorithm for block proportional–integral transmission power control. It combines the ideas of updating the transmission powers of different connections in blocks of chosen connections and using a multiple-input, multiple-output proportional–integral controller in the transmission power balancing. The algorithm is compared to the single-input, single-output proportional–integral controller scenario and is seen to offer faster convergence to the optimal transmission powers. Adaptive beamforming weight vector prediction algorithms are introduced for decreasing the negative impact of the beamformer delay on the system performance. The prediction algorithms are based on autoregressive-moving average models, where parameters are updated using recursive least squares technique. This thesis takes practical approaches to joint beamforming and power control. Separate solutions are proposed for the receiving and transmission beamforming systems. Both solutions are based on making SINR estimates according to the covariance matrices of desired signals, which can be applied in transmission power control of corresponding connections.

For transmission rate management, the feasibility of applying the power control point of view is taken. Solutions are based on the channel measurements and allocation of rates on the basis of the interference. The approach results in rate allocations that are fairer between users than those obtained via maximisation of communications capacity.

In addition to cellular radio systems, this thesis addresses radio resource management of wireless sensor networks. Antenna array beamforming solutions are considered in receivers and transmitters of star-topology sensor networks.

Keywords Radio resource management, power control, beamforming, wireless communication

ISBN (printed)	978-951-22-8821-2	ISSN (printed)	0356-0872
ISBN (pdf)	978-951-22-8822-9	ISSN (pdf)	
Language	English	Number of pages	92 + 71

Publisher Helsinki University of Technology, Control Engineering Laboratory

Print distribution Helsinki University of Technology, Control Engineering Laboratory

☒ The dissertation can be read at http://lib.tkk.fi/Diss/

VÄITÖSKIRJAN TIIVISTELMÄ	TEKNILLINEN KORKEAKOULU PL 1000, 02015 TKK http://www.tkk.fi

Tekijä Vesa Hasu

Väitöskirjan nimi

Radioresurssien hallinta langattomassa tietoliikenteessä: keilanmuodostus, lähetystehon ja -nopeuden säätö

Käsikirjoituksen päivämäärä 11.12.2006	Korjatun käsikirjoituksen päivämäärä 18.5.2007

Väitöstilaisuuden ajankohta 14.6.2007

☐ Monografia	☒ Yhdistelmäväitöskirja (yhteenveto + erillisartikkelit)

Osasto	Automaatio- ja systeemitekniikan osasto
Laboratorio	Systeemitekniikan laboratorio
Tutkimusala	Systeemitekniikka
Vastaväittäjä(t)	Professori Tapani Ristaniemi, TkT Zekeriya Uykan
Työn valvoja	Professori Heikki Koivo
Työn ohjaaja	Professori Heikki Koivo

Tiivistelmä

Radiospektrin tehokas jakaminen on tärkeää nykyisissä ja tulevaisuuden monen käyttäjän radiokommunikaatiojärjestelmissä tiedonvälityskapasiteetin maksimoimiseksi. Tehokas jakaminen vaatii tavoiteltujen signaali-interferenssi –suhteiden saavuttamista kaikkien käyttäjien kohdalla mahdollisimman vähin käytetyin resurssein. Tässä väitöskirjassa kolmea radioresurssien hallintatekniikkaa, lähetystehon säätöä, keilanmuodostusta ja lähetysnopeuden säätöä, käytetään yhdessä ja erikseen radioresurssien hallinnassa. Lähetystehon säätö tasapainottaa eri yhteyksien signaali-interferenssi –suhteita, keilanmuodostus suodattaa signaaleita tilallisessa suunnassa moniantennijärjestelmissä ja lähetysnopeuden säätö määrää tiedonvälitysnopeudet järjestelmän kaikille moninopeuksisille yhteyksille.

Tämä väitöskirja ehdottaa lähetystehon säätöön lohkotyyppistä PI-säädintä. Se yhdistää ideat lähetystehojen päivityksestä usean lähettimen ryhmissä ja MIMO-tyyppisen PI-säätimen käyttämisessä. Algoritmia verrataan yhden lähettimen PI-säädettyyn versioon ja se tarjoaa nopeamman suppenemisen optimaaliseen lähetystehoon. Adaptiivisen keilanmuodostuksen painovektorin ennustamiseen esitellään algoritmit vähentämään keilanmuodostimen viiveen aiheuttamaa tehokkuuden laskua. Ennustusalgoritmit perustuvat autoregressiivisiin liikkuvan keskiarvon malleihin, joissa parametrit päivitetään rekursiivisen pienimmän neliösumman menetelmällä. Väitöskirja ottaa käytännöllisiä näkökulmia yhdistettyyn keilanmuodostukseen ja tehönsäätöön. Eri ratkaisuja on tutkittu lähettävien ja vastaanottavien moniantenniryhmien tapauksissa. Ratkaisut perustuvat signaali-interferenssi –suhteen arvioimiseen signaaleiden kovarianssimatriiseista, joiden avulla tehosäätöä voidaan parantaa.

Väitöskirjassa kehitetään lähetysnopeuden säätöä tehonsäädön toteutettavuusnäkökulmasta. Ratkaisut perustuvat kanavamittauksiin ja nopeuksien asettamiseen interferenssin perusteella. Tuloksena saadaan tasapuolisempia lähetysnopeuksien jakoja käyttäjien välille kuin algoritmeilla, jotka perustuvat lähetyskapasiteetin maksimoimiseen.

Solukkoradioverkkojen lisäksi väitöskirja käsittelee langattomien anturiverkkojen radioresurssien hallintaa. Moniantennijärjestelmiä tutkitaan sekä lähettimissä että vastaanottimissa tähtitopologian omaavissa anturiverkkojärjestelmissä. Erityisesti käsitellään anturinoodeja, jotka eivät sisällä vastaanotinta.

Asiasanat Radioresurssien hallinta, lähetystehon säätö, keilanmuodostus, langaton tietoliikenne

ISBN (painettu)	978-951-22-8821-2	ISSN (painettu)	0356-0872
ISBN (pdf)	978-951-22-8822-9	ISSN (pdf)	
Kieli	Englanti	Sivumäärä	92 + 71

Julkaisija Teknillinen korkeakoulu, Systeemitekniikan laboratorio

Painetun väitöskirjan jakelu Teknillinen korkeakoulu, Systeemitekniikan laboratorio

☒ Luettavissa verkossa osoitteessa http://lib.tkk.fi/Diss/

Preface

This thesis presents the research work that I have done in the field of radio resource management. I have worked in Control Engineering Laboratory of Helsinki University of Technology under the supervision of professor Heikki Koivo.

The work done for this thesis started sometime around year 2000. Therefore I must thank professor Koivo for his exceptional patience towards my thesis work. Actually, he was so patient that the submission of the first draft of this thesis was a complete surprise to him (I work undercover). Professor Koivo deserves, of course, additional thanks for his unique leadership and supervision in the working community.

In addition to professor Koivo, final touches of this thesis are much influenced by the pre-examination done by professors Tapani Ristaniemi and Seong-Lyun Kim, from which I am very grateful of. In regards to this thesis, I thank also doctor Elmusrati for being the last man standing in the telecommunication group in Control Engineering Laboratory. Additionally, I thank the old "partners in crime": professor Riku Jäntti and doctor Matti Rintamäki for fruitful discussions.

I am very grateful for the financial support I have received from Academy of Finland, National Technology Agency of Finland (TEKES), Jenny and Antti Wihuri Fund, Tekniikan edistämissäätiö, Emil Aaltonen Fund, Nokia Foundation and especially Automation Fund of Finland, which has funded many of my conference trips.

I thank the staff of Control Engineering Laboratory, past and present, for a good company during sometimes excessively long coffee breaks. Many of them I can truly call also friends. In addition, I'd like to thank my friends for… hmm, wait a minute – how have contributed to this thesis? By giving a naked-and-oiled man-wrestling show in New Year's Eve? OK, let's just leave it to "thanks".

I thank also my parents for their support. Most of all, I want to thank my wife Vappu, my humongously big love, for being there for me.

Vesa Hasu

Wagner: "Sain väitöskirjani valmiiksi."
Viivi: "Mitä?!"
Wagner: "Olen tehnyt sitä salaa, etten masentaisi sinua henkisellä ylivoimallani."
Viivi: "Näytäpäs vähän sitä pumaskaa. – Tuhmia piirroksia, ostoslista ja pari kestolottokuponkia!"
Wagner: "Se on poikkitieteellinen."

Wagner: "I finished my doctoral thesis."
Viivi: "What?!"
Wagner: "I've done it secretly, so I wouldn't depress you with my intellectual superiority."
Viivi: "Show me that sheaf a bit. – Dirty drawings, a shopping list and a couple of lottery tickets!"
Wagner: "It is interdisciplinary."

Juba Tuomola: Viivi ja Wagner –comic, originally published 27 January 2007 in Helsingin Sanomat.

List of Publications

P1 V. Hasu, H. Koivo, ”A Block MIMO PI-Power Control Algorithm for Cellular Systems”, Proceedings of IEEE 54th Vehicular Technology Conference, VTC-Fall 2001, Atlantic City, NJ, USA, October 2001, vol. 3, pp. 1927–1931.

P2 V. Hasu, “Eigenvalue Approach to Joint Power Control and Beamforming for CDMA Systems”, Proceedings of IEEE Seventh International Symposium on Spread Spectrum Techniques and Applications, ISSSTA 2002, Prague, Czech Republic, April 2002, vol. 2, pp. 561–565.

P3 V. Hasu, H. Koivo, ”Self-Tuning Prediction of Beamforming Vector”, Proceedings of European Personal Mobile Communications Conference, EPMCC 2003, Glasgow, Great Britain, April 2003, pp. 49–53.

P4 V. Hasu, “Power Control Scheme for Systems With Transmission Beamforming”, Proceedings of the 2nd IASTED International Conference on Communications, Internet, & Information Technology, CIIT 2003, Scottsdale, AZ, USA, November 2003, 5 p.

P5 V. Hasu, H. Koivo, “Fair Finite-State Uplink Transmission Rate Allocation for Cellular Systems”, Proceedings of IEEE 61st Vehicular Technology Conference, VTC-Spring 2005, Stockholm, Sweden, May-June 2005, vol. 4, pp. 2369–2373.

P6 V. Hasu, H. Koivo, “SDMA in Connections between Wireless Sensors and Wired Network”, Proceedings of 10th IFIP International Conference on Personal Wireless Communications, PWC'05, Colmar, France, August 2005, 8 p.

P7 V. Hasu, H. Koivo, “SINR Estimation for Power Control in Systems with Transmission Beamforming”, IEEE Communications Letters, October 2005, vol. 9, no. 10, pp. 885–887.

P8 V. Hasu, H. Koivo, “Fair Transmission Rate Allocation: A Power Control Feasibility Approach”, Proceedings of The Tenth IEEE International Conference on Communications Systems, IEEE ICCS 2006, Singapore, October 2006, 5 p.

P9 M. Elmusrati, V. Hasu, “Random Switched Beamforming for Uplink Wireless Sensor Networks”, Proceedings of the IEEE 65th Vehicular Technology Conference, VTC Spring-2007, Dublin, Ireland, April 2007, pp. 3150–3154.

Contributions of the Author

[P1], [P3]	Professor Koivo contributed with the idea level, but the author generated the all results and wrote the paper.
[P2], [P4]	The author carried out the whole work related to the publications.
[P5],[P6],[P7],[P8]	The author carried out the work of the publications. Professor Koivo supervised the work and helped in the writing process.
[P9]	In addition to the text-writing, the author made simulations, reviewed mathematical formulations derived by Dr. Elmusrati.

Nomenclature

In general, in this thesis bolded lowercase symbols stand for vectors, bolded uppercase symbols stand for the matrices, and lowercase symbols stand for scalars.

Matrix operations

$\overline{f}$	complex conjugate of f,
$\mathbf{f}^H$	hermitian transpose (*i.e.* complex conjugate and transpose) of $\mathbf{f}$,
$f^{(k)}$, $f(k)$	time series f in a time step k,
$\hat{f}(k+1\|k)$	estimate of f in time step $k+1$, while data is known to step k,
$\mathbf{f}^{\mathrm{T}}$	transpose of $\mathbf{f}$,
$\Vert\mathbf{f}\Vert_1$	l_1-norm of $\mathbf{f}$,
$\Vert\mathbf{f}\Vert_\infty$	l_∞-norm of $\mathbf{f}$,
$\otimes$	elementwise product of matrices.

Symbols

$\mathbf{A}_m$	beamforming prediction coefficients of method m = 1, 2, 3,
$\mathbf{a}_{ij}$	steering vector between base station antenna array i and mobile j,
B	set of indices of the connections in the system,
B_n	set of indices of the connections in block n (Chapter 4) or mobiles in the same cell as transmitter n (Chapter 6),
$B(q^{-1})$	ARMA model delay polynomial,
$C(q^{-1})$	ARMA model delay polynomial,
g_{ij}	link gain between the transmitter i and receiver j,
$\mathbf{H}$	normalized link gain matrix,
$\mathbf{H}_{ij}$	normalized link gain matrix between blocks i and j,
$\mathbf{I}$	identity matrix,
$\mathbf{I}_n$	external interference of block n,
k	discrete time step,
l_{ij}	path loss between transmitter j and receiver i,

n_a	number of antenna elements in the antenna array,
n_i	noise power in the receiver i,
$\mathbf{P}$	inverse of data covariance matrix of state vector in RLS technique,
p_i	transmission power used in the connection between base station and mobile user i, uplink or downlink,
$\mathbf{p}$	power vector,
$\mathbf{p}_{opt}$	optimal power vector,
$\mathbf{p}_{max}$	vector of maximum powers,
$\mathbf{p}_n$	power vector of block n,
q	forward time-shift operator (*i.e.* $qf(k) = f(k+1)$, $q^{-1}f(k) = f(k-1)$),
s_{ij}	shadow fading between transmitter j and receiver i,
$\mathbf{W}_m$	beamforming vector history of method $m = 1, 2, 3$,
$\mathbf{w}_i$	beamforming weight vector of antenna array i,
$\hat{\mathbf{w}}_i$	beamforming weight vector estimate,
$\mathbf{x}$	signals received by an antenna array,
y	output signal of a beamformer,
α	the *path loss exponent*,
$\boldsymbol{\alpha}_n$	BPIPC parameter matrix of proportional part for block n,
β	RLS forgetting factor,
$\boldsymbol{\beta}_n$	BPIPC parameter matrix of integral part for block n,
Δ	update step size,
$\mathbf{\Phi}_i$, $\mathbf{\Phi}_{ds,i}$, $\mathbf{\Phi}_{in,i}$, $\mathbf{\Phi}_{s,i}$	covariance matrices of antenna array input, signal after despreading correlator, interference, and desired signal of connection i, respectively,
Γ_i	SINR experienced in the connection between base station and mobile user i, uplink or downlink,
$\hat{\Gamma}_i$	SINR estimate,
γ	target SINR (in general),
γ_i	target SINR of the connection between base station and mobile user i, uplink or downlink,
$\gamma(k)$	Kalman gain at time step k in RLS technique,
$\boldsymbol{\eta}$	normalized noise vector,
$\rho(\mathbf{H})$	the spectral radius of matrix $\mathbf{H}$,

Abbreviations

1G	first generation;
2G	second generation;
3G	third generation;
ARMA	auto-regressive-moving-average;
asBPC	alternative sub-optimal beamforming and power control;
BER	bit-error-rate;
BF	beamforming;
BP1, BP2, BP3	beamforming prediction algorithms;
BPC	block power control;
BPIPC	block proportional-integral power control,
CDMA	code-division multiple access;
CIR, C/I,	carrier-to-interference-ratio;
DPC	distributed power control;
DS-CDMA	direct sequence CDMA;
E_s/I_0	symbol energy to interference and noise spectral density ratio;
EDGE	enhanced data rates for GSM Evolution;
FDD	frequency division duplex;
FDMA	frequency division multiple access;
FH-CDMA	frequency hopping CDMA;
FSPC	fixed step PC;
FER	frame-error-rate;
F/TDMA	hybrid FDMA-TDMA system;
GSM	Global System of Mobile Communications;
LOS	line of sight;
LS-DRMTA	least squares de-spread re-spread multitarget array;
MGBF	maximum gain beamforming;
MIMO	multiple input – multiple output;
MSBF	maximum SINR Beamforming;

MT-DD	multitarget decision-directed algorithm;
NLOS	non-line-of-sight;
NMT	Nordic Mobile Telephone;
PC	power control;
PI	proportional–integral;
PIPC	proportional–integral power control;
QoS	quality of service;
RAN	radio access network;
RLS	recursive least squares;
RNC	radio network controller;
RRM	radio resource management;
sBPC	rub-optimal beamforming and power control;
SDMA	space division multiple access;
SEAPC	SINR estimate assisted power control;
SINR	signal-to-interference-and-noise-ratio;
SIR	signal-to-interference-ratio;
TDD	time division duplex;
TDMA	time division multiple access;
TRA	transmission rate allocation;
UMTS	Universal Mobile Telecommunications System;
UTRAN	Universal Terrestrial Radio Access Network;
WSN	wireless sensor network.

Contents

1. Introduction

1.1 Background and Motivation

The origins of wireless communication date back to the 19th century. The first steps toward utilising electromagnetic waves in communications were the prediction of Maxwell's equations (1864) of the existence of waves propagating at the speed of light, the experimental verification of the theory by Hertz (1897), and the first radiotelegraph transmissions by Marconi in 1899 [20]. Since then, radio communication has developed step by step at an increasing speed.

In recent years, demand for wireless communication services has been immense. Even the near future sets new challenges for the performance of the cellular multiple access wireless communication systems in the form of pressure for more sophisticated, as well as resource-consuming, multimedia services for the users. In addition, while enabling the mobility of the users, the future systems must assure **quality of service** (QoS) for all customers.

Essentially QoS means that users are admitted to the wireless network, the transmission quality is good enough to support the services that the users desire, and the services are supported as long as the users need them without being disconnected. The QoS demands mean that the radio spectrum available for the different communication systems must be used intelligently in varying channel conditions. Therefore, radio resource management [99] is even more important in third-generation (3G) and beyond wireless communication systems than in the second-generation (2G) systems.

In addition to cellular systems, wireless communication has become a very important tool in various applications. One of the most interesting applications of wireless systems is so called-wireless sensor networks. Basically, the wireless sensor nodes offer new possibilities for sensors, which can now be liberated from the burden of wires. Since wireless sensor networks use a similar radio channel to cellular networks, similar radio resource problems are present. Therefore, **radio resource management** (RRM) is important for securing QoS.

There are many tools available for RRM in the wireless communication systems. The tools relevant for RRM of services in both cellular and other networks that are central to this thesis are **power control**, **adaptive beamforming** and **rate allocation** (see, *e.g.*, [60] and [100]).

Here, power control in wireless communication refers to intelligent setting and balancing of the transmission powers in respect of the available radio resources in the system. A famous source separation metaphor is the so-called **cocktail party problem**, wherein several people are talking simultaneously at a cocktail party and one is trying to follow a single discussion. If somebody does not hear the speech well enough, the speaker must increase the volume. Unfortunately, this simultaneously increases the interference in other discussions at the cocktail party and the other parties have to increase their volume also. To avoid this upward spiral being realised in multiple access radio communication, transmission power control must be used.

Adaptive beamforming provides a way to do spatial filtering of the signals in multiple-antenna systems in order to amplify the desired waveforms in respect to the interfering signals. In the cocktail party metaphor, the adaptive beamforming corresponds to a listener's ear being pointed in the speaker's direction or the speaker steering his mouth in the listener's direction.

Transmission rate allocation controls communication speeds of all connections with variable transmission rates in the system. In the cocktail party metaphor, the transmission rate allocation corresponds to speaking slowly when the level of background noise is high or rapidly while the level of background noise is low.

1.2 Objectives

The main objective of the thesis is to examine new methods to combine and use beamforming, transmission power control, and transmission rate allocation in wireless communications.

The emphasis is placed on cellular systems, and intelligent combination of the radio resource management methods mentioned above. The basic objective is to find new algorithms to increase network performance and the quality of service. In cellular systems, the basic approach considers the angle of power control – *e.g.*, power consumption and outages.

An additional topic of this thesis is wireless sensor networks and especially radio resource management in cases where wireless transmitters have no receiver. The most intriguing topic here is to see how well transmission power control and beamforming can compensate for the absence of the feedback channel related to the receiver of wireless nodes.

1.3 Summary of Publications

The first advance in this thesis is in the field of transmission power control of cellular systems. A new power control algorithm [P1] combines the ideas of block power control (BPC) and proportional–integral power control (PIPC). In control engineering terms, the result is a **multiple-output, multiple-input** (MIMO) proportional–integral controller (PI controller) controlling the block transmission powers according to the interblock interference and channel conditions. Tuning of the block PI power control (BPIPC) algorithm is discussed in relation to Gerschgorin's theorem. BPIPC is compared with PIPC in snapshot simulations.

The joining of beamforming in the base stations of cellular systems and transmission power control is considered in uplink [P2] and downlink [P4], [P7]. The uplink approach is based on applying code-division multiple access (CDMA) similar ideas to [45] to the joint problem formulation of [68] and [69]. The maximum **signal-to-interference ratio** (SINR) in beamforming can be achieved on the basis of the signal covariance matrices before and after the despreading correlator, instead of using the signal and interference covariance matrices. [P2] discusses the performance degradation of adaptive beamforming by way of examination of the corresponding power control efficiency. Downlink transmission beamforming is joined to power control in the form of making SINR estimates in the transmitter end of the connection. This enables using more sophisticated power control algorithms even if the relay feedback channel is assumed.

The beamforming weight prediction [P3] is based on application of **autoregressive-moving-average** (ARMA) models with **recursive least squares** (RLS) parameter estimation into vector-sized weights. Three different ARMA-model configurations are considered and tested through simulations. The advantages of the approach include adaptability to all kinds of adaptive beamformers without special initialisation. Simulations show that the approach is efficient, especially in cases with a mobile transmitter moving with a large angular speed in relation to the receiving beamformer.

The power control feasibility approach to rate allocation of cellular systems [P5] [P8] is based on the spectral radius estimation of a **normalised link gain matrix**. [P5] uses an indirect method to estimate the feasibility of the power control, whereas [P8] estimates the spectral radius directly. The proposed approach looks at transmission rate allocation from the power control point of view instead of the normal throughput maximisation of so-called greedy algorithms. According to the simulations, the power control view results in transmission rate allocations with better fairness and outage behaviour than throughput maximising 'greedy' rate allocation.

In addition to cellular systems, beamforming is considered also in wireless sensor networks. [P6] considers beamforming as a multiple access technique in base stations for wireless sensor networks with a star topology. The beamforming approach is examined in case simulations. In [P9], transmission beamforming to random directions is used with wireless sensors. The transmission technique offers more diversity in wireless sensor network transmissions and therefore enables occasional throughput from nodes with bad channel conditions. The advantage of the approach is that outage is reduced in certain cases and a feedback channel is not required.

1.4 Contributions of the Author

The author's contributions can be summarised as follows:

- A new type of transmission power control for cellular radio networks is developed through an extension of PI-type transmission power control into the block power control framework. The new algorithm shows an improvement in performance over the PIPC algorithm.
- A more practical approach is proposed for joint power control and receiving beamforming in CDMA systems. Availability problems of the desired and interference signal covariance matrices for adaptive beamforming are solved by using covariance matrices before and after the despreading correlator. The convergence properties are examined in terms of power control efficiency.
- Prediction of beamforming weight vector is developed using adaptive and recursive methods. Beamforming prediction has not been addressed before in the literature.
- Downlink SINR level estimation – especially for transmission power control in transmission beamforming systems – is developed. The new SINR estimation algorithm increases the performance, and it does not require any new signalling or measurements.
- A power control feasibility approach is taken to the transmission rate allocation, resulting in fairer rate allocation and good throughput in beamforming systems. Although some similarities to stepwise removal algorithms can be seen, the point of view is novel in addressing the transmission rate allocation problem.
- Space-division multiple access (SDMA) and transmitters with no receivers and no feedback channel are proposed for wireless sensor networks. Applying this idea reduces the complexity of the wireless sensor nodes, thus reducing the price and power requirements of the nodes.
- Random switched transmission beamforming is examined in wireless sensor networks with sensor nodes without receiver. The approach results in fewer nodes that never get a transmission through in star-type sensor networks with many nodes.

1.5 Structure and Organisation of the Thesis

This thesis is organised as follows. In Chapter 2, the basic features of wireless cellular communication are presented in order to help the reader grasp the topic of the thesis. Radio resource management techniques, power control, and adaptive beamforming are presented and previous work in the field is examined in more detailed fashion in Chapter 3. The level of detail and the scope of chapters 2 and 3 is not meant to be comprehensive; they are to help the reader to understand some basic concepts dealt with in this thesis. More detailed descriptions can be found in the standard texts of the field (see *e.g.* [36], [47], and [100]).

A summary of the publications related to this thesis is provided in chapters 4–9, and the final conclusions are covered in Chapter 10. The publications mentioned above are included at the end of the thesis. Chapter 4 summarises the block PI transmission power control algorithm. Chapters 5 and 6 discuss joining transmission power control and adaptive beamforming in the uplink and in the downlink, respectively. Beamforming weight vector prediction is examined in Chapter 7, and transmission rate allocation from the power control feasibility point of view is considered in Chapter 8. Beamforming in wireless sensor networks is examined in Chapter 9.

The results presented in chapters 4–8 concentrate on cellular radio systems, whereas Chapter 9 examines radio resource management from the wireless sensor angle.

2. Wireless Communication Systems

What exactly does the concept 'wireless communication system' mean? The Encyclopædia Britannica dictionary [16] defines 'communication' as 'interchange of thoughts or opinions through shared symbols', and 'system' as 'an organized integrated whole made up of diverse but interrelated and interdependent parts'. The 'communication system' can be understood to refer to the physical plants and apparatus for disseminating information between people and other equipment. In the context of communication systems, 'wireless' refers to a network of communication apparatus without a physical connection. The non-physical connection between transmitter and receiver is formed when information is sent through the **radio channel**.

Wireless communication systems can have a wide variety of characteristics, including those based on the network topology, multiple access schemes, and device specifications. The most important wireless communication types for purposes of this thesis are cellular networks and wireless sensor networks with star topology. This chapter describes both network types, multiple access techniques, digital radio communication systems, and radio wave propagation, which are essential to the work of the thesis.

2.1 Multiple-User Access Schemes

Since the cellular systems must support several connections using high-capacity communication services in each base station at the same time, there is demand for schemes that share the available radio spectrum among many users, reducing the interference. These are called **multiple access** schemes.

The most common multiple access schemes are frequency-division multiple access (FDMA), time-division multiple access (TDMA), code-division multiple access (CDMA), and their combinations, such as frequency-time-division multiple access (F/TDMA). Additionally, the radio channel can be divided by means of many techniques, but the most important of these is division of the radio channel based on the radio wave direction of motion, space-division multiple access (SDMA).

In Fig. 2.1, the division principles of FDMA, TDMA, F/TDMA, and CDMA are illustrated. In FDMA, the interference from other users is avoided by allocating different narrow frequency bands for each user, whereas in TDMA the full bandwidth is in use for one user at a time. Ideally, FDMA and TDMA systems do not experience interference. Unfortunately, systems using just FDMA or TDMA have a very poor capacity, and in practice hybrid F/TDMA systems are used (*e.g.*, in GSM), where both FDMA and TDMA are applied simultaneously.

In CDMA, the radio spectrum is divided by assigning different *spreading codes* to each user. CDMA systems can be divided into two categories: frequency hopping CDMA (FH-CDMA) and direct sequence CDMA (DS-CDMA). In the first, the spreading code is used for rapid transmission frequency changes. In the latter, the transmitted data bits are multiplied with a spreading code, and the received data bits are despread with the same code in order to get the actual sent data bit. Most of the commercial CDMA systems use DS-CDMA; for example, 3G-standard UMTS uses DS-CDMA for multiple access.

In this thesis, only DS-CDMA systems are considered and the term 'CDMA' always refers to DS-CDMA. Since the spreading codes in CDMA are not perfectly orthogonal, CDMA systems are critical to the interference level, and hence effective radio resource management is needed. More details on CDMA can be read in [87].

SDMA systems divide the radio channel according to directions of motion of radio waves – *i.e.*, on the basis of directions of arrival in receiving SDMA systems and the directions of departure in transmission SDMA systems. SDMA can be implemented by sectorised antennas or antenna arrays with **beamforming**. In this thesis, SDMA is considered in the form of adaptive beamforming, in which signals of antenna array are weighted in order to amplify the desired radio wave directions. SDMA is considered for the cellular systems *e.g.* in [34]. More details on adaptive beamforming are given in Section 3.2.

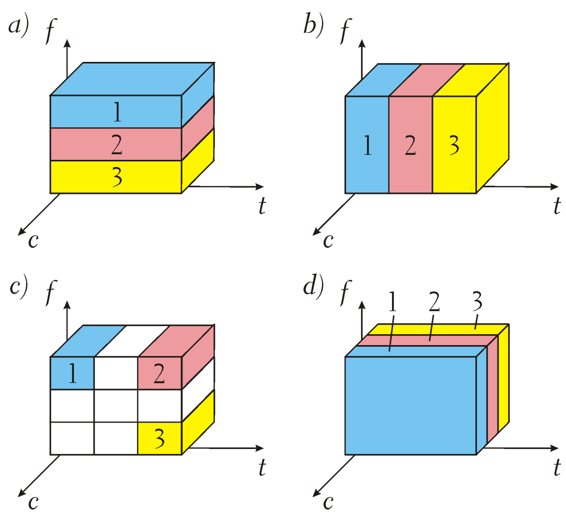

Fig. 2.1: Users 1, 2, and 3 are separated in multiple access schemes, with respect to frequency (*f*), time (*t*), and code (*c*) axes. Schemes are *a)* FDMA, *b)* TDMA, *c)* F/TDMA, and *d)* CDMA.

2.2 Cellular Networks

In the context of wireless communications, 'cellular' is related to a communication system divided into small sections, where mobile users are served by a base station with limited range. Cellular systems include also **mobile stations**, which are usually allocated to a base station. The mobile station is the device used by the user, which can both transmit and receive information – this is usually a mobile phone, but it can be, for example, a personal digital assistant, a computer, or a wireless sensor.

The base station is the other end of the wireless connection to the user, which includes also transceivers. They are the fixed antenna apparatus that are connected to the backbone wired network, which is traditionally the wire-line telephone network. Each base station can support more than one but a limited number of connections to mobile users. An example sketch of the wireless cellular communication network is presented in Fig. 2.2. The connection from a base station to a mobile user is called **downlink** (sometimes **forward link**), and the inverse connection is called **uplink** (or **reverse link**).

The cellular radio communication concept was originally suggested by Bell System in 1947. However, the first cellular networks were installed in 1979. The original, first-generation (1G), systems used analogue voice signalling and digital control signalling. An example of a 1G system is Nordic Mobile Telephone (NMT). With the rapid development of digital signal processing, voice processing became more feasible, and it was already in use in second-generation (2G) systems in the 1980s, such as in the Global System for Mobile Communications (GSM) [20]. Further development resulted in third-generation (3G) systems, enabling higher-data-rate services. One of the most widespread 3G systems is the Universal Mobile Telecommunications System (UMTS).

In practice, the radius of each cell varies according to the area type. The radius is essentially inversely proportional to the mobile user density. On the basis of the radius, cells can be divided into macrocells (radius of kilometres), microcells (radius of tens of metres), and picocells (radius of metres). The transmission frequencies of adjacent cells can be different from one another in order to reduce the intercell interference. As an example of frequency reuse of three different frequencies, see the background colours of the cells in Fig. 2.2.

Frequency reuse is important, especially in systems using FDMA. If the adjacent cell were using the same frequencies, the co-channel interference would be too great for successful communication. The CDMA systems use a wider frequency band than FDMA systems for communication, but they have to use a frequency reuse factor of 1. Hence, the limiting co-channel interference in CDMA systems is vital and radio resource management is very important. Details of the most important radio resource management techniques addressed by this thesis are presented in Chapter 3.

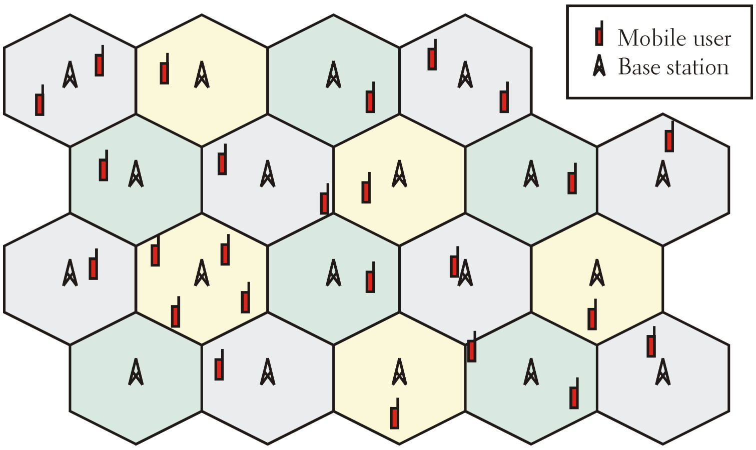

Fig. 2.2: An example of cellular structure in a communication system.

In addition to the separate multiple users, the uplink and downlink transmissions must be separated from each other. The methods for this are called duplexing techniques. Duplexing can be done by **frequency-division duplex** (FDD) **and time-division duplex** (TDD) techniques, which correspond to FDMA and TDMA separation of the users, respectively. FDD is utilised more in commercial systems. For example, in UMTS, uplink transmissions are sent in a 5-MHz band with a 1900-MHz carrier frequency, and the downlink transmits around a 2100-MHz carrier frequency.

The mobile users are assigned to cells offering the best signal quality. Since the users are mobile, the base station offering the best signal quality can change and these changes must be dealt with according to a procedure at base station level. This procedure is called **handoff** (see [61]). In soft handoff, the mobile is connected to multiple cells during the handoff.

In the wireless systems, RRM is done in the radio access network (RAN), which basically manages the link and functions between the mobile user and core communication network. A RAN consists of two main components: base stations and radio network controllers (RNCs) [40]. An example RAN is drawn in Fig. 2.3 (adapted from [40]), which includes a sketch of a Universal Terrestrial Radio Access Network (UTRAN) of UMTS networks.

Base stations handle the wireless connection between the mobile unit and the network. RNCs control the base stations and connections of the RAN to mobile units and to the core network. RNCs of different network subsystems are connected to each other for co-operation. RNCs implement all RRM functions of the sorts presented in this thesis.

2.3 Wireless Sensors and Wireless Sensor Networks

Wireless sensors and **wireless sensor networks** (WSNs) constitute emerging fields in wireless communication. Sensor networks are expected to be one of the key

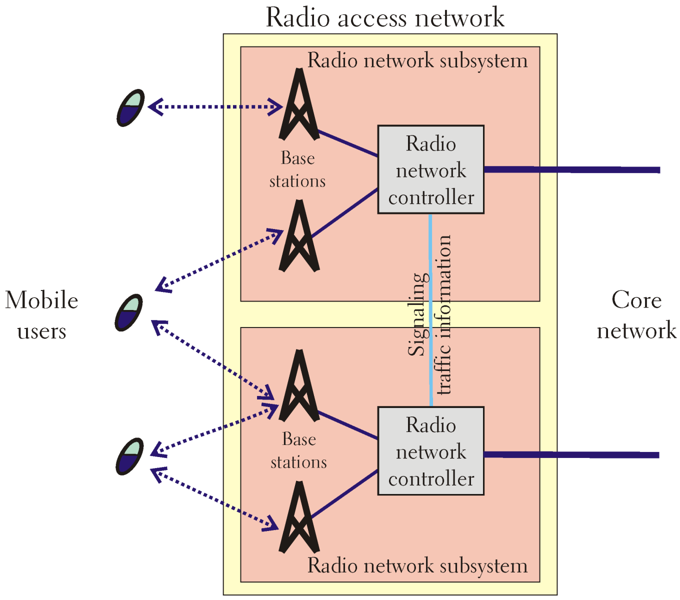

Fig. 2.3: An example radio access network structure, UTRAN-type (adapted from [40]).

technologies in the future [11]. The usual wireless sensor network scenario is that a large number of equal sensors, from tens to thousands, is overlaid on the physical world for various types of monitoring applications.

The communication can also take place in a network of identical transmitter-receiver devices relaying the messages from one to another. In these cases, the communication topology is referred to as being *ad hoc*, due to the temporary nature of the whole network configuration. The transmitter-receiver devices of *ad-hoc* networks are often referred to as **nodes**.

Many consider WSNs to be only *ad-hoc*-type networks, but in practice also star and cluster topologies are used (*e.g.* [11]). Here, '*ad hoc* topology' is used to refer wireless sensor nodes communicating via other sensors. In a star topology, wireless sensors communicate always via an access point – *i.e.*, a base station. In a cluster topology, sensors are clustered and communication to other clusters and access point is done via a cluster head. Examples of these topologies are shown in Fig. 2.4.

Among other factors, affecting the design of WSN network topology, transmission range and sensor mobility must be taken into account [91]. Characteristics and requirements of WSN devices listed in [83] are energy-efficiency, low cost, distributed sensing, wireless infrastructure, multi-hop nature, and distributed processing. The requirement for energy-efficiency is obvious for battery-powered sensors – a long sensor node servicing interval is desired. The desire for low cost is related to the large scale of WSNs. Overly pricey sensor nodes prevent large-scale WSNs. This is an important difference between devices in cellular network and WSN: the radio communication devices in WSN use must be cheap and simple.

Wang *et al.* [90] list the performance metrics of energy-efficiency, QoS and fairness. In WSNs, fairness is an especially important radio performance factor. If a node can

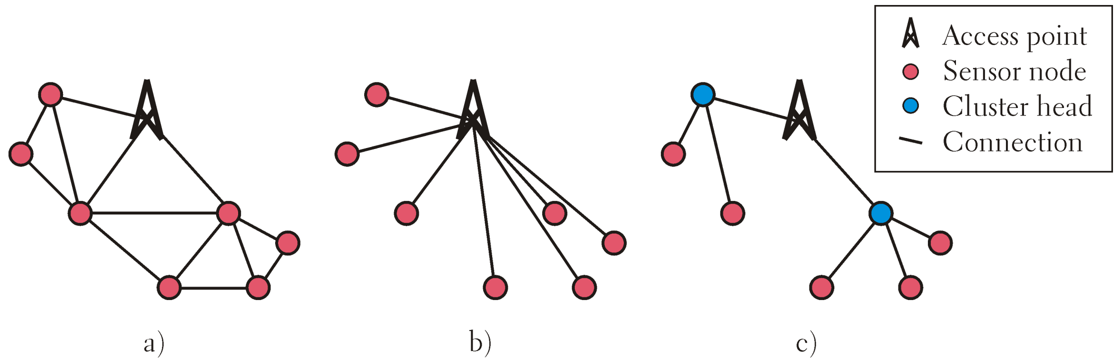

Fig. 2.4: Examples of communication routes in one access point and wireless sensor topologies: a) ad hoc, b) star, and c) cluster topology.

not get the messages through the network, it is essentially useless and it is only causing undesired radio interference in the network.

2.4 Overview of the Digital Radio Communication Systems

This section gives a very brief overview of how radio communication systems work. For detailed information about radio communication, consulting some foundation texts for the field (*e.g.*, [36] and [47]) may be of use.

In analogue radio communication systems – *e.g.*, in 1G wireless cellular systems – the transmitter consists of filtering and modulation of the message signal onto the carrier signal, and in the receiver the signal is demodulated. Since the present second-generation systems and future generations are digital radio communication systems, greater emphasis is put on digital communication here.

The general phases of sending information, or a message, over a digital wireless communication system are presented in Fig. 2.5 (redrawn from [29]). The **source encoder** is the actuator converting the message into bits. The message can be, *e.g.*, a voice waveform or a text message. Some redundancy is added to this message bit sequence by the **channel encoder**, in order to guarantee a reliable transmission. Since 0s and 1s cannot be sent in the air, in the **modulation** the bit stream is merged with an analogue carrier signal, which is sent to the **radio channel**.

The estimation of the message in the receiver is done by **demodulation**, **channel decoding**, and **source decoding**, which, as their names indicate, are the inverse operations of modulation, channel encoding, and source encoding, respectively. The channel decoder exploits the message redundancy introduced by the channel encoder in order to reduce and correct errors caused by the radio channel.

Fig. 2.5 also includes interference in the radio channel, which degrades the quality of the transmission. There are many different quantities that measure that quality. In Fig. 2.5, the **signal-to-interference ratio** (SIR), the **bit-error rate** (BER), and the

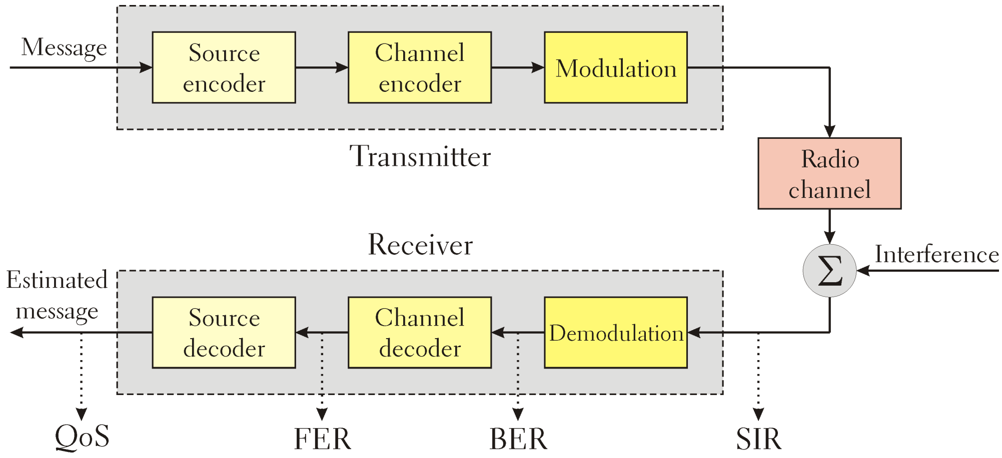

Fig. 2.5: A block diagram of a general digital communication system.

frame-error rate (FER), in addition to QoS (describing user satisfaction), are presented.

SIR, referred to also as **signal-to-interference-and-noise ratio** (SINR) to emphasise the presence of background noise, is the ratio between the power of the desired signal and the power of the interference (plus noise). BER indicates the error rate in the decoded information sequence after the demodulation of the incoming signal. FER is the error rate of the data blocks containing several bits.

Several quantities related to describing the level of difference of the desired signal and interference are closely related to SINR. For example, for CDMA systems, the **symbol energy-to-interference-and-noise-spectral-density** (E_s/I_0) is SINR multiplied by the number of information bits modulated by the spreading code, whereas the **carrier-to-interference-and-noise-power ratio** (CIR or C/I) is equal to E_s/I_0 divided by the length of the spreading code. It must be noted that, since the differences between the quantities are just in the scale (*e.g.*, the difference between SINR, which is used in this thesis, and CIR, used in a variety of papers) and since this thesis is not interested in absolute power levels as opposed to relative, the differences of the quantities are not essential.

Of the quantities expressing quality, SIR, BER, and FER are mostly technical and mathematically well-defined concepts, whereas QoS is a slightly more abstract term. QoS can include admission control, ratio of dropped data packets, error rates, transmission delays, throughput levels, and so on [16]. In other words, the QoS is related to how good a service the customer is getting.

2.5 Radio Wave Propagation in the Radio Communication Channel

In principle, the radio channel mentioned in Section 2.4 behaves as the solution to the Maxwell equations describes. However, the derivation of these solutions in practical situations is too complex a task, not to mention the utilisation of the results. Hence, the use of simplified, more intuitive models is a necessity. In this section, insight is given into the simulation models that are used in the later portions of this thesis.

In the field of power control, the most interesting aspect of the radio channel is the **link gain**, which describes the ratio between the power of the observed wave in the receiver and the power of the transmitted wave. Since the wave does not actually gain any more power in the channel, the channel gain is also called **attenuation**. Attenuation is due to the reflections, diffractions, and partial absorptions that objects in the terrain cause to the radio wave.

In simple statistical models, which are used in the simulations in this thesis, the channel gain is influenced by **path loss**, which is related to the distance between the transmitter and the receiver, and **shadow fading**, which is caused by terrain variations. The link gain g_{ij} between transmitter j and receiver i is modelled as the product of the path loss l_{ij} and shadow fading s_{ij}. If the terrain of the channel area has large objects, as is usually the case, **multipaths** of the signal can also be present, which refer to reflected copies of the transmitted signal.

According to [36], the path loss l_{ij} between transmitter j and receiver i can be approximated as

$$l_{ij} = \frac{C_p}{r_{ij}^{\alpha}}, \tag{2.1}$$

where r_{ij} is the distance between the transmitter and receiver, C_p is a parameter depending on antenna-specific parameters, degree of urbanisation and the transmitted wavelength; and α is the **path loss exponent** (or sometimes propagation constant). According to measurements, the range of the path loss exponent is $2 \leq \alpha \leq 4.35$, where the case $\alpha = 2$ corresponds to the free space propagation and higher values correspond to more and more urban environments with tall buildings and so on. In the simulations applied in this thesis, the powers are scaled so that the parameter C_p can be set to one, and the path loss exponent $\alpha = 3$ is used, unless noted otherwise.

In various sources (see, *e.g.*, [36] and [87]) the shadow fading s_{ij} is modelled as a random variable with log-normal distribution,

$$s_{ij} = 10^{\zeta_{ij}/10}, \tag{2.2}$$

where the random variable ζ_{ij} has a zero-mean Gaussian distribution with standard deviation σ. In the case of a cellular network, it can be assumed that shadow fading parameters of different base stations have a joint Gaussian distribution [87].

In simulations with moving mobiles, the autocorrelation of the shadow fading must be known since the fading is a spatial phenomenon [31]. A theoretically derived autocorrelation can be found in the literature [23]. The autocorrelation model is based on taking the zeroth-order Bessel function of the product of angular Doppler frequency and sampling time. Gudmundson [28] has also proposed an autocorrelation model with respect to the spatial alteration of the radio link.

The modelling of the multipath components is very tedious, since it is so much dependent on, *e.g.*, the terrain. In this thesis, the simulation of multipath components in an urban environment is done according to the model presented Martin [55].

The Martin model is based on the assumptions that the number of multipath components has a binomial distribution with an average of five, the relative **directions-of-arrivals** of multipath components in respect to the **line-of-sight** component obey a zero-mean Gaussian distribution with standard deviation of 15°, and the relative channel gains of the multipath components with respect to the line-of-sight components satisfy a log-normal distribution with mean of –6 dB and standard deviation of 6 dB.

The signals of the multipath components are delayed compared to the line-of-sight component, which causes **intersymbol interference**. The frequency corresponding to the time of delay spread is called a **coherence bandwidth**. If the coherence bandwidth is larger than the signal bandwidth, the channel is **called frequency-selective**. If the coherence bandwidth is smaller than the signal bandwidth, the channel is **frequency-flat** [31]. If the channel is frequency-selective, multipath signals can cancel each other out in part.

Additionally, if the transmitter or receiver is in motion, signals suffer from a Doppler effect, causing dispersion to the signal power spectrum [31]. The time for which the signal can be assumed to be coherent in spite of the Doppler effect is called **coherence time**. The channel is called **time-flat** or **time-selective** if the coherence time is less or more than the symbol period [31]. Time-selective fading is often referred to as **fast fading**.

2.6 Simulation of Wireless Communication Systems in the Thesis

The main purpose of the simulations is to compare new algorithms to the ones in the literature. Simulations in this thesis are done in both snapshot and dynamic frameworks. The snapshot simulations utilised are very similar to the ones in [37], and some of the assumptions are used also in the dynamic simulations of this thesis. The choice between snapshot and dynamic simulations depend on the scope of the system being examined, and therefore the simulations have some characteristics that change from case to case.

In the simulations performed for this thesis, as in [37], the use of a Viterbi equaliser [87] is assumed, and hence the influence of the intersymbol interference may be ignored. Additionally, handoffs are omitted in all simulations of this thesis. The main reasons for this are mainly the relatively short length of the dynamic simulations and cell sizes being chosen such that attenuation does not exclude any transmitter.

All signal powers are relative. Powers are always scaled so that the maximum transmission power is one, if transmission powers are constrained. In multicell simulations, the base giving the lowest attenuation is assigned to each mobile. When beamforming is applied, simulations include linear antenna arrays with a half-wavelength element spacing.

When multipath signals are assumed, the radio channel is considered to be frequency-selective. In these simulations, a rake receiver is assumed. The rake receiver [31] is assumed to find all multipath components of the desired signal.

A combination of Martin multipath model [55] and Bessel function autocorrelation models [23] is chosen for the dynamic simulations of multipath components over *e.g.* the celebrated Jakes model [36] in this thesis, for the more realistic assumptions on directions of arrival. This is a necessity in the simulations considering beamforming systems.

This multipath and autocorrelation combination is almost identical to the model for fast fading channels for multi-antenna systems described in [106]. The only difference is that in here the spatial characteristics of the multipath channel are taken from the Martin model, which is based on measurements [55]. The autocorrelation function takes into account fast fading effects.

All in all, the simulations follow the models described above. Unfortunately, numerous exceptions were made due to the nature of the case study work. Below, the main exceptions are listed.

- The dynamical simulations in Section 7.1 include only line-of-sight-components.
- An exception to the linear arrays is the simulations in Section 9.2, where tetrahedron- and triangle-type antenna array configurations (see Subsection 3.2.1) are used. Additionally, all signals in beamforming simulations are assumed to arrive on the plane (constant elevation angle of $\pi/2$) except in simulations in Subsection 9.2.2.
- Shadow fading is not modelled in Subsection 9.2.2 as in (2.2); instead, a more ray-tracing-oriented approach is used type for a case study simulations.

Additionally, examination of the results shows that the exact level of outage is very much case-dependent, due to the different statistical characteristics of SINR variation around the SINR target (for more details, see Subsection 3.1.2).

3. Radio Resource Management: Power Control, Adaptive Beamforming, and Rate Allocation

The aim of radio resource management in wireless cellular communication networks is to share the available and often rather limited radio spectrum between users as efficiently as possible. Here, 'efficiency' refers to use of capacity in the sense of maximising the data traffic load with respect to satisfying the QoS requirements of as many mobile users as possible, and overcoming the fundamental difficulties of radio wave propagation in the environment [61], such as introduced in Section 2.5.

The cellular networks employ several techniques for monitoring and controlling the network traffic. This chapter provides an overview of three radio resource management techniques essential to this thesis project: transmission power control, adaptive beamforming and transmission rate allocation.

In addition to the radio resource management techniques considered in more detail in this chapter, radio resources are managed in many ways. The first radio resource management mechanism that a user new to the network encounters is the **admission control**, which decides upon the admission of the new user according to whether the services of the new user can be supported in the current traffic situation. Care in the admittance process is necessary, since admittance of several users requiring demanding services could result in unacceptable outage and dropping potential for the users already in the network. If overload in the system should occur anyway, use of **connection removal algorithms** is obligatory to remove as few users as possible to guarantee the desired QoS level to the others.

Radio resource management algorithms that are in constant use include **power control** (PC) and, in cellular radio systems, **handoff** (see Section 2.2). The transmission PC is used to keep the interference levels at an acceptable level for all users. This will be discussed in a more detailed manner in Section 3.1.

Other radio resource management algorithms include, *e.g.*, packet scheduling for non-real-time packet data applications and allocation of transmission waveforms and access ports [99].

Techniques closely related to radio resource management and PC are **beamforming** and **adaptive beamforming** (sometimes referred to as **smart antennas**). They are related to using antenna arrays instead of single antennas, mostly in base stations, to reduce the interference level in the receivers. Details of beamforming (BF) are discussed in Section 3.2.

Many modern wireless communication protocols and standards support multiple transmission rates also. Users can subscribe to a variety of different services, which can be used with different transmission rates, depending on the services and the associated QoS standards. Transmission rate allocation is discussed in Section 3.4.

3.1 Transmission Power Control in Cellular Systems

Transmission power control is a key technique for the resource allocation of wireless radio communication networks. The history of PC in the cellular radio systems lies in the research of broadcasting networks in the 1960s and satellite systems in the 1970s.

PC battles against the near/far problem in the cellular networks, and the stochastic nature of radio channel. PC reduces the interference level significantly by balancing the transmission powers suitably. The interference reduction due to PC is especially vital for the 3G direct-sequence CDMA systems, since PC rejects interference from adjacent cells. The growth of PC's importance to the systems can be seen in the PC update periods. In 2G GSM systems, PC updating is performed no more than twice a second, whereas in the 3G UMTS standard the PC frequency is 1500 Hz. There are several good reviews of PC available in the literature; see, *e.g.*, [3], [29], [73], and [100].

3.1.1 Power Control Problem

The problem for PC to solve in cellular radio systems is to use as low a total transmission power as possible while guaranteeing the desired QoS level for every user. The desired QoS levels are defined here by target SINRs. The SINR for the connection i (between transmitter i and receiver i), Γ_i, is defined by

$$\Gamma_i = \frac{g_{ii}p_i}{\sum_{j \neq i} g_{ij}p_j + n_i}, \tag{3.1}$$

where g_{ij} is the link gain between the transmitter j and receiver i, p_i is the transmission power of the connection i, and n_i is the power of the noise experienced by the receiver i. In CDMA systems, the SINR definition (3.1) is multiplied by the

processing gain L_i, which is the ratio between the transmission bandwidth W and the transmitted data rate r_i, $L_i = W/r_i$.

In mathematical terms, the overall transmission PC problem described above can be stated as

$$\min \sum_{k \in B} p_k, \text{ s.t. } \Gamma_i \geq \gamma_i \ \forall i \in B, \tag{3.2}$$

where Γ_i is SINR experienced by the receiver of the connection i, B is the set of indices of connections in the system, and γ_i is the SINR target assigned to the connection i. Note that it is not defined whether the connections are uplink or downlink, since the problems are identical in both directions.

The optimal solution of the above power control can be solved analytically. If the column vector $\boldsymbol{\eta}$ and the matrix $\mathbf{H}$ are defined as $[\boldsymbol{\eta}]_i = \gamma_i n_i / g_{ii}$, $H_{ij} = [\mathbf{H}]_{ij} = \gamma_i g_{ij} / g_{ii}$, when $i \neq j$, and $H_{ii} = [\mathbf{H}]_{ii} = 0$, the QoS requirement in (3.2) for the whole system can be written using (3.1) as

$$(\mathbf{I} - \mathbf{H})\mathbf{p} \geq \boldsymbol{\eta}, \tag{3.3}$$

where $\mathbf{p}$ is the transmission power vector and $\mathbf{I}$ is an identity matrix of suitable dimensions. Since the optimal situation is to make satisfying connections with minimum power, the optimal solution $\mathbf{p}_{opt}$ can be found as the solution of

$$(\mathbf{I} - \mathbf{H})\mathbf{p}_{opt} = \boldsymbol{\eta}. \tag{3.4}$$

In practical situations the power is also often limited; *i.e.*, $\mathbf{0} < \mathbf{p} \leq \mathbf{p}_{\max}$, where $\mathbf{p}_{\max}$ is the maximum transmission power vector.

According to the Perron-Frobenius theorem [65], [37], (3.4) leads to

$$\mathbf{p}_{opt} = (\mathbf{I} - \mathbf{H})^{-1} \boldsymbol{\eta}, \tag{3.5}$$

if the spectral radius of the normalised link gain matrix $\mathbf{H}$ is smaller than one, *i.e.* $\rho(\mathbf{H}) < 1$. If $\rho(\mathbf{H}) \geq 1$, the inverse of $\mathbf{I} - \mathbf{H}$ does not exist. The system is said to be *feasible*, if the above spectral radius requirement is fulfilled, and in the constrained cases the optimal power satisfies $\mathbf{0} < \mathbf{p}_{opt} \leq \mathbf{p}_{\max}$. [37]

One may ask why so many power control algorithms are needed if the optimal power can be solved so easily. The problem is that application of the optimal solution (3.5) is not simple at all in practice. First of all, the solution would require lots of measurement and signalling; the link gains between every transmitter and receiver and noise levels in every receiver should be measured accurately and transmitted rapidly to the controller, and in addition the transmission powers must be sent to the transmitters. Secondly, the controller based on the matrix algebra solution should be centralised; all of the available data of possibly a very wide network should be transmitted to one place. In addition, in real-life networks the dimensions of the problem can be large, thus causing very heavy matrix calculations with possible numerical problems. Hence, a different algorithmic solution must be implemented in practice.

3.1.2 About Power Control Algorithms

According to [3], good PC algorithms and protocols from a communications and practical point of view are **distributed**, **simple**, **agile**, **robust**, and **scalable**. In [3], 'distributed' refers to ability for autonomous execution of PC at link level, 'simple' refers to ability to be implemented in real time, 'agile' refers to the tracking of the channel changes, 'robust' points to adaptation ability for coping with congestion situations without collapsing, and 'scalable' refers to maintaining high performance in networks of different scales.

In addition to the above list, in [29] more aspects are listed to be considered in the PC design, especially from a control engineering point of view. These are **capacity and system load**, **global stability and system performance**, **feedback bandwidth**, **constraints**, **time delays**, and **controller bandwidth**. In this list, 'load' refers to the suitable maximum number of mobile users that can be supported and 'global stability and performance' points to stability and performance of PC, while interconnecting several mobile stations with distributed PC. 'Feedback bandwidth' refers to the level of information required to be sent from the receiver to the transmitter, 'constraints' points to the limited power levels set by the hardware used, 'time delays' means the delays in measurements and sending of the control signals, and 'controller bandwidth' describes which channel variations can be mitigated.

In general, the SINR-measurement-based PC algorithms have either centralised or distributed (*i.e.*, decentralised) nature. In centralised PC algorithms, the decision of the level of the transmitted power of all connections in the network is made by one controller. Several centralised PC algorithms can be found in the literature – *e.g.*, the algorithm studied in [101]. However, centralised algorithms are not that interesting, since distributed nature is necessity for real-life PC algorithms, and hence the emphasis in this thesis is laid fully on distributed algorithms.

The literature suggests a couple of methods for examination of the convergence properties of PC algorithms. The first ([95], [33]) is based on defining the PC algorithm as an interference function, and the second one [37] is based on presenting PC algorithms as a linear iteration. Even though these analysis frameworks are based on the assumption of a very slowly changing radio channel, these asymptotic rates of convergence examinations provide valuable insight on the differences of PC algorithms. Simulations with constant link gain values are called **snapshot simulations**.

Even though many PC algorithms are based on balancing SINR levels, one should note that the PC algorithms are not restricted to the SINR-balancing-based algorithms. There exists an information theory approach to PC in order to improve link performance, such as optimal adaptive transmission schemes [22], and PC schemes applying different novel computing algorithms – *e.g.*, a game-theoretical approach [24], neural networks [46], and fuzzy computing [8]. For an overview of power control, see [30].

One important and sometimes restricting issue for the PC algorithms is the feedback bandwidth applied in the controlled wireless system. Many practical standards, such as UMTS, use only one-bit feedback for PC. This means, in essence, that a wide variety of PC algorithms using SINR levels for transmission power determination will be useless for direct implementation. However, the SINR-based algorithms are important for the examination and understanding of the PC problem itself, and they have more practical versions also.

A general sketch of a standard distributed PC feedback loop is presented in Fig. 3.1. The QoS requirement of the connection is fed to the outer loop PC, which decides the SINR target γ suitable for the connection. Especially worthy of note is that the SINR target is not equal to the minimum required SINR for the current QoS level. This is due to the variation in the radio channel, which causes the actual SINR level to vary around the SINR target, and to avoid constant outage the target must be set to be larger than the minimum required SINR.

The SINR target is fed into the inner loop PC, which is based on the feedback message from the received signal quality estimation. Taking the difference between the target value and the quality estimate sets the incremental transmission power change Δp. In Fig. 3.1, the channel variations are presented in terms of change in channel gain Δg, the noise power n, and the interference power I.

3.1.3 A Brief Overview of Power Control Algorithms

Algorithms Using SINR Levels

There are a great many different variations on the theme of distributed power control algorithms based on setting the new power level according to the experienced SINR

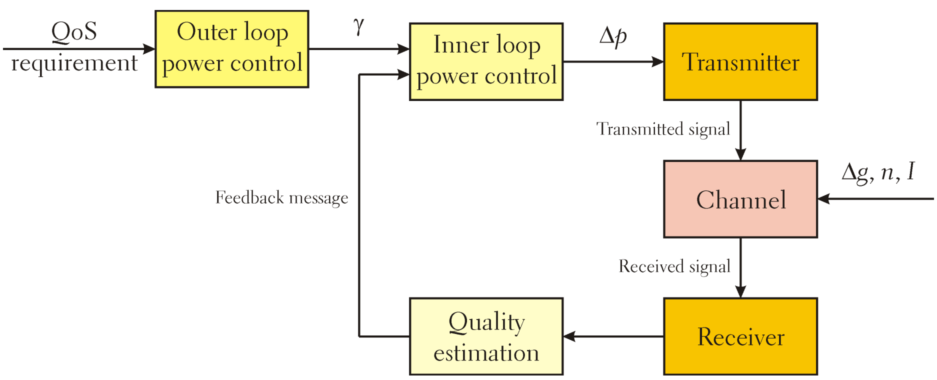

Fig. 3.1: A sketch of the general components in the PC loop.

between the transmitter and receiver. These algorithms include the distributed balancing algorithm (DBA) by Zander [102], distributed power control (DPC) by Grandhi *et al.* [26], the Foschini and Miljanic algorithm (FMA) [19], second-order power control (SOPC) by Jäntti and Kim [38], and PI power control (PIPC) by Uykan *et al.* [81]. More novel algorithms are, *e.g.*, accelerated DPC via Steffensens iterations [49], and multi-objective distributed power control [12].

Now is a good point at which to examine a few of the PC algorithms that are the most essential for this thesis. The power update in DBA [102] is the following:

$$p_i(k+1) = p_i(k)\gamma_i(k)\left(1 + \frac{1}{\Gamma_i(k)}\right). \tag{3.6}$$

A very similar power control algorithm is DPC [26], which updates the transmission power according to

$$p_i(k+1) = p_i(k)\frac{\gamma_i(k)}{\Gamma_i(k)}. \tag{3.7}$$

Both DBA and DPC originally included a normalisation parameter β in the power update equation instead of SINR target. However, in [19] it is established that the normalisation is not necessary in the noisy case. In [19] FMA is presented, in which the power updates are

$$p_i(k+1) = (1-\beta_i)p_i(k)\left(1 + \frac{\beta_i}{1-\beta_i}\frac{\gamma_i(k)}{\Gamma_i(k)}\right), \tag{3.8}$$

where β_i is a algorithm parameter, $\beta_i \in (0, 1]$. Note that by setting β_i to 1 FMA equals DPC. In [58] it is shown that the above FMA algorithm converges to optimal solution even in the case of asynchronous updates of the transmission powers.

The SOPC transmission power update formula [38] is

$$p_i(k+1) = \omega(k)\frac{\gamma_i(k)}{\Gamma_i(k)}p_i(k) + \big(1-\omega(k)\big)p_i(k-1), \tag{3.9}$$

where $\omega(k)$ refers to a nonincreasing sequence of control parameters satisfying $\omega(k) \in (1,2)\ \forall\ k \in \mathbb{Z}^+$, $\omega(2n-1) = \omega(2n)\ \forall\ n \in \mathbb{Z}^+$, and $\lim_{k\to\infty}\omega(k) = 1$. The greatest difference between SOPC and the above algorithms is that SOPC utilises the two previous power levels in the update, as can be seen by comparing (3.9) to (3.6) – (3.8). In PIPC, the power level update [81] is done by

$$p_i(k+1) = \left(1-(\alpha+\beta)\left(1-\frac{\gamma_i(k)}{\Gamma_i(k)}\right)\right)p_i(k) + \alpha\left(1-\frac{\gamma_i(k)}{\Gamma_i(k-1)}\right)p_i(k-1), \tag{3.10}$$

where α and β are the gains of the proportional and integral parts of a discretised PI-controller, respectively. For convergence, it is required that

$$\alpha > -\frac{1}{1-\rho(\mathbf{H})}, \beta > 0, \tag{3.11}$$

where $\rho(\mathbf{H})$ is the spectral radius of the normalised link gain matrix [81]. Note that, in addition to the information used by SOPC, PIPC also utilises the two previous SINR levels.

Fast PC convergence can be obtained by a multi-objective distributed PC (MODPC) algorithm, which is proved to converge more rapidly than DPC, DBA and FMA [13]. In MODPC, the transmission powers are updated according to

$$p_i(k+1) = \frac{\lambda p_{i,\min} + (1-\lambda)\gamma_i(k)}{\lambda p_i(k) + (1-\lambda)\Gamma_i(k)} p_i(k),$$

where λ is a weighting parameter, $\lambda \in [0,1]$, and $p_{i,min}$ is the minimum transmission power of the station. Although MODPC converges rapidly, it has a downside – instead of the SINR target γ_i, it converges to $\gamma_i - \frac{\lambda}{1-\lambda}(p_{i,ss} - p_{i,\min})$, where $p_{i,ss}$ stands for the steady state transmission power.

Constrained Power Control

In practice, so-called constrained versions of the PC algorithms should be applied, since the transmission powers have their upper limits. In general, the constraints are applied to the update as in [27]. If the PC algorithm suggests a new transmission power of $\tilde{p}_i(k+1)$, the power

$$p_i(k+1) = \min\left(p_{\max}, \tilde{p}_i(k+1)\right) \tag{3.12}$$

is used instead. For a control engineering insight, in [29] it is stated that the constrained version of DPC corresponds to an antiwindup I-controller in dB scale with integration time of unity. Additionally, the constrained versions are also proved to converge geometrically into optimal solution [33].

An extension to the power constraint is generalised distributed constrained power control (GDCPC) [7]. The main idea in GDCPC is that the power levels saturated to maximum powers are set to a somewhat lower level than the maximum power, which is used in the standard constrained PC in (3.12).

Relay Power Control

Another very essential limitation in real life is the power control feedback from the receiver to the transmitter. The feedback of accurate SINR measurements or power levels uses too much of the valuable radio spectrum; hence, the power level update should be limited to as small a quantity of data as possible. Therefore in the real-life systems the feedback is done by relay type one-bit up/down commands. In 3G systems, the received CIR is used as the decision variable in the relay controller, as suggested in [88].

The fixed-step PC (FSPC) algorithm based on the SINR measurement [2] is

$$\left(p_i(k+1)\right)_{dB} = \left(p_i(k)\right)_{dB} + \delta \operatorname{sgn}(\gamma_i(k) - \Gamma_i(k)),$$

where $(\cdot)_{dB}$ stands for values in decibels, δ is the **power control step**, and sgn is the signum function with sgn(0) = 1. This is referred to also as relay power control, since in every power update the transmission power is either increased or decreased by a power control step.

The literature also addresses several additions and improvements for the relay PC, such as dynamic step-size PC for UMTS [61], generalised minimum-variance PC [70], predictive fast PC [84], adaptive step power control [72], and generalised predictive PC [71]. All of these use the one-bit feedback in more advanced algorithms to decide the transmission power changes.

Other Algorithms

In addition to the algorithms above, there exist several modifications and additions to the PC algorithms. These include block power control (BPC) [37], variance minimisation stochastic PC [66], and PC by measuring intercell interference [103].

In BPC, PC of the whole network is done in sub-blocks of connections, in which the link gains between all transmitters and all receivers are known in addition to the SINRs of the connections. The algorithm is, in fact, centralised PC within the connection blocks and distributed between the blocks. In mathematical terms, one defines the normalised link gain matrix **H**, the normalised noise power vector $\boldsymbol{\eta}$, and the power vector **p** defined in Subsection 3.1.1 in block formation; *i.e.*,

$$\mathbf{H} = \begin{bmatrix} \mathbf{H}_{11} & \mathbf{H}_{12} & \cdots & \mathbf{H}_{1N} \\ \mathbf{H}_{21} & \mathbf{H}_{22} & \cdots & \mathbf{H}_{2N} \\ \vdots & \vdots & \ddots & \vdots \\ \mathbf{H}_{N1} & \mathbf{H}_{N2} & \cdots & \mathbf{H}_{NN} \end{bmatrix}, \boldsymbol{\eta} = \begin{bmatrix} \boldsymbol{\eta}_1 \\ \boldsymbol{\eta}_2 \\ \vdots \\ \boldsymbol{\eta}_N \end{bmatrix}, \mathbf{p} = \begin{bmatrix} \mathbf{p}_1 \\ \mathbf{p}_2 \\ \vdots \\ \mathbf{p}_N \end{bmatrix}, \qquad (3.13)$$

and the following block-diagonal parameter matrices:

$$\boldsymbol{\Omega} = \begin{bmatrix} \boldsymbol{\Omega}_{11} & 0 & \cdots & 0 \\ 0 & \boldsymbol{\Omega}_{22} & \ddots & 0 \\ \vdots & \ddots & \ddots & \vdots \\ 0 & 0 & \cdots & \boldsymbol{\Omega}_{NN} \end{bmatrix}, \boldsymbol{\Psi} = \begin{bmatrix} \boldsymbol{\Psi}_{11} & 0 & \cdots & 0 \\ 0 & \boldsymbol{\Psi}_{22} & \ddots & 0 \\ \vdots & \ddots & \ddots & \vdots \\ 0 & 0 & \cdots & \boldsymbol{\Psi}_{NN} \end{bmatrix}, \qquad (3.14)$$

where all of the diagonal block matrices $\boldsymbol{\Omega}_{ii}$, $\boldsymbol{\Psi}_{ii}$, $i = 1,\ldots N$ are of size $|B_i| \times |B_i|$, satisfying elementwisely $\mathbf{0} \le \boldsymbol{\Omega}_{ii} \le \mathbf{I}$, $\det(\boldsymbol{\Omega}_{ii}) \ne 0$, $\mathbf{0} \le \boldsymbol{\Psi}_{ii} \le \boldsymbol{\Omega}_{ii}\mathbf{1}$, where B_i is the set of indices of the connections belonging to block i, and $\mathbf{1}$ refers to a square matrix consisting of ones. According to [37], $\mathbf{\Omega}_{ii}$s constitute a damping factor for the controller and $\mathbf{\Psi}_{ii}$s describe reliability of the elements in the block. Then the unconstrained version of BPC can be written as

$$\mathbf{p}_i(k+1) = \left(\mathbf{I} + \left(\mathbf{I} - \mathbf{\Psi}_{ii} \otimes \mathbf{H}\right)^{-1} \mathbf{\Omega}_{ii} \left(\mathbf{X}_{ii}(k) - \mathbf{I}\right)\right) \mathbf{p}_i(k), \tag{3.15}$$

where $\mathbf{X}_{ii}$ is a diagonal matrix with ratios γ_j / Γ_j, $j \in B_i$, in the diagonal in the same order as in the other matrices.

PC is also combined with several different radio resource management techniques, including base station assignment [96], soft handoff [25], and admission control [4]. Joining of PC and adaptive BF is examined more closely in Section 3.3.

An Illustrative Example

An example PC iteration is drawn in Fig. 3.2. It demonstrates the differences among a PC algorithm, its constrained version, and its corresponding one-bit-version. The unconstrained SINR balancing algorithm is DPC, the constrained version is CDPC with maximum power of unity, and the one-bit feedback algorithm is FSPC with PC step on 0.5 dB. The simulated system has two mobiles transmitting to the same base station.

Fig. 3.2a shows the convergence of the transmission power to the optimal power vector [0.167 0.5]. The vector norm difference is shown in Fig. 3.2b. The results

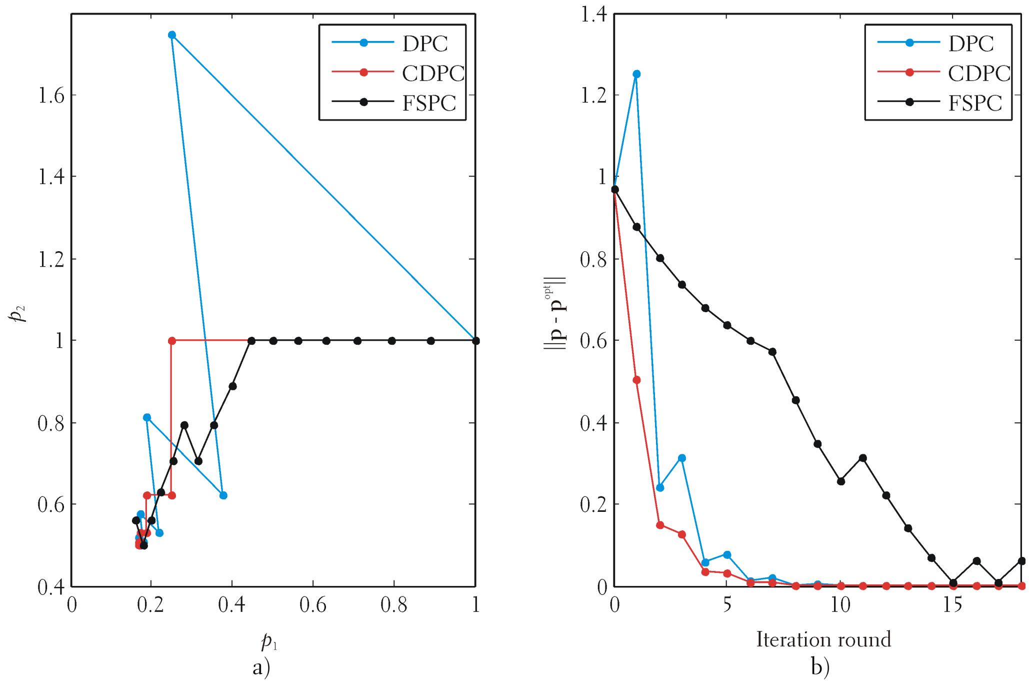

Fig. 3.2: An power control example, a) transmission power traces, b) norm of the difference between the applied and the optimal transmission power vector.

show that CDPC offers the fastest convergence. The example also shows the effect of low feedback bandwidth; FSPC is clearly the slowest, and its transmission power does not converge asymptotically to the exact optimal power vector.

3.2 Beamforming

Beamforming (BF) is a technique for spatial filtering of radio signals in antenna arrays. An antenna array is a system of, usually omnidirectional, antennas in parallel. The spatial filtering is done by controlling the radiation pattern of the antenna array. The beamforming can be done in both receiving and transmitting arrays.

BF techniques can be classed roughly by the adaptiveness of the system [52]. Fixed and switched beam systems rely on constant, pre-defined radiation patterns, which are chosen in advance. In adaptive BF techniques, radiation patterns are adjusted according to measurements.

The gain beams in the spatial dimension are formed by balancing the weighting of the antennas according to set rules. The different antenna weights lead to constructive interference in some directions and destructive interference in other directions due to the phase and gain differences between the signals in different antennas. Fig. 3.3 shows a simple example of BF gains in different directions in the form of BF lobe (*i.e.*, a longer lobe corresponds to a larger gain).

BF as a technique has its origin in the early 1960s and in the field of sonar and radar signal reception [60]. BF is used also in seismology, to locate and detect remote seismic activity. Several excellent overviews of BF are available in the literature – *e.g.*, [82] – as well as foundation textbooks in the field [52], [60].

3.2.1 Antenna Array Model

In antenna arrays, several antennas in a certain physical configuration are connected under the same system. In general, the output of the receiving antenna array at time t, $y(t)$ is a linear combination of outputs of the antennas in the array; that is,

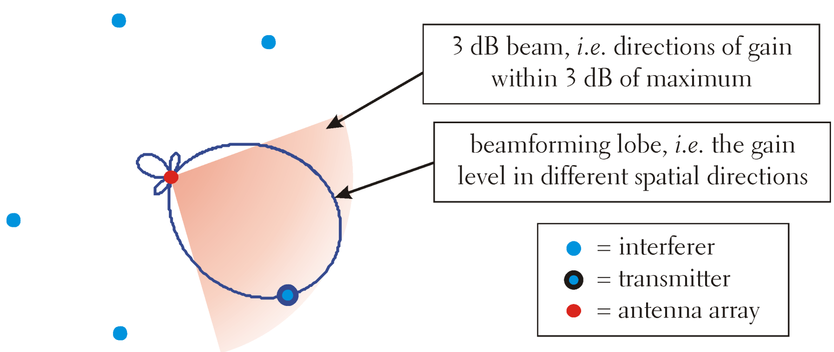

Fig. 3.3: An example of beamforming with five antenna array elements and four interferers.

$$y(t) = \mathbf{w}(t)^H \mathbf{x}(t)\,, \tag{3.16}$$

where **x** is the signal column vector, and **w** is the BF weight vector of the same size. For a sketch of a BF system, see Fig. 3.4. There exist a few different BF types, namely fixed beam systems and adaptive BF systems [52]. The main difference is that in the fixed beam systems a set of BF weight vectors is predefined, and the most suitable one is selected for BF. In adaptive BF, the weight vector is updated constantly according to the measurements. Since the results presented in this thesis concerns mostly adaptive BF systems, the details of fixed beam systems are omitted, for further details on these implementations, see ,*e.g.*, [52].

Let us consider a cellular system with several base stations with n_a antenna elements in the antenna arrays, and M mobile stations. Here it is assumed that the multipath delay spread is dealt with via equalisers, and it is also assumed that the fading channels vary slowly enough to be approximated as a constant between updates. In the uplink transmission, the received signal in the base station assigned to the mobile is

$$\mathbf{x}_i(t) = \sum_{j=1}^{M} \sqrt{p_j g_{ji}}\,\mathbf{a}_{ji} s_j(t - \tau_j) + \mathbf{n}_i(t)\,, \tag{3.17}$$

where $s_j(t)$ is the transmitted signal from user j, τ_j is the corresponding time delay, $\mathbf{n}_i$ is the thermal noise vector at the input of the antenna array of the ith receiver, $\mathbf{a}_{ji}$ is the antenna array response (or spatial signature) from the jth transmitter to the ith receiver, and p_j is the transmission power of the jth transmitter [69]. The antenna array response vector $\mathbf{a}_{ji}$ is given by

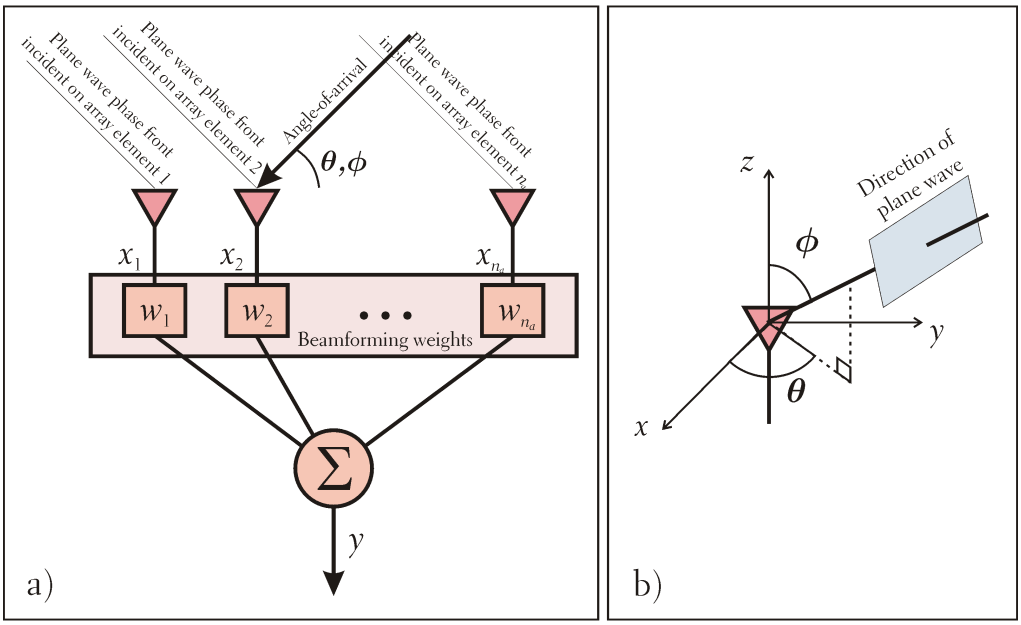

Fig. 3.4: a) A sketch of a beamforming system and b) angle geometry used in the expressions of direction of arrival at antenna element.

$$\mathbf{a}_{ji} = \sum_{l=1}^{L} \alpha_{ji}^{l} \mathbf{v}_j(\theta_l, \phi_l), \tag{3.18}$$

where α_{ij}^{l} is the attenuation due to shadowing of the multipath l, θ_l and ϕ_l are the azimuthal and elevation angle of arrival of the lth path with respect to the base station, and $\mathbf{v}$ is the steering vector. The elevation angle is measured from the z-axis; *i.e.*, the horizontal plane corresponds to $\phi = \pi/2$. The steering vector $\mathbf{v}$ is defined by

$$\mathbf{v}(\theta,\phi) = \begin{bmatrix} 1 \\ e^{-j\frac{2\pi}{\lambda_c}\left(\Delta x_2 \cos(\theta)\sin(\phi) + \Delta y_2 \sin(\theta)\sin(\phi) + \Delta z_2 \cos(\phi)\right)} \\ \vdots \\ e^{-j\frac{2\pi}{\lambda_c}\left(\Delta x_{n_a} \cos(\theta)\sin(\phi) + \Delta y_{n_a} \sin(\theta)\sin(\phi) + \Delta z_{n_a} \cos(\phi)\right)} \end{bmatrix}, \tag{3.19}$$

where λ_c is the carrier wavelength of the signal and Δx_i, Δy_i and Δz_i are the distances in the x, y, and z directions from the ith antenna element to the reference element 1 [52]. Note that in (3.19) 'j' stands for the imaginary unit; *i.e.*, $j = \sqrt{-1}$.

The only condition for the physical geometry of a BF antenna array is that the spacing between elements be small enough that there is no variation of amplitudes in received signals of different antenna elements [52]. Usually, a half-wavelength antenna element spacing is used for signal cancellation benefits and efficient usage of beamwidth [60]. Array geometries used in this thesis are depicted in Fig. 3.5.

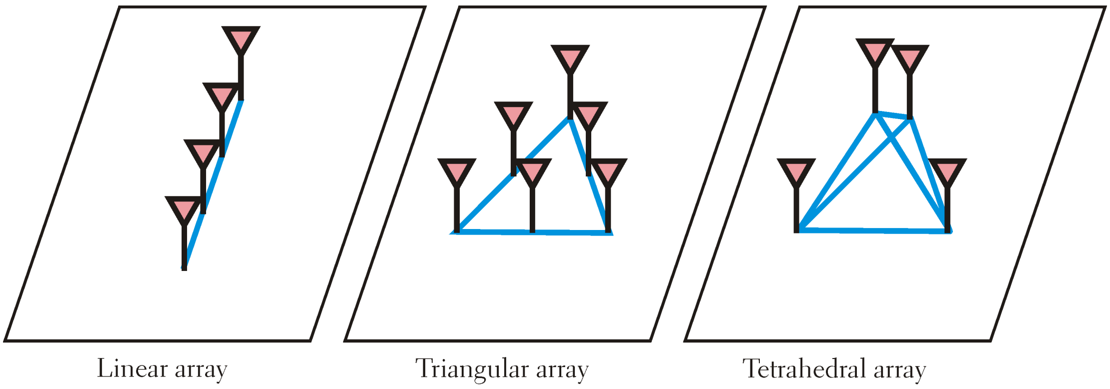

Fig. 3.5: Selected antenna array geometries.

If the message signals s of the transmitters in the system are uncorrelated and zero-mean, the covariance matrix of the incoming signal $\mathbf{x}$ of the antenna array is

$$\mathbf{\Phi}_i = \sum_{j \neq i} p_j g_{ji} \mathbf{a}_{ji} \mathbf{a}_{ji}^H + n_i \mathbf{I} + p_i g_{ii} \mathbf{a}_{ii} \mathbf{a}_{ii}^H = \mathbf{\Phi}_{in,i} + \mathbf{\Phi}_{s,i}, \tag{3.20}$$

where n_i is the noise power in each of the antennas in the array, $\mathbf{\Phi}_{in,i}$ is the covariance matrix of the interference in the connection i, and $\mathbf{\Phi}_{s,i}$ is the signal covariance matrix of the connection i. The covariance matrices are defined by

$$\begin{aligned}\mathbf{\Phi}_{in,i} &= \sum_{j\neq i} p_j g_{ji} \mathbf{a}_{ji} \mathbf{a}_{ji}^H + n_i \mathbf{I}, \\ \mathbf{\Phi}_{s,i} &= p_i g_{ii} \mathbf{a}_{ii} \mathbf{a}_{ii}^H .\end{aligned} \tag{3.21}$$

It should be noted that the above covariance matrices (3.21) may not be estimated directly in practice. However, in [10] and [45] a solution for CDMA systems is presented. The covariance matrices $\mathbf{\Phi}_{in,i}$ and $\mathbf{\Phi}_{s,i}$ can be expressed by known covariance matrices by

$$\begin{aligned}\mathbf{\Phi}_{in,i} &= \frac{1}{L-1}\left(L\mathbf{\Phi}_i - \mathbf{\Phi}_{ds,i}\right), \\ \mathbf{\Phi}_{s,i} &= \frac{1}{L-1}\left(\mathbf{\Phi}_{ds,i} - \mathbf{\Phi}_i\right),\end{aligned} \tag{3.22}$$

where L is the processing gain of the CDMA system used and $\mathbf{\Phi}_{ds,i}$ is the covariance matrix of the incoming signal after the despreading correlator. The SINR level of the connection i can be calculated with

$$\Gamma_i = \frac{\mathbf{w}_i^H \mathbf{\Phi}_{s,i} \mathbf{w}_i}{\mathbf{w}_i^H \mathbf{\Phi}_{in,i} \mathbf{w}_i} = \frac{\mathbf{w}_i^H \mathbf{\Phi}_{ii} \mathbf{w}_i}{\mathbf{w}_i^H \left(\sum_{j\neq i} \mathbf{\Phi}_{ji} + n_i \mathbf{I} \right) \mathbf{w}_i} = \frac{\mathbf{w}_i^H p_i g_{ii} \mathbf{a}_{ii} \mathbf{a}_{ii}^H \mathbf{w}_i}{\mathbf{w}_i^H \left(\sum_{j\neq i} p_j g_{ji} \mathbf{a}_{ji} \mathbf{a}_{ji}^H + n_i \mathbf{I} \right) \mathbf{w}_i} . \tag{3.23}$$

In the case of CDMA systems, the above SINR value is multiplied by the processing gain.

The above examination of the antenna array model is for the receiving BF. Transmission BF – *i.e.*, the BF in downlink in the base stations – is as a model almost the same. With a similar antenna array model, the SINR level of the downlink connection i is

$$\Gamma_i = \frac{\mathbf{w}_i^H \mathbf{\Phi}_{ii} \mathbf{w}_i}{\sum_{j\neq i} \mathbf{w}_j^H \mathbf{\Phi}_{ji} \mathbf{w}_j + n_i} = \frac{\mathbf{w}_i^H p_i g_{ii} \mathbf{a}_{ii} \mathbf{a}_{ii}^H \mathbf{w}_i}{\sum_{j\neq i} \mathbf{w}_j^H p_j g_{ji} \mathbf{a}_{ji} \mathbf{a}_{ji}^H \mathbf{w}_j + n_i} , \tag{3.24}$$

where the **w**'s are the transmission BF weights. Transmission BF is very hard to carry out in real systems, because of the need for the channel measurements.

3.2.2 A Brief Summary of Adaptive Beamforming Algorithms

As in the case of PC, there exist several different algorithms for BF – *e.g.*, statistically optimal beamformers and adaptive beamformers. In this subsection, the most important of them are reviewed.

Statistically Optimal Beamforming

In [82] and [52], a few statistically optimal BF methods are mentioned. They include a minimum mean square error beamformer, the maximum SINR beamformer, and the linearly constrained minimum variance beamformer. Note that all signals presented, their covariance matrices, and BF weight vectors are time-dependent even though the dependency is not explicitly noted.

In minimum mean square error BF the error between the output of the array and a given reference signal is minimised. The optimal weights $\mathbf{w}_{MMSE}$ for this BF method are given by

$$\mathbf{w}_{MMSE} = \mathbf{R}_x^{-1}\mathbf{p},$$

where $\mathbf{R}_x$ is a correlation matrix for the antenna array data vector, $\mathbf{R}_x = E\{\mathbf{x}\mathbf{x}^H\} = \mathbf{\Phi}_s + \mathbf{\Phi}_{in}$, and $\mathbf{p}$ is the cross-correlation between the data vector and the desired signal, $\mathbf{p} = E\{\mathbf{x}^H s\}$. The disadvantage of this method is that a known reference signal must be generated, which uses the radio spectrum.

Maximum gain beamforming (MGBF) is done by solving the principal eigenvector of the covariance matrix of the desired signal. That is, the BF weights $\mathbf{w}_{MGBF}$ are solved from

$$\mathbf{\Phi}_{s,i}\mathbf{w}_{MGBF} = \lambda_{MGBF}\mathbf{w}_{MGBF}. \tag{3.25}$$

The maximum SINR beamformer (MSBF) weights are given by the principal eigenvector $\mathbf{w}_{MSBF}$ of the generalised eigenproblem between the signal and interference covariance matrices. For instance, the eigenproblem for connection i is

$$\mathbf{\Phi}_{s,i}\mathbf{w}_{MSBF} = \lambda_{MSBF}\mathbf{\Phi}_{in,i}\mathbf{w}_{MSBF}. \tag{3.26}$$

Statistically this procedure finds the principal axis of the **Fisher discriminant** (introduced in [18]). The benefit of this method is that it maximizes SINR. The downside of this method is that the covariance matrices must be known, and the numerical solution of (3.26) can be a heavy computational task.

The linearly constrained minimum variance BF method is based on minimising the variance at the output of the antenna array subject to linear constraint of $\mathbf{w}^H\mathbf{c} = g$, where $\mathbf{c}$ is the steering vector in the direction of the constraint, $\mathbf{c} = \mathbf{a}(\theta)$. The solution for the weights $\mathbf{w}_{LCMV}$ is

$$\mathbf{w}_{LCMV} = \mathbf{R}_x^{-1}\mathbf{c}\left(\mathbf{c}^H\mathbf{R}_x^{-1}\mathbf{c}\right)^{-1} g. \tag{3.27}$$

This is the general formulation of the problem; the constraint weight vector $\mathbf{c}$ should be equal to the desired direction-of-arrival component. The computation of this vector is the drawback of this algorithm.

Blind Adaptive Beamforming

Fully adaptive algorithms include least mean squares (LMS) BF and recursive least squares (RLS) BF. The downside of both of these methods is the need for either a training sequence or the desired direction [52]. The update equations for the LMS beamforming weights $\mathbf{w}_{LMS}$ are

$$\begin{aligned} \mathbf{w}_{LMS}(k) &= \mathbf{w}_{LMS}(k-1) + \mu\mathbf{x}(k-1)\overline{y}(k-1) \\ y(k) &= y_d(k-1) - \mathbf{w}_{LMS}^H(k)\mathbf{x}(k) \end{aligned} \tag{3.28}$$

where $\mathbf{u}$ is the data vector of the antenna array, y_d is the training sequence, and μ is the update gain, which must satisfy $0 < \mu < \mathrm{trace}(\mathbf{R}_x)^{-1}$ [82]. The corresponding update equation for the RLS approach is

$$\begin{aligned} \mathbf{k}(k) &= \frac{\mathbf{P}(k-1)\mathbf{x}(k)}{\mathbf{x}^H(k)\mathbf{P}(k-1)\mathbf{x}(k) + \beta}, \\ \alpha(k) &= y_d(k) - \mathbf{w}_{RLS}^H(k-1)\mathbf{x}(k), \\ \mathbf{w}_{RLS}(k) &= \mathbf{w}_{RLS}(k-1) + \mathbf{k}(k)\overline{\alpha}(k), \\ \mathbf{P}(k) &= \left(\mathbf{I} - \mathbf{k}(k)\mathbf{x}(k)^H\right)\mathbf{P}(k-1)/\beta, \end{aligned} \tag{3.29}$$

where α is the update gain, $\mathbf{P}$ is the inverse of the estimated covariance matrix of $\mathbf{x}$, and λ_f is the forgetting factor satisfying $0 < \beta < 1$ [82].

Among blind adaptive algorithms – *i.e.*, algorithms that do not need a training sequence – is Bussgang technique [52]. The Bussgang algorithm is equivalent to the LMS approach except that the second equation of Equation Set (3.28) becomes

$$y(k) = g_e\left(\mathbf{w}_{LMS}^H(k)\mathbf{x}(k)\right) - \mathbf{w}_{LMS}^H(k)\mathbf{x}(k), \tag{3.30}$$

where $g_e(\cdot)$ is a non-linear zero-memory estimator function. This may be a simple relay function or something more complex, such as in the constant modulus approaches [82].

Other approaches include maximum power BF, and more novel algorithms for the BF in CDMA systems – *e.g.*, the multitarget decision-directed algorithm (MT-DD) and least squares de-spread re-spread multitarget array (LS-DRMTA) [82]. The maximum power BF essentially searches for the principal eigenvector of the desired signal covariance matrix, in other words: it is a simplified version of the maximum SINR algorithm. MT-DD and LS-DRMTA are essentially steepest-descent algorithms using the error between the respread data bits and received signal. In [21], LS-DRMTA simulation results in a UMTS system show that the best performance is achieved with four to six antenna elements and that element spacing of less than half-wavelength increases BER only by a factor of two.

Transmission Beamforming

There exist also adaptive schemes for transmission BF; one of the most used ideas is that of virtual uplink BF (see, *e.g.*, [85]). Basically, it involves computing virtual BF and PC for the uplink, and applying the same BF weight vectors to the downlink transmission. The virtual uplink algorithm is discussed more in Subsection 3.2.3 and Section 6.1.

3.2.3 Joining of Adaptive Beamforming and Power Control

The joint examination of BF and PC is recognised as an efficient addition to radio resource management. The effectiveness of applying both techniques in the same system was noticed in [62]. The basic papers on the joint BF and PC problem were written by Rashid-Farrokhi *et al.* [69], [68].

The joint receiving BF and PC algorithm, which is presented in [68], involves iterating the BF and PC steps alternately. The BF step is to solve for the maximum SINR BF weight vector (*e.g.*, by solving (3.26)). The PC step is to apply DPC applying (3.7), using the SINR value estimated with the BF weight vector obtained in the preceding BF step. Mathematically the algorithm is as follows:

1. BF update step: $\mathbf{w}_i^{(k)} = \arg\max_{\mathbf{w}_i} \frac{\mathbf{w}_i^H \mathbf{\Phi}_{s,i} \mathbf{w}_i}{\mathbf{w}_i^H \mathbf{\Phi}_{in,i} \mathbf{w}_i}$. (3.31)

2. PC update step: $p_i^{(k+1)} = \gamma_i p_i^{(k)} \frac{\left(\mathbf{w}_i^{(k)}\right)^H \mathbf{\Phi}_{in,i} \mathbf{w}_i^{(k)}}{\left(\mathbf{w}_i^{(k)}\right)^H \mathbf{\Phi}_{s,i} \mathbf{w}_i^{(k)}}$. (3.32)

The convergence and optimality of the solution of this algorithm is proved in [69]. In the transmit BF and PC algorithm, a virtual uplink BF scheme with virtual centralised PC is applied with centralised PC [68]. In mathematical terms, this is

1. virtual uplink BF step: $\mathbf{w}_i^{(k)} = \arg\max_{\mathbf{w}_i} \frac{\mathbf{w}_i^H \mathbf{\Phi}_{s,i} \mathbf{w}_i}{\mathbf{w}_i^H \mathbf{\Phi}_{in,i} \mathbf{w}_i}$, (3.32)

2. virtual uplink power $\mathbf{p}$ update: $\mathbf{p}^{(k+1)} = \mathbf{D}_w^{(k)} \mathbf{F}_w^{(k)} \mathbf{p}^{(k)} + \mathbf{u}_w^{(k)}$, (3.33)

3. downlink power $\tilde{\mathbf{p}}$ update step: $\tilde{\mathbf{p}}^{(k+1)} = \mathbf{D}_w^{(k)} \left(\mathbf{F}_w^{(k)}\right)^T \tilde{\mathbf{p}}^{(k)} + \tilde{\mathbf{u}}_w^{(k)}$, (3.34)

where matrices $\mathbf{D}_w$ and $\mathbf{F}_w$, and vector $\mathbf{u}_w$, are defined as

$$\left[\mathbf{F}_w\right]_{ij} = \mathbf{w}_i^H \mathbf{\Phi}_{ji} \mathbf{w}_i,\ \forall i, j \in B,$$

$$\mathbf{D}_w = \mathrm{diag}\left\{\frac{\gamma_1}{\mathbf{w}_1^H \mathbf{\Phi}_{11} \mathbf{w}_1}, \ldots, \frac{\gamma_M}{\mathbf{w}_M^H \mathbf{\Phi}_{MM} \mathbf{w}_M}\right\},$$

and

$$\left[\mathbf{u}_w\right]_i = \frac{\gamma_i N_i}{\mathbf{w}_i^H \mathbf{\Phi}_{ii} \mathbf{w}_i}, \forall i \in B.$$

A similar approach for joint uplink BF and PC with additional joint multi-user detection was presented in [97], which is essentially the same as the additional multitap receiver diversity combiner suggested in the appendix of [68]. In [50] joint transmission BF, PC, and data rate allocation are discussed. An adaptive QoS application to the joint BF and PC systems is introduced in [56]. Feasibility results related to the joint problem in single-cell CDMA systems are presented in [79]. The problem of joint PC and MIMO BF is discussed in [12].

3.3 Transmission Rate Allocation

In modern wireless communication systems, phone calls are not the only services to be supported. Hence, multiple services requiring different and perhaps variable transmission rates must be supported by the system. Transmission rate allocation (TRA) aims for allocating the transmission rates among the subscribers according to QoS requirements and channel conditions.

Variable transmission rates can be implemented in various ways. The two main methods are changing the modulation scheme to control transmission rates and using variable spreading lengths – *i.e.*, changing the spreading factor. For example, the EDGE technique in GSM applies the first type by using different modulation and coding schemes [92], and UMTS controls the data rates by using different CDMA spreading factors – *i.e.*, changing processing gain.

3.3.1 The Rate Allocation Problem

Unfortunately, the TRA problem is not as well defined as the PC problem. First of all, maximisation of the throughput is desired; *i.e.*,

$$\max J_T = \max \sum_i r_i \, , \tag{3.35}$$

where J_T is the throughput and r_i is the transmission rate used by the transmitter i. Secondly, the PC problem requirements are valid. This means that it is desirable to keep transmission powers as low as possible and less than maximum as long as all SINR constraints are met. Mathematically this corresponds to

$$\min \sum_i p_i \text{ , s.t. } \Gamma_i = \frac{L_i g_{ii} p_i}{\sum_{j=1, j\neq i}^{M} g_{ji} p_j + n_i} \geq \gamma_i \text{ , } i = 1,\ldots,M, \tag{3.36}$$

$$0 \leq p_i \leq p_{\max,i} \text{ , } i = 1,\ldots,M, \tag{3.37}$$

where L_i is the processing gain of transmission i – *i.e.*, the ratio between the transmission bandwidth and the transmission rate of the connection, W/r_i. As mentioned in Subsection 3.1.1, the minimum total transmission power is obtained when equalities hold in all SINR constraints of (3.36).

The TRA problem is made yet more difficult by a requirement that the applicable transmission rates be chosen from a predefined set of discrete rates, thus:

$$r_i \in R_i \text{ ,} \tag{3.38}$$

where R_i is the set of acceptable rates for connection i. For example in the UMTS uplink, transmission rates can vary from 15 kbit/s to 960 kbit/s with multiplication factor 2 (*i.e.* R_i = {15, 30, 60, 120, 240, 480, 960} kbit/s). The corresponding processing gains vary between 256 and 4.

These requirements alone make the TRA problem NP-complete. If, additionally, fair treatment of all users is added as the third requirement, the problem becomes even more challenging due to conflicting demands.

The natural problem in fair transmission rate allocation is the definition of fairness. Fairness in transmission rate allocation in wireless networks is considered in [80], where the concept of fairness is adapted from the wired communication framework [59]. One of these authors' generalised fairness criteria is harmonic mean fairness. It corresponds to maximisation of the harmonic mean of the transmission rates over the connected mobiles. The fair rate allocation problem is solved through optimisation methods in [80].

The criterion applied here for fair maximization is harmonic mean fairness, as suggested in [59],

$$J_H = \left(\frac{1}{M} \left(\sum_{i=1}^{M} \frac{1}{r_i} \right) \right)^{-1} \tag{3.39}$$

In [80], J_H is maximised within the constraints (3.36) and (3.37).

3.3.2 A Brief Overview of Transmission Rate Allocation Algorithms

The literature includes a wide variety of TRA algorithms. One of the fundamental differences between the algorithms is the nature of the set of acceptable rates R_i.

Some of them do not restrict rates, some allow using continuous rates, and others restrict and use discrete set of rates.

Optimal throughput can be achieved via the greedy algorithms [64], [6]. The basic idea for throughput maximisation is to allocate as many transmitters with the best channel conditions as possible to transmit at full rate, then allocate the next best users for transmission at full power and allocate the next user as high a rate as possible [35]. In other words, users with the best channels transmit at full rate, users with the next best channels transmit at full power, at most one user with the next best channel transmits with less than full power and full rate, and the other users do not transmit at all.

Continuous rates can be allocated also by means of other algorithms. Maximum throughput power control (MTPC) is presented in [9]. This is a power control algorithm that maximises the product of SINR values in the system. With a continuous and unrestricted set of rates, this solution maximises also the throughput. The centralized minimum total transmission power algorithm [75] solves the TRA problem as an optimisation problem. A multi-objective optimisation approach is taken in multi-objective distributed power and rate control [14].

Additionally, more practical TRA algorithms for a discrete set of rates are suggested. These include the Lagrangian multiplier power control approach, which solves the transmission rate allocation by updating rates according to Lagrangian multipliers and the transmission power according to DCPC [42], and selective power control with active link protection, which utilises a stress signal to indicate the need for transmission rate changes [39].

If the throughput is maximised instantaneously, all TRA methods face a problem with the changing radio channel. Hence, some kind of safety margins should be used and, for example, greedy TRA algorithms can not be used at their exact limit.

Mathematical details of the algorithms are omitted here.

4. Block PI Transmission Power Control

Block PI power control (BPIPC) as introduced in [P1] is based on similar model to the BPC algorithm defined in Subsection 3.1.3, particularly in terms of the block structure of the PC problem defined in (3.13), and the PIPC algorithm defined by (3.10). The only factor constraining the selection of the blocks is that the diagonal normalised link gain block matrices $\mathbf{H}_{nn}$ $\forall$ $n = 1,\ldots, N$, of $\mathbf{H}$ and the interference to every receiver coming from the outside of the block, $\mathbf{I}_n$, must be known.

4.1 BPIPC Algorithm

Let us define the external interference column vector $\mathbf{I}_n$(k) of block n as

$$[\mathbf{I}_n(k)]_i = \gamma_i \frac{\sum_{j\notin B_n} g_{ij}p_j(k)+n_i}{g_{ii}} = \left[\sum_{\substack{l=1\\ l\neq n}}^{N} \mathbf{H}_{ln}\mathbf{p}_l(k)+\boldsymbol{\eta}_n\right]_i, \ \forall\ n = 1,\ldots, N,\ i \in B_n. \quad (4.1)$$

The discretised control law of BPIPC is

$$\begin{aligned}\mathbf{p}_n(k+1) = &\left(\mathbf{I}-(\boldsymbol{\alpha}_n+\boldsymbol{\beta}_n)(\mathbf{I}-\mathbf{H}_{nn})\right)\mathbf{p}_n(k)\\ &+\boldsymbol{\alpha}_n(\mathbf{I}-\mathbf{H}_{nn})\mathbf{p}_n(k-1)+\boldsymbol{\alpha}_n(\mathbf{I}_n(k)-\mathbf{I}_n(k-1))+\boldsymbol{\beta}_n\mathbf{I}_n(k),\end{aligned} \quad (4.2)$$

where k refers to the time step, n is the block number, and $\boldsymbol{\alpha}_n$ and $\boldsymbol{\beta}_n$ are the parameter matrices of the proportional and integral parts of the controller in the block n. This control law is drawn in the block diagram formation in Fig. 4.1.

In practice, the transmission power is limited, and thus the algorithm should be applied in a constrained version – *i.e.*,

$$\begin{aligned}\mathbf{p}_n(k+1) = \min\{&\mathbf{p}_{n,\max}, \left(\mathbf{I}-(\boldsymbol{\alpha}_n+\boldsymbol{\beta}_n)(\mathbf{I}-\mathbf{H}_{nn})\right)\mathbf{p}_n(k)\\ &+\boldsymbol{\alpha}_n(\mathbf{I}-\mathbf{H}_{nn})\mathbf{p}_n(k-1)+\boldsymbol{\alpha}_n(\mathbf{I}_n(k)-\mathbf{I}_n(k-1))+\boldsymbol{\beta}_n\mathbf{I}_n(k)\},\end{aligned} \quad (4.3)$$

where $\mathbf{p}_{n,\max}$ is the maximum transmission power vector of the block n.

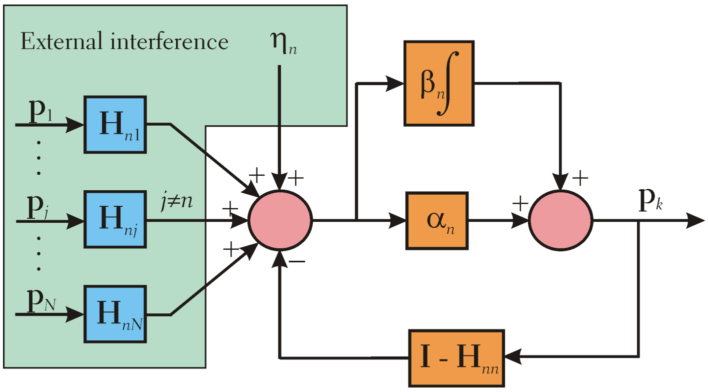

Fig. 4.1: Block MIMO PI-controller.

4.2 BPIPC Properties

According to the standard theory of difference systems, the BPIPC algorithm, (4.2), converges if the eigenvalues of the system matrix are inside the unit circle. In the case of BPIPC, the state-space representation corresponding to (4.2) is

$$\begin{bmatrix} \mathbf{p}_n(k+1) \\ \mathbf{p}_n(k) \end{bmatrix} = \begin{bmatrix} \mathbf{I}-(\boldsymbol{\alpha}_n+\boldsymbol{\beta}_n)(\mathbf{I}-\mathbf{H}_{nn}) & \boldsymbol{\alpha}_n(\mathbf{I}-\mathbf{H}_{nn}) \\ \mathbf{I} & \mathbf{0} \end{bmatrix} \begin{bmatrix} \mathbf{p}_n(k) \\ \mathbf{p}_n(k-1) \end{bmatrix} + \begin{bmatrix} \boldsymbol{\beta}_n \\ \mathbf{0} \end{bmatrix} \mathbf{I}_n(k), \quad (4.4)$$

and hence the system matrix is

$$\begin{bmatrix} \mathbf{I}-(\boldsymbol{\alpha}_n+\boldsymbol{\beta}_n)(\mathbf{I}-\mathbf{H}_{nn}) & \boldsymbol{\alpha}_n(\mathbf{I}-\mathbf{H}_{nn}) \\ \mathbf{I} & \mathbf{0} \end{bmatrix}. \quad (4.5)$$

In addition, if the algorithm converges to some fixed point, it converges to the optimal solution. This point can be solved from (4.2):

$$\begin{aligned} \mathbf{p}_n &= \left(\mathbf{I}-(\boldsymbol{\alpha}_n+\boldsymbol{\beta}_n)(\mathbf{I}-\mathbf{H}_{nn})\right)\mathbf{p}_n + \boldsymbol{\alpha}_n(\mathbf{I}-\mathbf{H}_{nn})\mathbf{p}_n + \boldsymbol{\alpha}_n(\mathbf{I}_n-\mathbf{I}_n) + \boldsymbol{\beta}_n\mathbf{I}_n \\ &= \left(\mathbf{I}-\boldsymbol{\beta}_n(\mathbf{I}-\mathbf{H}_{nn})\right)\mathbf{p}_n + \boldsymbol{\beta}_n\mathbf{I}_n, \end{aligned}$$

and hence

$$\boldsymbol{\beta}_n(\mathbf{I}-\mathbf{H}_{nn})\mathbf{p}_n = \boldsymbol{\beta}_n\mathbf{I}_n \Rightarrow (\mathbf{I}-\mathbf{H}_{nn})\mathbf{p}_n = \mathbf{I}_n = \sum_{l\neq n}\mathbf{H}_{ln}\mathbf{p}_l + \boldsymbol{\eta}_n. \quad (4.6)$$

The last formulation of (4.6) shows that if all of the block solutions are combined, the block transmission powers $\mathbf{p}_i$, $i = 1,\ldots,N$, equal the solution (3.5).

The tuning of a controller is an important problem in practice. In the case of BPIPC, the question is how to find matrices $\boldsymbol{\alpha}_n$ and $\boldsymbol{\beta}_n$ such that the convergence is guaranteed as rapidly as possible. In [54], one necessary condition for the convergence for MIMO PI-controllers can be found: the determinant of $\boldsymbol{\beta}_n$s must be positive. As mentioned above, the algorithm converges if eigenvalues of matrix defined by (4.5) are inside the unit circle. Since there does not exist any straightforward solution to the tuning problem, the following tuning based on reasoning according to Gerschgorin's theorem (see, *e.g.*, [57]) is suggested [P1]:

$$\alpha_{ij,n} = \begin{cases} 1-\beta_{ij,n}, \text{ if } i=j, \\ -\beta_{ij,n}, \text{ if } i \neq j, \end{cases} \quad \forall\, i, j = 1,\ldots, |B_n|, \tag{4.7}$$

where $\alpha_{ij,n}$ and $\beta_{ij,n}$ refer to the element in the ith row and jth column in $\boldsymbol{\alpha}_n$ and $\boldsymbol{\beta}_n$, respectively. Since the determinant of $\boldsymbol{\beta}_n$ must be positive, it is advantageous to select diagonal values to be positive and much larger than non-diagonal values. Determination of the magnitudes of the parameters is a tedious task; the examination in [P1] imply that setting small values for the non-diagonal values and scaling them with the respective column in $\mathbf{H}_{nn}$ gives the best convergence results.

4.3 BPIPC Simulation

Below, the BPIPC algorithm presented above is simulated and compared to the PIPC algorithm in the uplink snapshot simulations. BPIPC is compared to PIPC, since it is the closest PC algorithm from a tuning perspective. For statistical reliability, the results are taken over 1000 simulation cases.

The constrained versions of BPIPC and PIPC are applied. The simulated DS-CDMA system includes 19 omni-bases located in the centres of 19 hexagonal cells with 190 mobiles randomly distributed throughout the system; see Fig. 4.2. CDMA processing gain was 128. Link gains were modelled as presented in Section 2.5. The base receiver noise is set to 10^{-12}. The SINR target is 8 dB.

PIPC is tuned with parameters α = -0.2 and β = 1.2, and BPIPC with the parameter matrices $\boldsymbol{\alpha}_n$ and $\boldsymbol{\beta}_n$, which have constants –0.2 and 1.2 in the diagonals, respectively, and the non-diagonal elements were 10^{-6} divided by the means of the respective

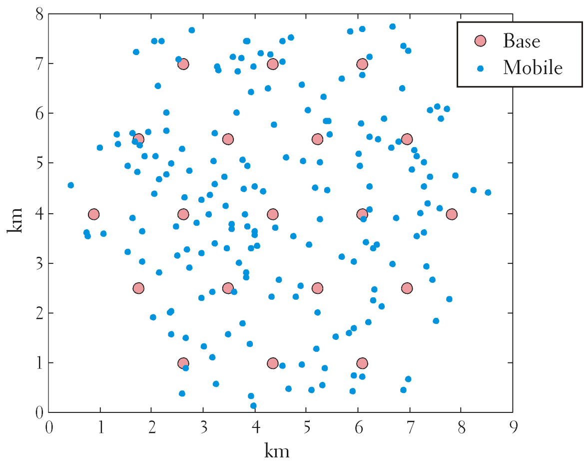

Fig. 4.2: An example showing a simulated case of a system with 19 base stations.

columns of $\mathbf{H}_{nn}$. The levels of non-diagonal elements were chosen in accordance with the description in Section 4.2. In the BPIPC case, the connections were divided among the blocks on the basis of the base station assignments, *i.e.* the system included 19 blocks.

The geometric means of errors of BPIPC and PIPC power vector in respect to the optimal power vector given by the matrix inversion in (3.5) in l_2- and l_∞-norms are plotted in Fig. 4.3. It can be seen that on the average, BPIPC converges to the optimum slightly more quickly than PIPC does. The results vary according to the iterations; for example, after 30 iteration rounds, the BPIPC power vector is closer (in respect to l_∞-norm) to the optimum than the PIPC power vector in 80% of the cases.

Fig. 4.4 presents the outage probabilities of the PC algorithms. The minimum SINR required to avoid outage is set 0.1 dB lower than the SINR target. It can be seen that, even though BPIPC has the advantage over PIPC in terms of convergence rate, there is no significant difference in the outage probabilities.

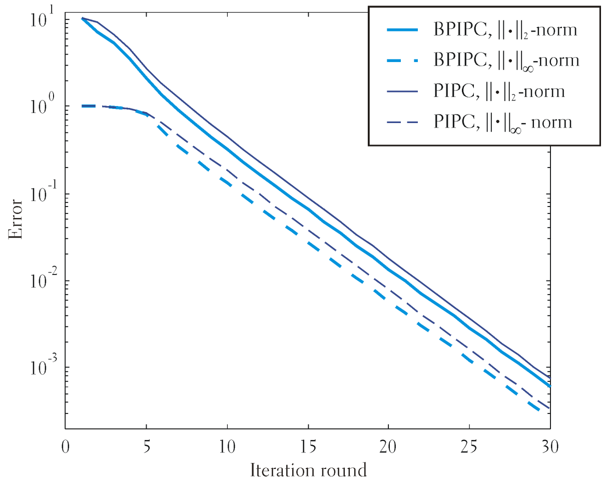

Fig. 4.3: Geometric means of errors in respect to the optimal power vector over 1000 simulations as functions of number of iterations.

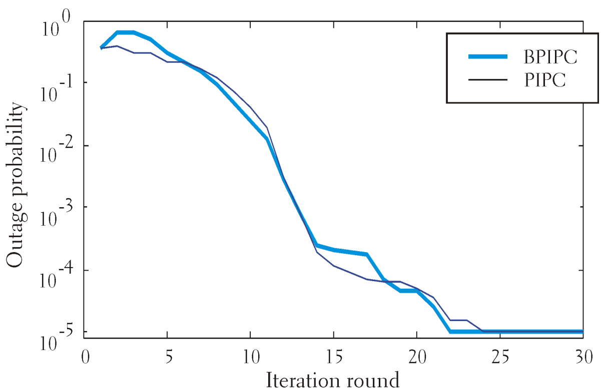

Fig. 4.4: Outage probabilities of BPIPC and PIPC over 1000 simulated cases.

5. Solutions for Combined Receiving Adaptive Beamforming and Power Control

This chapter considers practical solutions for joint adaptive receiving BF and PC. The uplink receiving BF and PC techniques are discussed on the basis of [P2].

5.1 Iterative Joint Adaptive Receiving Beamforming and Power Control Algorithms

As in (3.26), the maximum SINR BF weight vector can be determined by the generalised eigenproblem between the covariance matrices $\mathbf{\Phi}_{s,i}$ and $\mathbf{\Phi}_{in,i}$. If (3.26) is compared to the definition of the uplink SINR (3.23), the SINR level Γ_i corresponding to the principal eigenvalue $\lambda_{max,i}$ is obvious. Hence, if one solves for the maximum SINR BF, the corresponding eigenvalue can be used as an estimate of the SINR of the connection, which, for one, can be applied by the PC algorithm. This is the property that is used successively and iteratively in the joint receiving BF and PC algorithm introduced in [68]. However, it is not emphasised that the DPC algorithm applied is neither the only nor the best possible PC algorithm for systems with changing channel and noise conditions.

However, in the actual systems, implementing the above solution is problematic: the signal and interference matrices, $\mathbf{\Phi}_{s,i}$ and $\mathbf{\Phi}_{in,i}$, are not available. On the other hand, for the CDMA systems this problem can be solved using the relations presented in (3.22). If these definitions (3.22) are substituted into (3.26), we get

$$\begin{aligned} &\frac{1}{L-1}\left(\mathbf{\Phi}_{ds,i} - \mathbf{\Phi}_i\right)\mathbf{w}_i = \lambda_{\max,i}\frac{1}{L-1}\left(L\mathbf{\Phi}_i - \mathbf{\Phi}_{ds,i}\right)\mathbf{w}_i, \\ &\Rightarrow \left(1+\lambda_{\max,i}\right)\mathbf{\Phi}_{ds,i}\mathbf{w}_i = \left(1+\lambda_{\max,i}L\right)\mathbf{\Phi}_i\mathbf{w}_i, \end{aligned} \tag{5.1}$$

where L is the processing gain of the CDMA system. The eigenproblem that should be solved for the maximum BF in the CDMA systems is

$$\mathbf{\Phi}_{ds,i}\mathbf{w}_i = \Lambda_{\max,i}\mathbf{\Phi}_i\mathbf{w}_i \,, \tag{5.2}$$

where $\Lambda_{\max,i}$ is the principal eigenvalue of the problem, and it is related to the principal eigenvalue of (3.26) by

$$\Lambda_{\max,i} = \frac{1+\lambda_{\max,i}L}{1+\lambda_{\max,i}}\,, \tag{5.3}$$

which means that the eigenvalue SINR estimate $\lambda_{\max,i}$ can be solved via

$$\lambda_{\max,i} = \frac{\Lambda_{\max,i}-1}{L-\Lambda_{\max,i}}\,. \tag{5.4}$$

By applying this, *e.g.*, the DPC power update suggested in [68] becomes

$$p_i^{(k+1)} = \frac{\gamma_i}{\lambda_{\max,i}}p_i^{(k)} = \frac{\gamma_i\left(L-\Lambda_{\max,i}\right)}{\Lambda_{\max,i}-1}p_i^{(k)}\,. \tag{5.5}$$

Of course, the SINR estimate given by (5.4) can be used in the various PC algorithms making use of SINR levels, such as introduced in Section 3.1.

5.2 Practical Implementations: sBPC and asBPC

In practice, solving of the generalised eigenproblem can be computationally too expensive for many systems with a heavy traffic load. A cheaper way to solve this is to use iterative methods to solve the eigenproblem, and to use the estimates in the BF and PC operations. The iterative search of the principal eigenvector and eigenvalue can be done through, for example, a power method (see, *e.g.*, [74]) or a gradient method (see, *e.g.*, [45] or [43]). In this case the latter is computationally more efficient than the former, but it does not converge as rapidly.

With regard to the computational complexity of the power method approach, it is a relatively cheap method computationally. In each iteration round it requires one matrix-vector multiplication, and one Gaussian elimination between matrix and vector. Although these computations have a computational complexity of $O(n_a^2)$, where n_a is the number of antenna elements, the number of computations is acceptable, since the number of antenna elements is quite small in practice.

In the case of the combined eigenbeamforming and PC, for the CDMA systems – *i.e.*, equations (5.2) through (5.5) – with the power method iteration, the practical update algorithm is the following.

i) Choose an arbitrary initial eigenvector (*i.e.* BF vector) $\mathbf{w}_i^{(0)}$ with a unit norm;

ii) Update the eigenvector by solving

$$\mathbf{\Phi}_{ds,i}^{(k)}\mathbf{w}_i^{(k-1)} = \Lambda_{\max,i}^{(k)}\mathbf{\Phi}_i^{(k)}\mathbf{w}_i^{(k)},$$

where k is the iteration step, solving

$$\Lambda_{\max,i}^{(k)}\mathbf{w}_i^{(k)} = \mathbf{\Phi}_i^{(k)^{-1}}\mathbf{\Phi}_{ds,i}^{(k)}\mathbf{w}_i^{(k-1)} \tag{5.6}$$

by, *e.g.*, Gaussian elimination, and setting $\Lambda_{\max,i}^{(k)}$ to be the norm of the left hand side of (5.6);

iii) Use $\Lambda_{\max,i}^{(k)}$ to update the value of the power with the PC law in use;

iv) Update the covariance matrices $\mathbf{\Phi}_i$ and $\mathbf{\Phi}_{ds,i}$; and

v) Iterate steps ii through iv above.

This iteration can be used for solving the generalised eigenvalue problem (3.26). The power method iteration for joint BF and PC in the case of the eigenvalue problem (3.26) will be referred as **sub-optimal BF and PC** (sBPC), and in the case of (5.2) it will be referred as **alternative sub-optimal BF and PC** (asBPC) from here on.

Note that the power method iteration converges in the case of sBPC with a faster rate than asBPC does. This can be seen by comparing the ratios of the largest eigenvalues of sBPC and asBPC iterations, which give the decay speed of the components different from the principal eigenvector in the power iteration. If λ_1 and λ_2 with Λ_1 and Λ_2 are the largest and the second largest eigenvalues of (3.26) and (5.2), correspondingly, their ratios relate to each other as

$$\frac{\Lambda_2}{\Lambda_1} = \frac{(1+\lambda_2 L)(1+\lambda_1)}{(1+\lambda_2)(1+\lambda_1 L)} = \frac{1+\left(\lambda_1\lambda_2+\lambda_2\right)L+\lambda_1}{1+\left(\lambda_1\lambda_2+\lambda_1\right)L+\lambda_2} > \frac{\lambda_2}{\lambda_1}. \tag{5.7}$$

Hence, when the processing gain L increases from one to infinity, the ratio Λ_2 / Λ_1 changes from one to $(\lambda_2 + \lambda_1\lambda_2) / (\lambda_1 + \lambda_1\lambda_2)$. Since a smaller eigenvalue ratio corresponds to faster convergence to the principal eigenvector, this means that the BF convergence in asBPC is slower than the BF convergence in sBPC regardless of the value of the processing gain.

Additionally, PC is not synchronised with the joint algorithm of [68] in these practical implementations, since sBPC and asBPC use their approximations of the eigenvalues in the power control instead of the correct eigenvalue. However, this does not prevent sBPC and asBPC from converging to the optimal solution.

Another technique for solving the generalised eigenproblem iteratively that is mentioned above is the gradient method [43]. The first step of the gradient method update for the principal generalised eigenvector is

$$\mathbf{w}_i^{(k+1)} = \mathbf{w}_i^{(k)} + \Delta\mathbf{w}_i^{(k)}, \tag{5.8}$$

where the update vector $\Delta\mathbf{w}_i^{(k)}$ is defined by

$$\Delta \mathbf{w}_i^{(k)} = \alpha \left(\mathbf{\Phi}_{ds,i}^{(k)} \mathbf{w}_i^{(k)} - \Lambda_{\max,i}^{(k)} \mathbf{\Phi}_i^{(k)} \mathbf{w}_i^{(k)} \right), \tag{5.9}$$

with α being the update gain (a small positive number), and $\Lambda_{\max,i}^{(k)}$ being the estimated principal eigenvalue in the time step k. The second step is to scale $\mathbf{w}_i^{(k+1)}$ to the unity length, and update $\Lambda_{\max,i}$.

The PC papers in which the PC algorithms of Subsection 3.1.3 are introduced, present also convergence conditions. The results presented in Subsection 3.1.1 apply also for sBPC and asBPC; the difference is changing to the total link gains $g_{ji}|\mathbf{w}_i^H \mathbf{a}_{ji}|^2$. Basically, the convergence proofs lead to the conclusion that the algorithms converge for every feasible system – *i.e.*, if the normalised link gain matrix $\mathbf{H}$ has a spectral radius smaller than one. In this case, the elements of the normalised link gain matrix during the kth iteration, $\mathbf{H}^{(k)}$, are the following:

$$\left[\mathbf{H}^{(k)}\right]_{ij} = h_{ij}^{(k)} = \begin{cases} \gamma_i \dfrac{g_{ji} \mathbf{w}_i^{(k)H} \mathbf{a}_{ji} \mathbf{a}_{ji}^H \mathbf{w}_i^{(k)}}{g_{ii} \mathbf{w}_i^{(k)H} \mathbf{a}_{ii} \mathbf{a}_{ii}^H \mathbf{w}_i^{(k)}}, & \text{if } i \neq j, \\ 0, & \text{if } i = j. \end{cases} \tag{5.10}$$

The convergence of the joint BF and PC algorithms with the sub-optimal BF to the optimal solution can be proved with an approach similar to that applied for the convergence. Since in the fixed point of the iteration the BF vector is optimal, the convergence properties of the power control algorithms indicate that the fixed point of the iteration is indeed the optimal one.

Note that the above sBPC and asBPC algorithms can be easily extended to include multitap diversity combining by adjoining the output of the different taps into the covariance matrices, such as is presented in [68] and [97]. Of course, the estimated SINR through the eigenproblem can be applied in other radio resource management techniques, such as handoff or admission control.

5.3 Adaptive Receiving Beamforming and Power Control Simulations

It is worth examining first snapshot simulations in a 12-base station network with six-element antenna arrays in a quite similar fashion to the BPIPC in Section 4.3. The system includes 240 mobile users, no multipath components, and an FMA PC algorithm. The target SINR is set to 8 dB, and the CDMA processing gain is 128.

The means of the behaviour of SINR (in decibels) and relative power over 100 snapshots are presented in Fig. 5.1 and Fig. 5.2, respectively. They show that the joint BF and PC approach yields results superior to separate BF for every measurement; convergence to the SINR target is faster, and a smaller average power is used. Note that even the sub-optimal algorithms sBPC and asBPC have a superior convergence rate to separate BF and PC, and their results are not so far off the results of the joint algorithm with perfect BF.

Similar properties are visible in Fig. 5.3, which shows the relative frequency of the mobiles within 0.044 dB of the SINR target γ = 8 dB over 100 snapshots. More snapshot simulations are presented in [P2].

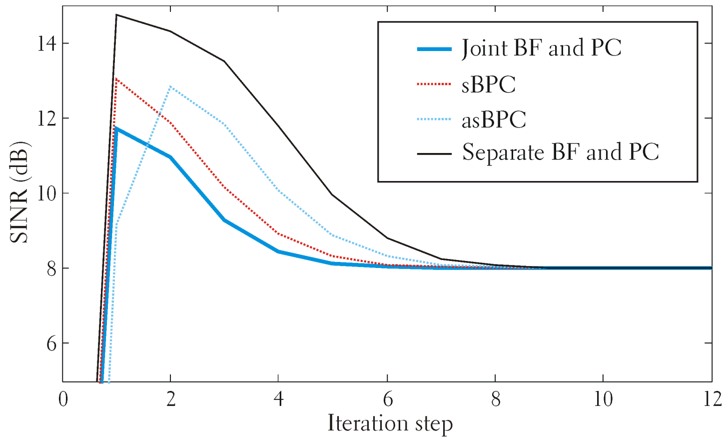

Fig. 5.1: Geometric mean of SINR in relation to iteration step.

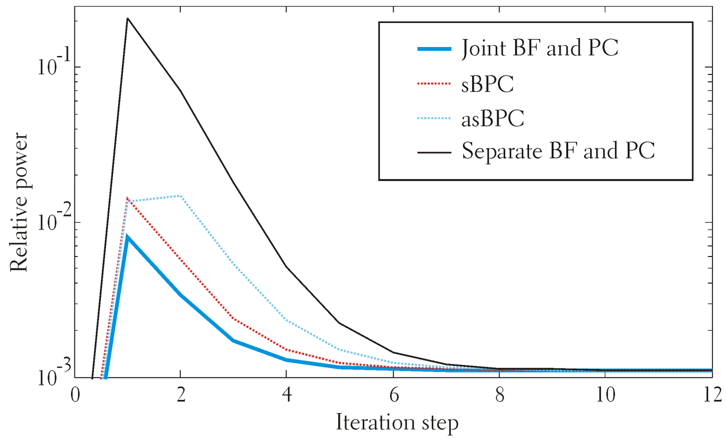

Fig. 5.2: Geometric mean of the relative power in relation to iteration step.

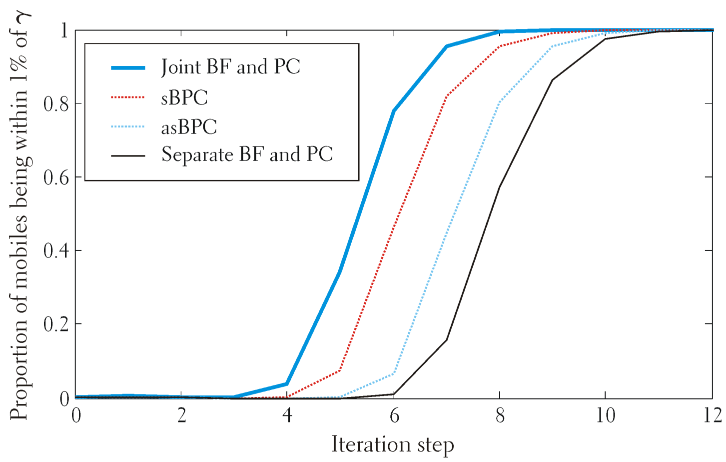

Fig. 5.3: Relative frequency of mobiles within 1% of the SINR target.

In addition, simulations with a dynamically changing channel were carried out. In the discussion that follows, the multipath channel model discussed in Section 2.6 is used. The simulated system has one base station with a four-element antenna array, and 30 moving mobile users; see Fig. 5.4. The speeds of the mobiles vary from 0 to 29.3 m/s, and mobiles move in random directions. An example of movements is depicted in Fig. 5.4 by movement vectors. The BF and PC update period is set to one millisecond (0.001 s), and a carrier frequency of 3 GHz is used.

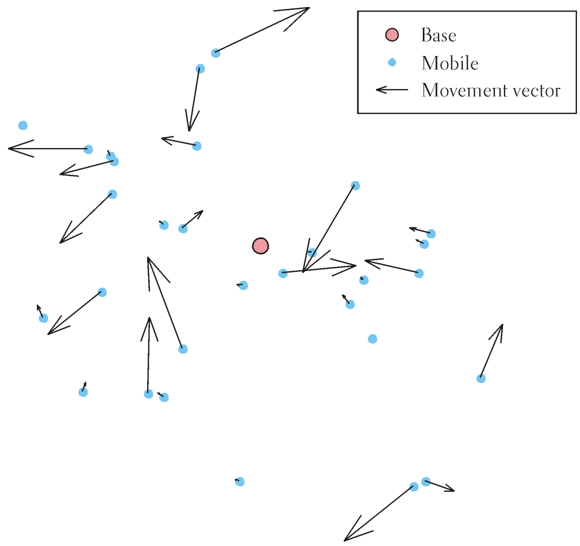

Fig. 5.4: An example simulated system. The cell radius is 1000 m.

Relay power control with power step of 0.5 dB is applied in all different BF and PC formulations. In addition to the algorithms simulated in the snapshot case, the joint gradient method BF and PC referred to in Section 5.2 are simulated. For the gradient method, $\alpha = 0.1$ is used.

The average SINR levels over 100 simulations are drawn in Fig. 5.5, which indicates almost equal performance of the algorithms. The greatest difference is in the convergence of the gradient method. Fig. 5.6 shows the corresponding transmission powers, and the slower initial convergence of gradient method is visible again.

After the convergence period, the results show that sBPC, asBPC and separate BF and PC result in 0.52%, 0.53%, and 1.28% greater power consumption than the joint approach, respectively. Meanwhile, the gradient-method-based estimation results in 0.07% lower power consumption than the joint BF and PC, but it reduces the average SINR by 0.11% as well. With sBPC, asBPC and separate BF and PC, the average SINR is increased by 0.25%, 0.23%, and 0.77%, respectively.

As discussed in Section 3.1, the minimisation of SINR level deviations is also essential for the PC performance. In compared to the joint BF and PC, the average standard deviation of SINR in sBPC, asBPC, the gradient method, and separate BF and PC algorithms are increased by 0.51%, 0.55%, 0.93%, and 1.09%, respectively.

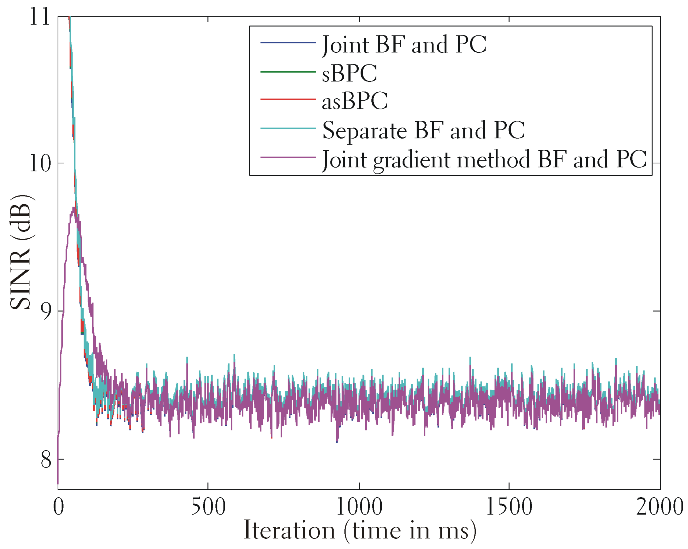

Fig. 5.5: Average SINRs of all mobiles in 100 simulations.

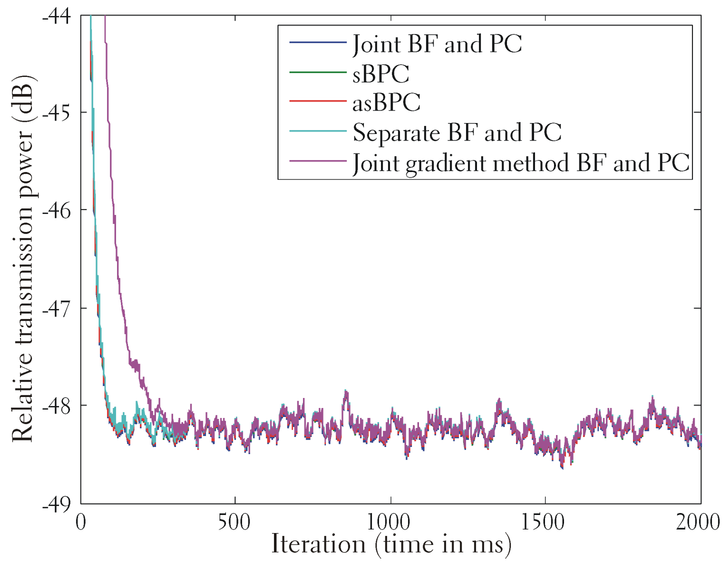

Fig. 5.6: Average transmission powers of all mobiles in 100 simulations.

6. Transmission Beamforming and SINR Estimation for Power Control

The downlink transmission BF and PC scheme is described according to [P4] and [P7]. The main idea of the scheme is to form an SINR estimate of the connection known to the transmitter to be used in PC. The only data needed for estimation are the covariance matrices of the links, which must be known, *e.g.*, in the maximum SINR virtual uplink BF, and the normal PC command.

In most cases, the joint problem of transmission BF and PC is solved by first determining the BF weight vector, then performing the PC step, and then iterating this procedure. However, reaching the global optimum is difficult if it is compared, for example, to the joint PC and receiving BF problem. This is since transmission BF in the base station of each mobile affects the SINR of every mobile, as can be seen in (3.24), and an easily solvable closed-form solution to the optimal BF weight vector is not available. However, this is not the problem considered in the following approach. The aim here is to increase the efficiency of PC.

6.1 Virtual Uplink Algorithm

One sub-optimal transmit BF algorithm is the so-called virtual uplink algorithm, used in, *e.g.*, [68]. The suboptimality is not mentioned there, but can be proved by a simple counterexample; consider the system consisting of two base stations and three mobile users as drawn in Fig. 6.1. If all uplink and downlink transmissions are made with equal transmission power and the path loss is modelled according to distance by d^{-3}, the virtual uplink BF algorithm produces 1.1% worse SINR in downlink than the optimal BF arrived at by an optimisation algorithm.

Essentially, the virtual uplink algorithm corresponds to using the receiving BF vector in the base station in the reciprocal transmission to the same mobile user, even though it solves a slightly different problem. In [76] and [77], Schubert and Boche prove that the optimal uplink receiving BF vector is also the optimal downlink

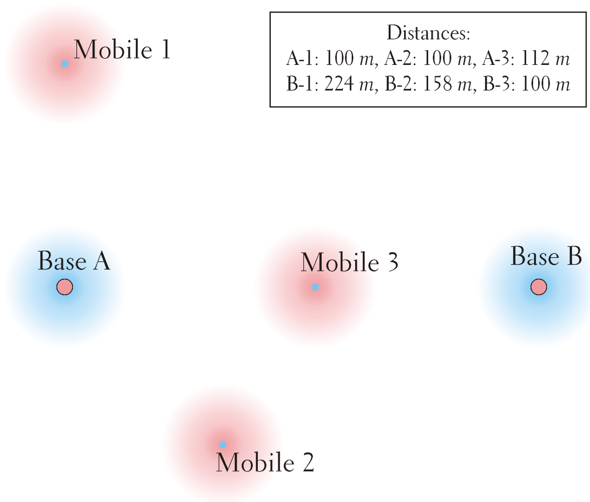

Fig. 6.1: A simple example system.

transmission vector for single-cell systems. This implies that virtual uplink is a good approximation for SINR maximisation and hence it can be used also in simulations.

As mentioned in [68], for transmission BF systems the covariance matrices – *i.e.*, channel information – are known in TDD systems fairly accurately, with a small delay, since the uplink and downlink channels are reciprocal. In FDD systems, measurements must be made from the feedback channel of suitable frequency.

6.2 Downlink SINR Estimation Using Transmission Beamforming

In the following approach to SINR estimation it is assumed that the BF vectors $\mathbf{w}_i$ are given by some transmission BF algorithm, such as the virtual uplink algorithm discussed above. The basic idea is to divide interference into intracell and intercell, referring to interference caused by the base station of the receiver's cell and the other base stations, respectively. If the interference in the receiver of mobile i in the denominator of the downlink SINR (3.24) is divided into intracell and intercell interference expressions, (3.24) can be written as

$$\Gamma_i = \frac{p_i \mathbf{w}_i^H \mathbf{\Phi}_{ii} \mathbf{w}_i}{\sum\limits_{\substack{j \neq i \\ j \in B_i}} p_j \mathbf{w}_j^H \mathbf{\Phi}_{ii} \mathbf{w}_j + \sum\limits_{l \notin B_i} p_l \mathbf{w}_l^H \mathbf{\Phi}_{il} \mathbf{w}_l + n_i} = \frac{p_i \mathbf{w}_i^H \mathbf{\Phi}_{ii} \mathbf{w}_i}{\sum\limits_{\substack{j \neq i \\ j \in B_i}} p_j \mathbf{w}_j^H \mathbf{\Phi}_{ii} \mathbf{w}_j + I_i}, \tag{6.1}$$

where B_i stands for the set of mobile indices assigned to the same base station as the mobile i and I_i is the combined intercell interference and noise power of the mobile i; *i.e.*,

$$I_i = \sum_{l \notin B_i} p_l \mathbf{w}_l^H \mathbf{\Phi}_{il} \mathbf{w}_l + n_i . \tag{6.2}$$

Equation (6.1) shows that Γ_i can be presented as a function of variables known to the base station, p_j, $\mathbf{w}_j$ and $\mathbf{\Phi}_{ii}$, where $j \in B_i$, and an unknown variable I_i. Now, if the level of the unknown intercell interference I_i is estimated on the basis of PC command coming from the mobile, all of the variables in (6.1) are known, and SINR can be estimated.

This SINR estimate update can be written as

$$\hat{\Gamma}_i^{(k)} = \frac{p_i^{(k)} (\mathbf{w}_i^{(k)})^H \mathbf{\Phi}_{ii}^{(k)} \mathbf{w}_i^{(k)}}{\sum_{\substack{j \neq i \\ j \in B_i}} p_j^{(k)} (\mathbf{w}_j^{(k)})^H \mathbf{\Phi}_{ii}^{(k)} \mathbf{w}_j^{(k)} + I_i^{(k)}}, \qquad (6.3)$$

where k refers to the iteration. The level of the intercell interference-and-noise factor $I_i^{(k)}$ is updated in each iteration round k on the basis of the PC command.

The advantage of the proposed SINR update is visible in (6.3). The most recent variations of the channel are to be taken into account more rapidly and accurately than with the normal relay PC. The information circulating in the update loop is presented in Fig. 6.2, where $\Delta_i^{(k)}$ is the PC command at time step k, and q^{-1} stands for the one-step delay operator of the discrete systems.

The proposed SINR estimate assisted power control (SEAPC) scheme is to use an SINR estimate $\hat{\Gamma}_i$ given by (6.3) in a chosen decentralised PC algorithm, which utilises the received SINR in the transmission power level update. In practice, the SEAPC scheme for mobile i would be as presented in Table 6.1.

The main advantage of SEAPC is using the recently updated SINR estimates, which are known to the transmitter, in PC. This is not usually the case. Hence more sophisticated distributed SINR-based PC algorithms can be applied in the inner loop PC instead of the simple relay control FSPC. Hence the changes of transmission power in the base station antenna array need not be fixed in SEAPC.

The cells with SEAPC can co-exist with cells with regular PC schemes and base stations without the transmission BF. This is because the intercell interference factor

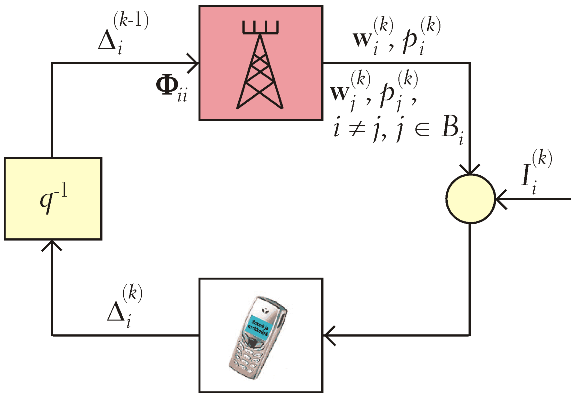

Fig. 6.2: Sketch of the SINR update loop.

Table 6.1: SEAPC scheme.

1. Choose initial values for the base station transmission power to user i, $p_i(0)$, and for the intercell interference $I_i(0)$.
2. Update the intercell interference by

$$I_i^{(k)} = I_i^{(k-1)} + \Delta_i^{(k-1)} \text{ (in dBs).} \tag{6.4}$$

   The update is written in dBs, which corresponds to multiplicative update in absolute values.
3. Update the signal covariance matrix $\mathbf{\Phi}_{ii}$, and the BF vectors $\mathbf{w}_j$, where $j \in B_i$.
4. Update the SINR estimate according to (6.3).
5. Use the chosen distributed power control algorithm using SINR for the PC update to determine $p_i^{(k)}$.
6. Iterate steps 2 – 5 in each iteration round.

I_i update utilises the normal relay PC command Δ_i and covariance matrices $\mathbf{\Phi}_{jj}$, $j \in B_i$, which are measured for adaptive BF purposes.

The down side of SEAPC is that the link covariance matrices $\mathbf{\Phi}_{ii}$ should be known quite accurately. This is due to the fact that their data are used in a feedforward style in the SINR estimation, hence also in the PC. The sensitivity of the SINR estimate $\hat{\Gamma}_i$ for the errors in the intercell interference factor I_i and the link covariance matrix $\mathbf{\Phi}_{ii}$, is an important issue. Differentiation of (6.3) shows that the error in I_i results in large SINR estimation errors when the level of the interference and noise is low. A similar approach indicates also that errors in the elements of $\mathbf{\Phi}_{ii}$ cause large SINR estimation errors if the corresponding elements in BF vectors $\mathbf{w}$ of the mobiles in the same cell are large in absolute value.

6.3 SEAPC Simulation

SEAPC and normal PC schemes were compared in a simulated 12-base-station system, in which every base station has a four-element linear omnidirectional antenna array with a half-wavelength spacing, including 72 mobile users. The maximum cell radius was set to 500 m and the mobiles were spread randomly within the system. The base station receiver relative noise power is set to 10^{-12} and the relative transmission power is allowed to vary between –156 dB and 0 dB.

The multipath propagation model presented in Section 2.3 is utilised. The BF and PC update time is set to 0.001 s. The transmission BF is done with the maximum SINR virtual uplink BF. The carrier frequency is 2 GHz, the processing gain is 128, and the SINR targets are set to 8 dB. Mobiles were set to random movements with 44% of them at low speeds (< 2 m/s) and others evenly distributed within the range 2–30 m/s.

The comparison is done between a transmission beamforming system with normal relay-type FSPC scheme applying a 0.5–dB PC step (corresponding to multiplication of power level by either 1.12 or 0.89), and SEAPC using FMA PC update (3.8) with β = 0.8. Any SINR-based PC algorithms, as well as different tunings, could have been chosen for use with SEAPC instead of FMA and the above choice of β. This corresponds to making FSPC updates according to

$$p_i^{(k)} = 10^{0.05\Delta_i^{(k-1)}} \cdot p_i^{(k-1)},$$

and the SEAPC updates via

$$p_i^{(k)} = \left(0.2 + 0.8\frac{\gamma_i}{\hat{\Gamma}_i^{(k-1)}}\right) \cdot p_i^{(k-1)}.$$

A few important details must be emphasised. Firstly, both PC schemes – normal PC with FSPC and SEAPC with FMA – use exactly the same signalling and measurement: one-bit power control feedback and BF signal covariance matrices. Secondly, note that one–step–delayed information is used in both power control updates.

Relative power means and downlink SINRs over all mobiles are shown in Fig. 6.3 and Fig. 6.4, respectively. In addition, the estimated SINR probability densities of the schemes over all of the mobiles are included in Fig. 6.5.

Fig. 6.3 shows that the mean transmission power is slightly lower in SEAPC than in the normal PC scheme. The mean relative transmission powers of all mobiles in the last 1200 iteration steps of the simulation for the normal PC and SEAPC schemes are 0.5055×10^{-4} and 0.5032×10^{-4}, respectively. The last 1200 iterations are examined in order to guarantee the convergence of the algorithms. This corresponds to SEAPC having 0.44 % lower power consumption than the normal relay FSPC in a similar system.

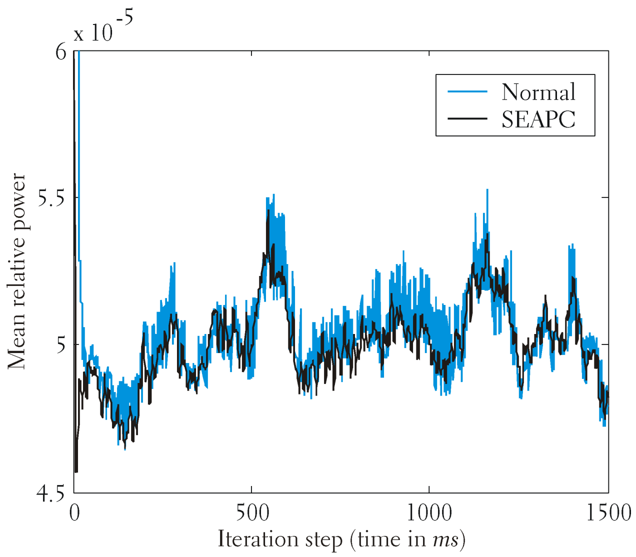

Fig. 6.3: Mean relative powers as a function of the iteration step.

Fig. 6.4 indicates that, after the convergence period, SINRs of the different schemes vary around the SINR target. To be precise, SEAPC has a 0.03% smaller mean SINR in the last 1200 iteration rounds. Hence, it can be stated that the performance follows the mean SINR and power consumption is roughly the same for the normal PC scheme and SEAPC. There is a noteworthy difference, however, in SINR behaviour between the schemes. The SINR variance around the target is much larger with the normal scheme than with SEAPC. This result can be validated by checking the estimated distributions of the experienced SINR in Fig. 6.5; the probability density of SINR is spread much wider in the relay PC case.

In addition to simulating the case with perfect estimation of covariance matrices $\mathbf{\Phi}_{ii}$, a simulation with erroneous estimation is considered. Multiplicative elementwise errors are simulated similar to the ones obtained in [51]. In this case, SEAPC has 0.18 % greater power consumption than the normal scheme. However, the SINR variance is still significantly smaller with SEAPC, as the probability densities in Fig. 6.5 show. In the normal and SEAPC schemes, the SINR safety margins for 2% outage are 0.78 dB and 0.55 dB, respectively.

As discussed in Section 3.1, the small variance of the SINR levels is very important in reducing the power consumption. This is because there are given required SINR levels, which must be satisfied constantly in order to guarantee the desired BER, or the connection could be dropped. In practice, this means that large variance of SINR around the target SINR leads to a need to increase the safety margin between the minimum required SINR and the PC target SINR. For example, in the simulation presented the probabilities of experienced SINRs being at least 7.5 dB of the normal and SEAPC schemes were 93.6% and 100%, respectively. In other words, the minimum required SINR of 7.5 dB for the given service would have been fully acceptable for SEAPC but not at all for normal relay PC.

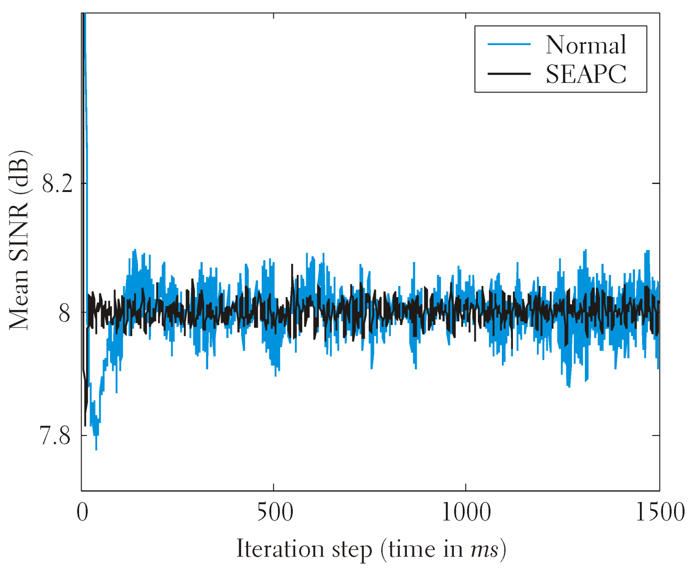

Fig. 6.4: Mean SINRs as a function of iteration step.

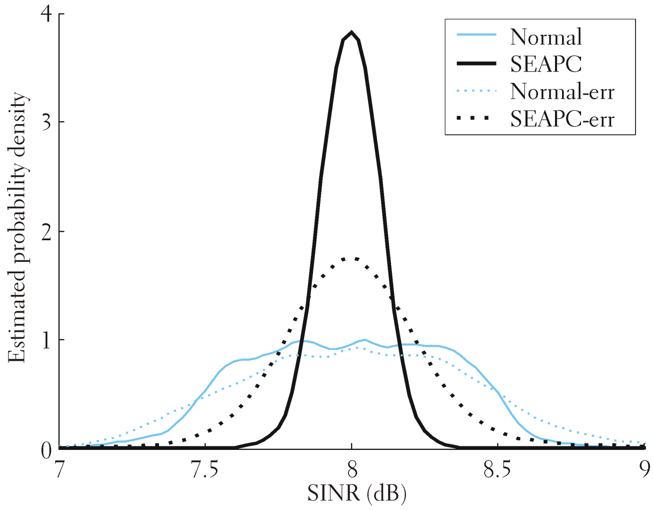

Fig. 6.5: The estimated SINR distributions of the power control schemes.

In further simulations, the similar scenario with erroneous signal covariance matrix estimation was simulated over 100 cases with different channel conditions and mobile station movements. The differences to the above simulation is that there is only 60 mobiles and simulations lasted for 1000 steps *i.e.* one second. The results shown in below are averaged after the initial convergence period (300 steps).

The corresponding SINR distributions are drawn in Fig. 6.6. In overall, the results seem similar to the ones presented in Fig. 6.5: SEAPC results in more narrow SINR distribution. In addition, 2 % tail values of both distributions are drawn in Fig. 6.6. Their numerical values are 7.31 dB and 7.54 dB for normal and SEAPC schemes, respectively. Although 2 % is not a realistic target for outage, the difference in tail values indicates the significantly better performance of SEAPC scheme.

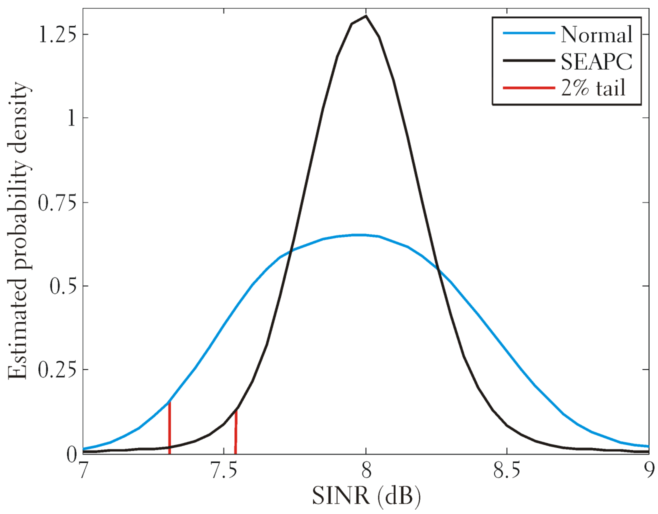

Fig. 6.6: The estimated SINR distributions of the power control schemes with erroneous covariance matrix estimation over 100 simulated cases.

7. Beamforming Weight Vector Prediction

The following self-tuning prediction of BF weight vector is based on the assumption that data points and predicted data points are dependent on each other according to an ARMA model. The desired future data value can be solved from the ARMA model, and the model is used for prediction. The core of the self-tuning predictor is estimation of parameters of the ARMA-model via RLS method [53]. An introduction to self-tuning predictors can be found, for example, in [32].

A similar self-tuning predictor scheme has been known in control engineering for a long time (see, *e.g.*, [44]). In a wireless telecommunication platform, a similar kind of predictor was introduced for inner-loop transmission PC, the fast PC, of third-generation cellular radio systems in [84] by Virtej *et al*. The most significant difference between a PC prediction and a BF prediction is that in the case of the PC prediction a scalar prediction is required, whereas in BF a vector prediction must be applied. This obviously increases degrees of freedom and complexity in the BF prediction, including even the choice of predictor model configuration.

7.1 Beamforming Prediction Models

In the case of BF, the basic assumption for ARMA models mentioned above is the BF vectors $\mathbf{w}$ and the predicted BF vectors $\hat{\mathbf{w}}$ being linearly dependent. Both vectors are of dimension n_a *x* 1, where n_a is the number of antenna elements in the array. In this case, the ARMA model is

$$B(q^{-1})\mathbf{w}(k) = C(q^{-1})\hat{\mathbf{w}}(k+1\,|\,k)\,, \tag{7.1}$$

where q^{-1} is the delay operator for difference systems, with $B(q^{-1})$ and $C(q^{-1})$ being polynomials, or polynomial matrices with respect to q^{-1}, depending on the model structure. C is limited to be monic with respect to the constant term. For details of the delay operator and related polynomial matrices, see, *e.g.*, [104]. The notation $(k + 1 \mid k)$ stands for the estimate at time step $k + 1$, while data until step k is known.

The BF prediction is performed on the basis of the following form of (7.1):

$$\hat{\mathbf{w}}(k+1|k) = B(q^{-1})\mathbf{w}(k) + (I - C(q^{-1}))\hat{\mathbf{w}}(k+1|k) \tag{7.2}$$

where I is a unit matrix suitable for the dimensions of C. This is the core of the following BF prediction algorithms; the predicted vector $\hat{\mathbf{w}}(k+1 \mid k)$ can be used in BF instead of $\mathbf{w}(k)$, the delayed vector, in time step k.

Since $\mathbf{w}$ and $\hat{\mathbf{w}}$ are column vectors in (7.2), there are several ways to form predictors, depending on the format of $B(q^{-1})$ and $C(q^{-1})$. Three different options are considered in this paper:

i) $B(q^{-1})$ and $C(q^{-1})$ are polynomials,

ii) $B(q^{-1})$ and $C(q^{-1})$ are diagonal matrices with polynomial entries, and

iii) $B(q^{-1})$ and $C(q^{-1})$ are matrices with polynomial entries.

Let us write the above prediction methods in linear algebra fashion. The representations of the three are, respectively:

i) If the BF history is collected as

$$\mathbf{W}_1(k) = \begin{bmatrix}\mathbf{w}(k) & \dots & \mathbf{w}(k-n) & \hat{\mathbf{w}}(k|k-1) & \dots & \hat{\mathbf{w}}(k-m|k-1-m)\end{bmatrix}, \tag{7.3}$$

where n and m correspond to the degrees of the polynomials B and C, respectively, and

$$\mathbf{A}_1(k) = \begin{bmatrix}b_0(k) & \dots & b_n(k) & -c_1(k) & \dots & -c_m(k)\end{bmatrix}^T, \tag{7.4}$$

then the first ARMA model can be expressed as

$$\hat{\mathbf{w}}(k+1|k) = \mathbf{W}_1(k)\mathbf{A}_1(k). \tag{7.5}$$

ii) If for every antenna element $i = 1,\dots,n_a$ the BF weight vector history is written as

$$\mathbf{W}_{i,2}(k) = \begin{bmatrix}w_i(k) & \dots & w_i(k-n) & \hat{w}_i(k|k-1) & \dots & \hat{w}_i(k-m|k-1-m)\end{bmatrix}, \tag{7.6}$$

and

$$\mathbf{A}_{i,2}(k) = \begin{bmatrix}b_{0,i}(k) & \dots & b_{n,i}(k) & -c_{1,i}(k) & \dots & -c_{m,i}(k)\end{bmatrix}^T, \tag{7.7}$$

then the second ARMA model can be written for every antenna element as

$$\hat{w}_i(k+1|k) = \mathbf{W}_{i,2}(k)\mathbf{A}_{i,2}(k). \tag{7.8}$$

The second ARMA model can be expressed collectively by combining the above equations, thus:

$$\begin{aligned}\mathbf{W}_2(k) &= \begin{bmatrix} w_1(k) & \dots & w_1(k-n) & \hat{w}_1(k|k-1) & \dots & \hat{w}_1(k-m|k-1-m) \\ \vdots & & \vdots & \vdots & & \vdots \\ w_{n_a}(k) & \dots & w_{n_a}(k-n) & \hat{w}_{n_a}(k|k-1) & \dots & \hat{w}_{n_a}(k-m|k-1-m)\end{bmatrix} \\ &= \begin{bmatrix}\mathbf{w}(k) & \dots & \mathbf{w}(k-n) & \hat{\mathbf{w}}(k|k-1) & \dots & \hat{\mathbf{w}}(k-m|k-1-m)\end{bmatrix},\end{aligned} \tag{7.9}$$

$$\mathbf{A}_{i,2}(k) = \begin{bmatrix} b_{0,1}(k) & \dots & b_{0,n_a}(k) \\ \vdots & & \vdots \\ b_{n,1}(k) & \dots & b_{n,n_a}(k) \\ -c_{1,1}(k) & \dots & -c_{1,n_a}(k) \\ \vdots & & \vdots \\ -c_{m,1}(k) & \dots & -c_{m,n_a}(k) \end{bmatrix}, \tag{7.10}$$

and

$$\hat{\mathbf{w}}(k+1 \mid k) = \operatorname{diag}\left(\mathbf{W}_2(k)\mathbf{A}_2(k)\right). \tag{7.11}$$

iii) If the history of the weight vectors is formulated as

$$\mathbf{W}_3(k) = \begin{bmatrix} \mathbf{w}(k) \\ \vdots \\ \mathbf{w}(k-n) \\ \hat{\mathbf{w}}(k \mid k-1) \\ \vdots \\ \hat{\mathbf{w}}(k-m \mid k-1-m) \end{bmatrix}, \tag{7.12}$$

and the parameters as

$$\mathbf{A}_3(k) = \begin{bmatrix} \mathbf{b}_{0,1}(k) & \dots & \mathbf{b}_{n,1}(k) & -\mathbf{c}_{1,1}(k) & \dots & -\mathbf{c}_{m,1}(k) \\ \vdots & & \vdots & \vdots & & \vdots \\ \mathbf{b}_{0,n_R}(k) & \dots & \mathbf{b}_{n,n_R}(k) & -\mathbf{c}_{1,n_R}(k) & \dots & -\mathbf{c}_{m,n_R}(k) \end{bmatrix}, \tag{7.13}$$

where

$$\begin{aligned} \mathbf{b}_{i,j}(k) &= \left[b_{i,j,1} \dots b_{i,j,n_R} \right], \\ \mathbf{c}_{i,j}(k) &= \left[c_{i,j,1} \dots c_{i,j,n_R} \right], \end{aligned} \tag{7.14}$$

then the third ARMA model can be written as

$$\hat{\mathbf{w}}(k+1 \mid k) = \mathbf{A}_3(k)\mathbf{W}_3(k). \tag{7.15}$$

Note that the order of matrices in the matrix product on the right-hand side of (7.15) differs from the multiplication order in (7.8) and (7.11). The prediction models represented by (7.8), (7.11), and (7.15) are referred to as BP1, BP2, and BP3 from here on. Note that according to the prediction model (7.2) n + 1 normal BF vectors and m estimated BF vectors are used to predict the new BF vectors.

The linear algebra formulations are illustrated in Fig. 7.1 to describe the model structures. In BP1 the predicted BF vector is a linear combination of the history BF vectors, BP2 is elementwise linear combination of the history BF vector, and in BP3 the predicted BF vector elements are based on all elements in the history BF vectors.

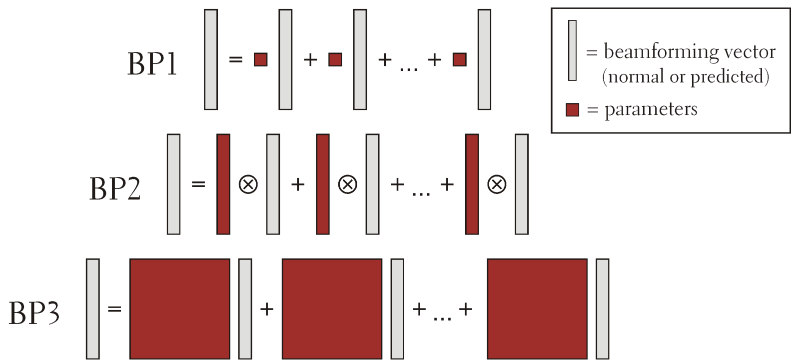

Fig. 7.1: A sketch of the differences of the prediction models.

7.2 RLS Algorithm for Parameter Estimation

The crucial question is how the prediction model weights $\mathbf{A}$ are updated in each time step. This is the point where the RLS algorithm comes into the picture. In the case of scalar prediction, the RLS update equations [53] are

$$\begin{aligned}\boldsymbol{\gamma}(k) &= \frac{\mathbf{P}(k)\mathbf{W}^T(k+1)}{\mathbf{W}(k+1)\mathbf{P}(k)\mathbf{W}^T(k+1)+\beta},\\ \mathbf{A}(k+1) &= \mathbf{A}(k)+\boldsymbol{\gamma}(k)\big(w(k+1)-\mathbf{W}(k+1)\mathbf{A}(k)\big),\\ \mathbf{P}(k+1) &= \big(\mathbf{I}-\boldsymbol{\gamma}(k)\mathbf{W}(k+1)\big)\mathbf{P}(k)/\beta,\end{aligned} \tag{7.16}$$

where $\boldsymbol{\gamma}(k)$ is the time-variable update gain, which is sometimes referred to as the Kalman gain; $\mathbf{P}(k)$ is the inverse of the covariance matrix of the variables in the history vector $\mathbf{W}(k)$; β is the forgetting factor; and $\mathbf{I}$ is a unit matrix with suitable dimensions. The forgetting factor β is chosen from the range (0, 1]. Its name comes from the fact that the weight of the older data points in RLS estimate decay exponentially with the factor β. Usually the forgetting factor is chosen to be close to 1.

For the prediction model BP1 (7.5), the RLS update equations are

$$\begin{aligned}\boldsymbol{\gamma}_1(k) &= \mathbf{P}_1(k)\mathbf{W}_1^T(k+1)\big(\mathbf{W}_1(k+1)\mathbf{P}_1(k)\mathbf{W}_1^T(k+1)+\beta\mathbf{I}\big)^{-1},\\ \mathbf{A}_1(k+1) &= \mathbf{A}_1(k)+\boldsymbol{\gamma}_1(k)\big(\mathbf{w}(k+1)-\mathbf{W}_1(k+1)\mathbf{A}_1(k)\big),\\ \mathbf{P}_1(k+1) &= \big(\mathbf{I}-\boldsymbol{\gamma}_1(k)\mathbf{W}_1(k+1)\big)\mathbf{P}_1(k)/\beta.\end{aligned} \tag{7.17}$$

In the case of BP2 (7.6) the RLS update equations are

$$\begin{aligned}\boldsymbol{\gamma}_{i,2}(k) &= \frac{\mathbf{P}_{i,2}(k)\mathbf{W}_{i,2}^T(k+1)}{\mathbf{W}_{i,2}(k+1)\mathbf{P}_{i,2}(k)\mathbf{W}_{i,2}^T(k+1)+\beta},\\ \mathbf{A}_{i,2}(k+1) &= \mathbf{A}_{i,2}(k)+\boldsymbol{\gamma}_{i,2}(k)\big(w_{i,2}(k+1)-\mathbf{W}_{i,2}(k+1)\mathbf{A}_{i,2}(k)\big),\\ \mathbf{P}_{i,2}(k+1) &= \big(\mathbf{I}-\boldsymbol{\gamma}_{i,2}(k)\mathbf{W}_{i,2}(k+1)\big)\mathbf{P}_{i,2}(k)/\beta,\end{aligned} \tag{7.18}$$

As far as BP3 is concerned, in (7.15) the matrix multiplication is done in reverse order compared to the others. Therefore in (7.16) **W**s are replaced by $\mathbf{W}_3^T$, and **A**s by $\mathbf{A}_3^T$, resulting in the following RLS equations:

$$\begin{aligned}\boldsymbol{\gamma}_3(k)&=\frac{\mathbf{P}_3(k)\mathbf{W}_3(k+1)}{\mathbf{W}_3^T(k+1)\mathbf{P}_3(k)\mathbf{W}_3(k+1)+\beta},\\ \mathbf{A}_3^T(k+1)&=\mathbf{A}_3^T(k)+\boldsymbol{\gamma}_3(k)\left(\mathbf{w}^T(k+1)-\mathbf{W}_3^T(k+1)\mathbf{A}_3^T(k)\right),\\ \mathbf{P}_3(k+1)&=\left(\mathbf{I}-\boldsymbol{\gamma}_3(k)\mathbf{W}_3^T(k+1)\right)\mathbf{P}_3(k)\big/\beta.\end{aligned} \tag{7.19}$$

In order to clarify the differences between the complexities of prediction algorithms, a summary of the matrix dimensions in the algorithms is presented in Table 7.1.

Table 7.1: Summary of the dimensions of the parameter matrices.

	W	γ	**A**	**P**
BP1	n_a x $(n+1+m)$	$(n+1+m)$ x n_a	$(n+1+m)$ x 1	$(n+1+m)$ x $(n+1+m)$
BP2	n_a x 1 x $(n+1+m)$	n_a x $(n+1+m)$ x 1	n_a x $(n+1+m)$ x 1	n_a x $(n+1+m)$ x $(n+1+m)$
BP3	$(n+1+m)n_a$ x 1	$(n+1+m)n_a$ x 1	$(n+1+m)n_a$ x n_a	$(n+1+m)n_a$ x $(n+1+m)n_a$

Building BF prediction N steps ahead (*i.e.*, estimating $\hat{\mathbf{w}}(k+N \mid k)$), is almost exactly the same as the one-step prediction presented. The only things that change are that $\mathbf{w}(k+1)$ is replaced by $\mathbf{w}(k+N)$ in RLS models, and the predicted elements in the matrices $\mathbf{W}(k)$ are of the form $\hat{\mathbf{w}}(k+N-j \mid k-j)$ instead of $\hat{\mathbf{w}}(k+1-j \mid k-j)$, while $j = 1,\ldots,m$. Otherwise the approach is similar.

7.3 Beamforming Prediction Simulation

Let us consider an uplink simulation case, which includes 10 mobiles moving with speeds from 11 m/s to 35 m/s assigned to the same base station; see Fig. 7.2. The base station has a four-element linear antenna array, and the maximum SINR BF is used. The model does not include multipath components, but the channel variations are dealt with via relay PC. The performance criteria are the power usage and the average SINR. The SINR target is set to 0.01, and the BF and PC update period is set to 0.01 s. Models with a history of two BF vectors and one predicted vector are used in prediction – *i.e.*, $n = 1$ and $m = 1$. A forgetting factor of $\beta = 0.9$ is used.

Mean relative powers of the BF schemes are drawn in Fig. 7.3 in terms of the iteration step. The corresponding results for the average power usage and SINR of the simulation with moving mobile stations are presented in Table 7.2. The work shows that not much difference exists in SINR levels between the BF schemes. However, since PC is on, there is considerable difference in the mean relative power used. The BF and PC system with prediction algorithm BP1 uses more power than the regular, delayed, BF. The cases with the prediction algorithms BP2 and BP3 have clearly lower power consumption than regular BF. On the other hand the system with the optimal, undelayed, BF has much better power efficiency, but the advantages of the BF prediction are clear.

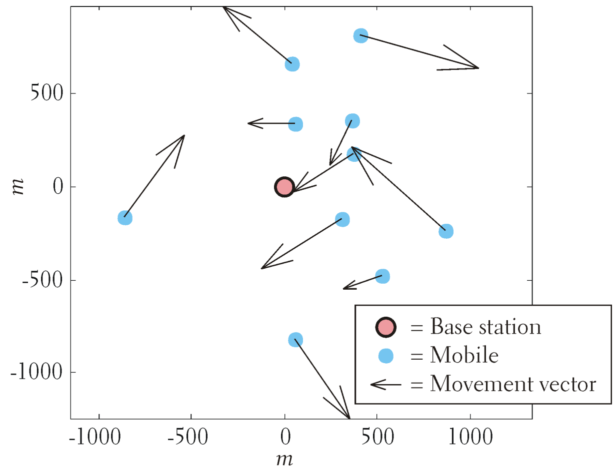

Fig. 7.2: The simulated case with moving mobiles.

Table 7.2: Average SINR and power usage in the simulation with moving mobiles.

Method	SINR	Relative power
Regular BF	0.0115	$0.524 \cdot 10^{-4}$
BP1	0.0115	$0.544 \cdot 10^{-4}$
BP2	0.0115	$0.506 \cdot 10^{-4}$
BP3	0.0113	$0.496 \cdot 10^{-4}$
Optimal BF	0.0109	$0.421 \cdot 10^{-4}$

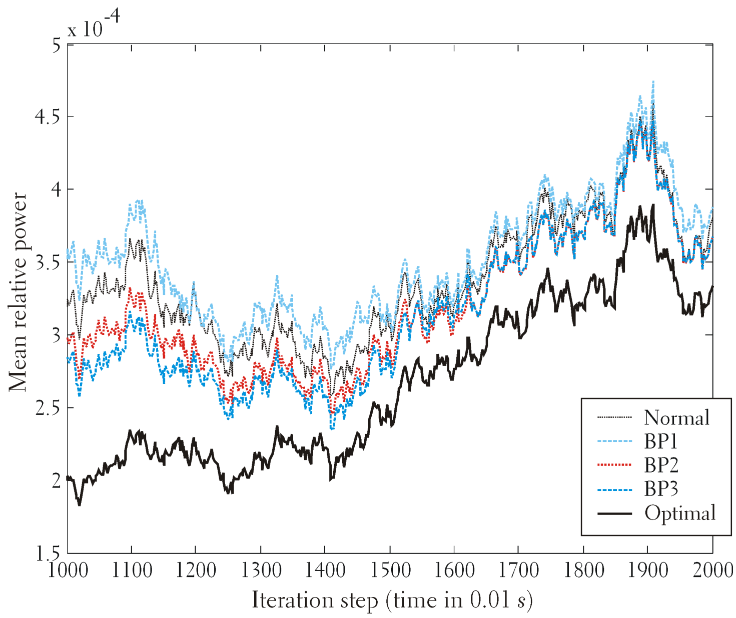

Fig. 7.3: Mean relative powers of different beamforming schemes.

8. A Power Control Approach to Transmission Rate Allocation

Most of the transmission rate allocation algorithms consider the throughput to be the only performance variable. However, in practice, the fairness should be taken into account in rate allocation. Service of all paying customers should be assured, and given QoS requirements should be met constantly for all users.

The maximum throughput rate allocation in single-antenna systems is shown in [35] to be such that the users with best channel conditions transmit at maximum rate, while others do not transmit at all. Additionally, [41] describes discovering that in the antenna array systems the residual capacity can be allocated to other users depending on the directions-of-arrivals of the signals to antenna arrays of base stations. The problem in the above allocations is that they are not fair to all users at all moments.

Since PC and TRA are closely related to each other, the TRA problem is approached through PC here. As mentioned in Subsection 3.1.1, the minimum total transmission power satisfying SINR constraints is obtained while the equality holds in (3.2). In the case of variable rates, the optimum transmission powers (3.5) are

$$\mathbf{p}_{opt} = (\mathbf{I} - W^{-1}\mathbf{R}\mathbf{H})^{-1} W^{-1}\mathbf{R}\boldsymbol{\eta}, \tag{8.1}$$

where $\mathbf{R} = diag\{r_1, \dots, r_M\}$ is the rate matrix with entries in the diagonal, and W is the transmission bandwidth. Equation (8.1) demonstrates the difficulty of rate allocation: increase of any transmission rate increases all transmission powers also.

8.1 Interference and Interference-Sensitivity Approaches

The key point in allocating transmission rates is to decide which transmitters get to transmit at high rate and which must settle for a lower rate. Since PC is closely related to TRA, the suggested approach is to allocate the highest data rates to those connections that cause least interference, instead of those with the best channel conditions, as in [35]. An iterative and cellwise rate allocation is practical due to low signalling and fast convergence speed. Allocations can be applied also at the network-wide level.

The sensitivity of transmission powers to interference can be examined from the steady-state solution of PC. The steady-state solution for the transmission power of connection i is

$$p_i = \frac{\gamma_i}{L_i g_{ii}}\left(\sum_{j=1, j\neq i}^{M} g_{ji} p_j + n_i\right) = \frac{\gamma_i r_i}{W}\left(\sum_{j\in B_i, j\neq i} \frac{g_{ji}}{g_{ii}} p_j + \frac{I_i}{g_{ii}}\right), \tag{8.2}$$

where L_i is the processing gain, defined as $L_i = W/r_i$; B_i is the set of indices of mobiles allocated to the same base station as i; and I_i is the intercell interference from the other cells in the system plus noise:

$$I_i = \sum_{j\notin B_i} g_{ji} p_j + n_i \,. \tag{8.3}$$

In order to measure the sensitivity of transmission powers p_i to the interfering transmission powers within a cell k, (8.2) can be differentiated with respect to interfering p_j:

$$\frac{\partial p_i}{\partial p_j} = \frac{\gamma_i r_i}{W}\cdot\frac{g_{ji}}{g_{ii}}, \; i, j \in B_k, \tag{8.4}$$

where B_k is the set of indices of connections allocated to the cell k of interest. The above can be collected in an interference-sensitivity matrix (ISM):

$$\mathbf{S}_{IS}^{k} = \left[\frac{\partial p_i}{\partial p_j}\right]_{ij} = \begin{cases} \left[\frac{\gamma_i r_i}{W}\cdot\frac{g_{ji}}{g_{ii}}\right]_{ij}, & i,j \in B_k, \, j\neq i, \\ 0, & j = i. \end{cases} \tag{8.5}$$

For fair allocation of transmission rates, it is desirable that connections with a high transmission rate have low sensitivity to interference. Practically, this corresponds to the connection corresponding to the smallest row and column sums of $\mathbf{S}_{IS}{}^{k}$.

An alternative measure for the rate allocation is to estimate the interference caused to connections within the cell. These measures can be collected in an interference matrix (IM):

$$\mathbf{S}_{I}^{k} = \begin{cases} \left[\frac{\gamma_i r_i}{W}\cdot\frac{g_{ji}}{g_{ii}}\cdot p_i\right]_{ij}, & i,j \in B_k, j\neq i, \\ 0, & j = i. \end{cases} \tag{8.6}$$

For fairness, it is desirable to give higher transmission rates to the connections, that do not suffer from or cause much interference. Hence, a kind of interference equalisation is obtained.

Interestingly, use of the interference-sensitivity matrix $\mathbf{S}_{IS}$ and the interference matrix $\mathbf{S}_I$ are similar to stepwise removal algorithms SRA [101] and SMIRA [48] criteria, respectively, with weighting by SINR targets and transmission rates. In those approaches, variables are used in determining which bases are removed from the cochannel set. In SRA and SMIRA, the criteria were taken into account by calculating row and column sums of corresponding matrices. Here we suggest a similar approach: for each connection i the TRA decision variable v_i is the maximum over the sums of corresponding rows and columns in $\mathbf{S}_{IS}$ or $\mathbf{S}_I$ – for example, in the ISM case:

$$v_i = \max\left\{\left\|[\mathbf{S}_{IS}^k]_{i\cdot}\right\|_1, \left\|[(\mathbf{S}_{IS}^k)^T]_{i\cdot}\right\|_1\right\}, \tag{8.7}$$

where $\|\cdot\|_1$ stands for an l_1-norm of row vector.

Since the ISM- or IM-based rate allocations are restricted to one cell, we notice that $g_{ji} = g_{ij}$ for single-antenna systems. Therefore, the decision variables are dominated by channel conditions between the mobiles and their allocated base stations. However, this is not the general case for BF systems, due to spatial filtering. For BF systems, ISM and IM are defined by

$$\mathbf{S}_{IS}^k = \left[\frac{\partial p_i}{\partial p_j}\right]_{ij} = \left[\frac{\gamma_i r_i}{W}\cdot\frac{g_{ji}\mathbf{w}_i^H\mathbf{a}_{ji}\mathbf{a}_{ji}^H\mathbf{w}_i}{g_{ii}\mathbf{w}_i^H\mathbf{a}_{ii}\mathbf{a}_{ii}^H\mathbf{w}_i}\right]_{ij},\ i, j \in B_k,\ j \neq i \text{ and} \tag{8.8}$$

$$\mathbf{S}_I^k = \left[\frac{\gamma_i r_i}{W}\cdot\frac{g_{ji}\mathbf{w}_i^H\mathbf{a}_{ji}\mathbf{a}_{ji}^H\mathbf{w}_i}{g_{ii}\mathbf{w}_i^H\mathbf{a}_{ii}\mathbf{a}_{ii}^H\mathbf{w}_i}\cdot p_j\right]_{ij},\ i, j \in B_k,\ j \neq i, \tag{8.9}$$

respectively. In fact, $g_{ji}\mathbf{a}_{ji}\mathbf{a}_{ji}^H$ is the signal covariance matrix between transmitter j and receiver i normalised by transmission power (see Subsection 3.2.1). Since many BF techniques are based on the measurement of these covariance matrices [52], the ISM- or IM-based allocations do not require any additional measurements.

8.2 Power Control Feasibility Approach

In order to obtain meaningful power allocations via (8.1), the corresponding PC problem must be **feasible**. This essentially means that the matrix inversion in (8.1) can be done. The necessary and sufficient condition for the existence of non-negative $\mathbf{p}$ in (8.1) for every non-negative $\boldsymbol{\eta}$ is that matrix $(\mathbf{I} - W^{-1}\mathbf{RH})^{-1}$ is non-negative [65]. Since $W^{-1}\mathbf{RH}$ is also non-negative, $(\mathbf{I} - W^{-1}\mathbf{RH})^{-1}$ is non-negative exactly when the spectral radius of $W^{-1}\mathbf{RH}$ is smaller than one [65]. This corresponds to PC problem being feasible if and only if

$$\rho(W^{-1}\mathbf{RH}) = \max_i \left|\lambda_i(W^{-1}\mathbf{RH})\right| < 1, \tag{8.10}$$

where ρ refers to the spectral radius and λ refers to an eigenvalue.

For unconstrained power transmissions, rates can be selected in any manner as long as (8.10) is satisfied. However, for a practical implementation, it should be kept in mind that if the spectral radius of $W^{-1}\mathbf{RH}$ is close to one while satisfying (8.10), the transmission powers (8.1) grow unboundedly. Since the actual transmission powers are always constrained, additional constraints must be introduced by the maximum transmission power constraint

$$\mathbf{0} < \mathbf{p} \leq \mathbf{p}_{\max}, \tag{8.11}$$

or by the total transmission power constraint

$$\mathbf{0} < \|\mathbf{p}\|_1 \leq \tilde{p}_1, \tag{8.12}$$

where $\tilde{p}_1$ is the maximum total transmission power in the cell. Usually uplink transmissions have a maximum transmission power constraint. In downlink, the transmission powers may be bounded in either way.

The PC feasibility approach to the rate allocation that is suggested is to maximise rates while satisfying constraint (8.10) with a predefined safety margin. In order to do this, the spectral radius of $W^{-1}\mathbf{RH}$ must be estimated first. The consequent allocation must secure the condition (8.10), but simultaneously maximising rates, which corresponds to spectral radius being as close to the margin as possible.

A good method for spectral radius approximation for positive irreducible matrices is given in [93]:

Theorem – *Let* $\mathbf{A} \geq 0$ *be an* n x n *irreducible matrix and* $\boldsymbol{q}_0$ *be an arbitrary positive* n*-dimensional vector. Defining* $\mathbf{q}_\nu = \mathbf{A}\mathbf{q}_{\nu-1} = \ldots = \mathbf{A}^\nu \mathbf{q}_0$, $\nu \geq 1$, *let*

$$\lambda_{1,\nu} = \min_{1\leq i\leq n}\left(\frac{\boldsymbol{q}_{\nu+1}^{(i)}}{\boldsymbol{q}_{\nu}^{(i)}}\right) \text{ and } \lambda_{u,\nu} = \max_{1\leq i\leq n}\left(\frac{\boldsymbol{q}_{\nu+1}^{(i)}}{\boldsymbol{q}_{\nu}^{(i)}}\right), \tag{8.13}$$

where the superscript i represents the ith component of a vector. Then

$$\lambda_{1,0} \leq \lambda_{1,1} \leq \lambda_{1,2} \leq \ldots \leq \rho(\mathbf{A}) \leq \lambda_{u,2} \leq \lambda_{u,1} \leq \lambda_{u,0}. \tag{8.14}$$

In a nutshell, this power-method-based algorithm provides bounds for spectral radius that becomes better with iteration.

The simplest way to estimate the spectral radius of any non-negative matrix is via minimum and maximum row and column sums [65], [93]. In this case, the same upper limit could be acquired byway of Gerschgorin's theorem [57], which interestingly gives also suprema for achievable rates r_i:

$$r_{u,i} = \frac{g_{ii}W}{\gamma_i \sum_{j=1,j\neq i}^{M} g_{ji}}, \; i = 1,\ldots,M. \tag{8.15}$$

The limit (8.15) obtained through Gerschgorin's theorem gives valuable insight about the dependency between spectral radius of $W^{-1}\mathbf{RH}$ and the allocated rates. The simultaneously maximised rates do not depend directly on each other; they depend only on the link properties. Additionally, the limit (8.15) suggests also an upper bound of possible transmission rates for all users simultaneously. This means that, on the basis of this measure, users are not classified only as those granted maximum rate and those granted minimum rate. Therefore, the rate allocation is fairer than in the case of maximising throughput.

8.3 Incremental Rate Allocation Algorithms

In addition to maximising the throughput and fairness, TRA algorithms must reduce the outage. Therefore, the system cannot be set to transmit near the theoretical capacity limit, due to channel variations. The discussion that follows suggests changing transmission rates on the basis of the maximum transmission power used in the cell.

The transmission rates (8.15), or rates close to them, are not applicable in practice, for a number of reasons. Firstly, the available rates are often members of a predefined discrete set of rates; they cannot be selected arbitrarily in a continuous interval. Secondly, as rates r_i tend toward their limits $r_{u,i}$ and the spectral radius of $W^{-1}\mathbf{RH}$ tends to one, transmission powers can grow infinitely, which is not the case in reality.

The rate allocations discussed in the previous sections are not always applicable, due to the required measurements of channel gain and the related signalling. These rate allocations are more useful if the channel gains can be estimated reciprocally – *i.e.*, if the base stations can estimate their channel gains to all mobiles in the system accurately enough. This channel estimation is required, *e.g.*, in BF systems.

In variable-transmission-rate systems, rates are applied in frames. This means that transmission rate levels are updated at a given interval, which is a multiple of the PC period. In practice, the easiest way to change the allocated rates is to do so incrementally – adjusting the rate applied by one step up or down.

8.3.1 Interference and Interference Sensitivity

The rate to be modified is chosen on the basis of the decision variables v_i introduced in Section 8.1. The outline of the TRA algorithm is given in Table 8.1.

The exact levels of δ_1 and δ_2 must be chosen according to the system. δ_1 should be the ratio between the current transmission rate and one level greater transmission rate. Thus, an outage should not occur if rule 2 of the algorithm is activated and transmission rate is increased. δ_2 should be chosen to prevent an outage if interference and/or channel conditions get worse between the rate updates.

Table 8.1: Incremental change rate allocation.

1. Determine the maximum transmission power $p_{maxused}$ used in the cell.
2. If $p_{maxused} \leq \delta_1 \cdot p_{max}$, where $0 < \delta_1 < 1$, then increase the rate of the connection not transmitting at full rate having the smallest ν.
3. If $p_{maxused} \geq \delta_2 \cdot p_{max}$, where $0 < \delta_1 < \delta_2 < 1$, then decrease the transmission rate of the connection not transmitting at minimum rate having the largest decision variable ν.
4. If $\delta_1 \cdot p_{max} \leq p_{maxused} \leq \delta_2 \cdot p_{max}$, where $0 < \delta_1 < \delta_2 < 1$, then increase the rate of the connection not transmitting at full rate or using at least $\delta_1 \cdot p_{max}$ transmission power having the smallest decision variable ν.
5. Apply the new transmission rates and resume with the next communication frame.
6. After the frame return to step 1.

Basically, δ_1 and δ_2 define the limits for the maximum transmission power applied in comparison to the maximum possible transmission power.

Note that the increased rate can be applied after one frame delay. This is because PC must converge in order to avoid outage. While the transmission rate decreases, the decreased rate must be used immediately, since PC begins to decrease the power level.

8.3.2 Power Control Feasibility

The PC feasibility is best taken into account in rate allocation in the form of making sure that the spectral radius of $W^{-1}\mathbf{RH}$ does not get too close to one. This can be done by estimating $\rho(W^{-1}\mathbf{RH})$ in every frame and adjusting the rates accordingly.

Another important issue is to decide which rate to increase or decrease according to the spectral radius estimate. In this case, the upper limits of spectral radius estimates (8.15) of Gerschgorin's Theorem are useful. In order to keep the upper limits as small as possible, if a rate can be increased, the one corresponding to the smallest row (or column) sum of $W^{-1}\mathbf{RH}$ should be chosen. If a rate must be decreased, the one corresponding to the largest row (or column) sum of $W^{-1}\mathbf{RH}$ should be chosen.

The implementation of the suggested rate allocation starts with an initialisation stage, in which the initial transmission rates and powers are determined. Additionally, a range for acceptable spectral radius estimates must be determined. Let us denote the range as $[\rho_{inf}, \rho_{sup}]$, where $0 < \rho_{inf} < \rho_{sup} < 1$.

If there is no upper limit of transmission power, the rate allocation algorithm applied after the initialisation is shown in Table 8.2. Note that steps 1–3 may have to be iterated a few times in each frame, depending on the level of the channel variation. This iteration guarantees that the spectral radius is within the desired range.

If there is an upper limit of the transmission power, the rate allocation algorithm must have additional power constraints requiring the maximum transmission power in cell $p_{maxused}$ to be at most $\delta \cdot p_{max}$, $0 < \delta < 1$. Hence, rates are allocated according to the algorithm in Table 8.3. The additional power constraints are aimed at preventing outage and guaranteeing the feasibility of the PC with power constraints.

8.4 Transmission Rate Allocation Simulations

In the following simulations, mobiles are divided randomly into four service classes, which have different possible rates and different SINR target levels. Details of the service classes are given in Table 8.4. Class 1 represents voice users. Class 2 is for streaming video users. Classes 3 and 4 are for high- and low-service-level data users, respectively. The lowest rate in Class 4 represents the case in which transmission is blocked. This rate is used because using (3.39) as a fairness measure does not give the opportunity to apply a zero data transmission rate.

The relay PC step is set to 0.5 dB, and the spreading bandwidth is set to 3.84 Mb/s. Link gains are modelled by $g_{ji} = s_{ji} d_{ji}^{-4}$, where s_{ji} is log-normally distributed shadowing factor and d_{ji} is the distance between transmitter j and receiver i. The relative noise power is set to 10^{-12}. The results shown are averaged over 100 simulation cases.

Transmission rate allocations using PC feasibility, ISM, and IM are compared with a maximum gain allocation similar to greedy algorithms [35], where the incremental

Table 8.2: Spectral radius estimation based rate allocation without a power constraint.

1. Determine the spectral radius estimate to predefined accuracy according to (8.13) and (8.14).
2. If the spectral radius estimate is larger than ρ_{sup}, decrease the rate of the connection not transmitting at the minimum rate and corresponding to the largest row sum of $W^{-1}\mathbf{RH}$. Go back to step 1.
3. If the spectral radius estimate is smaller than ρ_{inf}, increase the rate of the connection not transmitting at the maximum rate and corresponding to the smallest row sum of $W^{-1}\mathbf{RH}$. Go back to step 1.
4. Apply the new transmission rates and resume with the next communication frame.
5. After the frame, return to step 1.

Table 8.3: Spectral radius estimation based rate allocation with the maximum transmission power constraint (4).

1. Determine the spectral radius estimate to predefined accuracy according to (8.13) and (8.14).
2. If the spectral radius estimate is larger than ρ_{sup} or $p_{maxused} > \delta \cdot p_{max}$, decrease the rate of the connection not transmitting at the minimum rate and corresponding to the largest row sum of $W^{-1}\mathbf{RH}$. Go back to step 1.
3. If the spectral radius estimate is smaller than ρ_{inf} and $p_{maxused} < \delta \cdot p_{max}$, increase the rate of the connection not transmitting at the maximum rate and corresponding to the smallest row sum of $W^{-1}\mathbf{RH}$. Go back to step 1.
4. Apply the new transmission rates and resume with the next communication frame.
5. After the frame, return to step 1.

Table 8.4: Service class specifications.

Class	Possible transmission rate (kbit/s)	SINR target (dB)
1	15	4.3
2	60, 120, 240	7.8
3	15, 30, 60, 120, 240, 480, 960	8.5
4	1.9, 15, 30, 60, 120, 240	8.5

data rate modifications are decided by channel gains between the mobiles and the base stations. This means using decision variable $\nu_i = g_{ii}^{-1}$ or $\nu_i = (g_{ii}\mathbf{w}_i^H\mathbf{a}_{ii}\mathbf{a}_{ii}^H\mathbf{w}_i)^{-1}$ in single-antenna and BF systems, respectively.

The throughput and harmonic fairness results of the ISM, PC feasibility, greedy and IM allocations are depicted in figures 8.1 and 8.2, respectively. Simulations show that the greedy rate allocation results in the best throughput, as shown in Fig. 8.1. Additionally, the ISM allocation has the second largest throughput with the power control feasibility and IM allocations having almost equal throughput. If the fairness among the users is considered, Fig. 8.2 shows that the power control feasibility approach is superior to the others. The other allocation techniques are quite equal, with the greedy algorithm being a bit fairer than ISM and IM techniques.

The outage and the mean of the transmission powers applied in the same simulations are presented in figures 8.3 and 8.4, respectively. In these simulations, the power control feasibility approach to transmission rate allocation shows its superiority. Outage and the transmission power used are far less than in the other techniques. Additionally, ISM has a better performance than the greedy algorithm with respect to these variables. The IM rate allocation seems to conserve power, but it suffers from the largest outage probability.

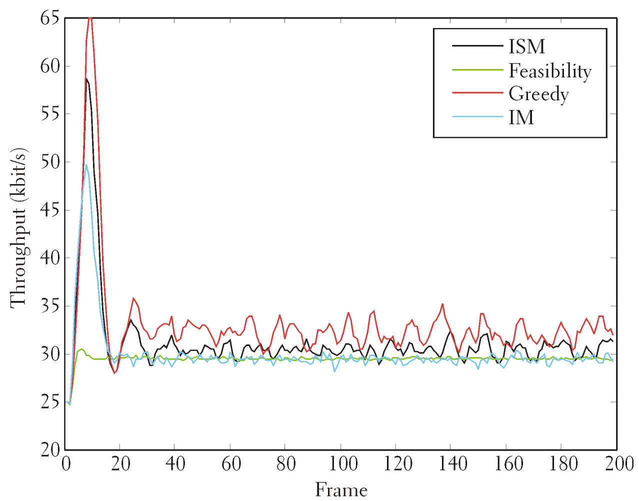

Fig. 8.1: Throughput of the rate allocation techniques considered.

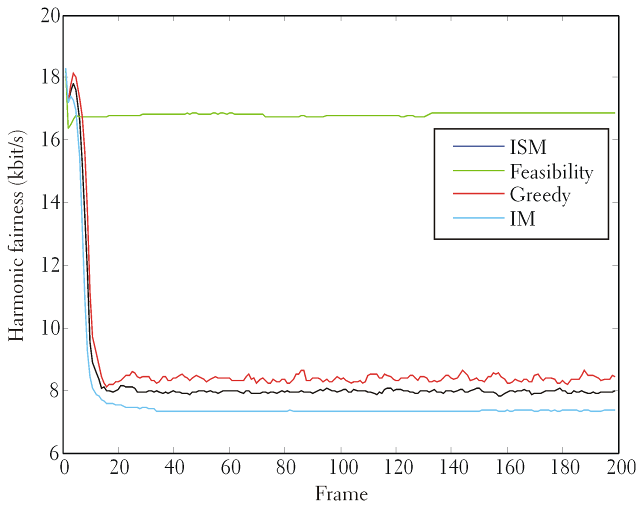

Fig. 8.2: Harmonic fairness of the rate allocation techniques considered.

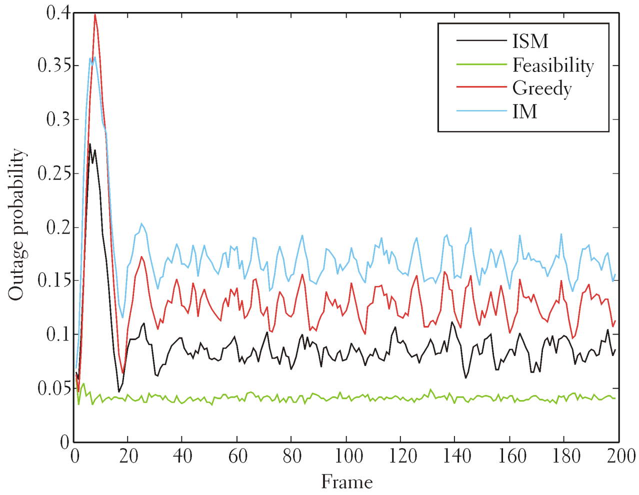

Fig. 8.3: Outage probabilities of the rate allocation techniques considered.

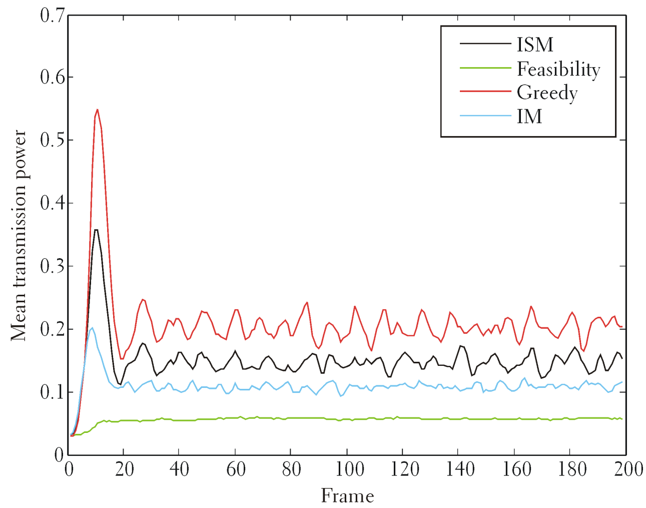

Fig. 8.4: Transmission power consumption of the rate allocation techniques considered.

9. Beamforming for Radio Resource Management in Wireless Sensor Networks

The purpose of this chapter is to examine to the usefulness of BF in the connection of wireless sensors and a fixed network. Saving on transmission power and reducing the complexity of wireless sensors is a necessity, and BF techniques can offer new views in this area.

As discussed in Section 2.3, the communication in wireless sensor networks is not always *ad-hoc*. For example in monitoring applications, wireless sensor nodes need to transmit to the wired network, where monitoring takes place. Additionally in very large *ad-hoc* networks, it might be more useful to utilise a wired network connection than a multi-hop route between two distant nodes. Hence, examination of efficient strategies between wireless and wired worlds is needed.

The BF techniques for wireless sensors are considered in two alternative ways. Firstly, the receiving BF is considered as a multiple access technique, space-division multiple access (SDMA), in the access point of a wired network receiving the transmission of wireless sensors. Secondly, random BF is examined as a transmission technique for wireless sensors.

Uplink SDMA is considered in the form of the receiving BF ([52], [60]) in the access point of the wired network. Compared to the other multiple access (MA) techniques, SDMA does not require as accurate scheduling as TDMA or as wide frequency band as FDMA. In addition, it is applicable simultaneously with the other MA techniques for better communicational capacity.

The switched random transmission BF approach aims to increase diversity between transmitting nodes in a congested network. The technique is considered also to increase the fairness among transmitting sensors. Previously, the fairness in sensor networks was examined using random transmission power in [15]. A random BF technique is considered in opportunistic BF as proposed in [86], which uses 'dumb antennas' as opposed to 'smart antennas'. The major difference is that [86] applies a feedback channel also.

Prior to the present work, BF had not been widely considered as a transmission technique for nodes of wireless sensor networks. In the related field of *ad-hoc* networks, for example, [67] tests BF antennas and determines that performance is significantly improved even with simple routing algorithms. Interestingly, the performance is improved even with a simple beam-switching antennas. BF nodes are suggested in [67] for, *e.g.*, fixed *ad-hoc* networks. In WSN use, BF is mostly considered through co-operation of omnidirectional transmitters/receivers of sensor nodes – that is, communication through distributed BF ([94], [5]). However, outside communication, BF is an important sensor technique for use with, for example, acoustic sensors (see, *e.g.*, [89]).

9.1 Link Between Wireless Sensors and Wired Network

What additional value can BF antenna arrays bring to the communication between wireless sensors and a wired network? In addition to the larger number of connections supported, they offer the prospect of using connections without feedback.

WSN, which communicate ad-hoc, are obviously able to communicate with feedback to wired stations. In those cases, communication capacity between the nodes and the access point can be restricted, and hence the use of SDMA is worthwhile. If the wireless nodes are distant to the access point or SINR is small, it is advisable to collect the information to a single node from a larger cluster of nodes and then send to the wired base station [63].

The up sides of connections without feedback are that they are lighter in hardware and software terms, leading to lower battery usage. The lack of feedback enables sensor node constructions without receivers. The advantage of the receiverless node is the smaller requirement for hardware and complex signal processing, and the lower power consumption. After all, the power consumption of the analogue/digital conversion of receivers is high (for examples, see [78] and [1]).

The down side of the feedbackless connections is the inability to use several multiple access and radio resource management techniques – *e.g.*, TDMA, FDMA, PC, and collision avoidance algorithms – and therefore the communication capacity is reduced. Of the BF applications considered, SDMA with BF requires a control signal channel for efficient interference rejection in bursty traffic and random BF can increase the packet-loss-ratio, if communication conditions are very easy.

While the interference reduction is vital in wireless communications, it is especially important in feedbackless systems. For SDMA systems, the reduction corresponds to an accurate steering of null gains towards interferers. In practice, BF techniques relying on the training sequences are more practical to implement than the SINR beamformer [52], especially in bursty traffic. In addition, a control signal is also needed for perfect null gain orientation. In random transmission BF systems, the interference reduction is a direct result of changes in the transmission direction.

9.2. SDMA in Connections Between Wireless Sensors and Wired Network

While connections without feedback and using SDMA are considered, one essential question is that of how often unacceptable signal conditions are expected to occur. The simulation results discussed below are applied in examining the effect of transmission power level and adaptive antenna specifications in a BF system.

9.2.1 Line-of-Sight Simulations

The simulations included transmitting wireless sensors and a BF base station. The sensor nodes were considered to be in randomly spread fixed locations in a space with radius *r*. The base station antenna array had two configurations: four elements in a tetrahedral arrangement or six elements in a triangle with half-wavelength spacing. The base station was set outside the node cluster, to distance *r*. The geometrical specifications simulate, for example, industrial processes in which system measurements are sent to a monitoring system. It would be more advantageous for an SDMA system to have more spatial distribution – *i.e.*, with the base between the sensor nodes. On the other hand, the near/far effect could become significant in those cases. The system uses MSBF. This means that there must be a control channel from wireless nodes to the base station in addition to the communication channel.

Signal path losses were modelled with an exponent of two. The relative noise power in the system was -80 dB throughout the simulations. The SINR target level for the connections was 7 dB, corresponding to a bit-error rate of 10^{-3} using coherent binary phase-shift-keying modulation [31].

The usefulness of SDMA in feedbackless communication with random transmission times combined with TDMA was examined. SINR levels of all combinations with 1–8 simultaneously transmitting nodes were simulated, and probabilities for supported connections were determined. As a definition, a connection was supported if SINR was larger than the SINR target. These results are good for comparing support probabilities in feedbackless connections and in SDMA/TDMA with multiple simultaneous transmitters.

Fig. 9.1a shows support probabilities in systems with 15 randomly spread nodes and a triangular antenna array with six elements. Fig. 9.1b presents support probabilities of a system with a tetrahedral four-element antenna array. In order to guarantee spatial diversity, results were averaged over 100 simulations.

Fig. 9.1's panes show that the BF theory holds quite well in the cases of high transmitting power: n_a simultaneous connections are supported, where n_a is the number of antenna array elements. On the other hand, n_a connections are not always supported. If transmitting nodes are in the same direction, the spatial resolution of the antenna array is not accurate enough and the signal cannot be separated from the interfering signal. In Fig. 9.1, the near/far effect of wireless communications can be seen as lower support percentages in cases with lower transmission powers. If the two panes of the figure are compared, it can be seen that the transmission power level is a much more significant factor in the case with fewer antenna elements.

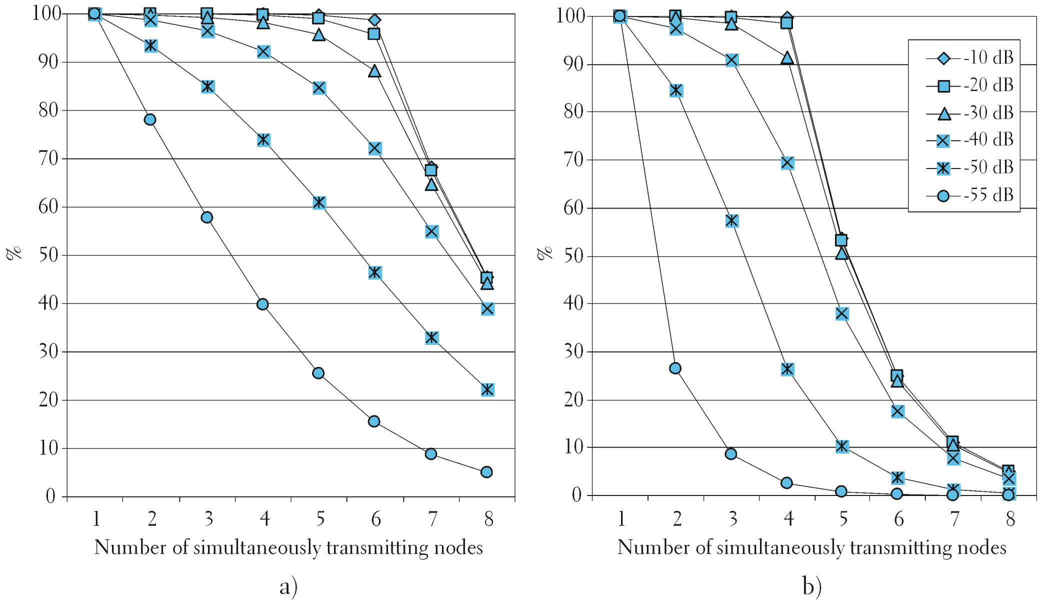

Fig. 9.1: Support probabilities with different transmission power levels. The system includes 15 randomly spread nodes and a triangular antenna array with a) six elements, b) four elements.

These results indicate that SDMA enables feedbackless communication between the wireless sensor nodes and the access points of a wired network, if the control channel can be utilised well enough (*e.g.*, BF can direct nulls). Performance limitations are related to the number of elements in the array n_a, as the BF theory suggests. If nodes transmit at random intervals and the average number of simultaneous connections is lower than n_a, the SDMA approach guarantees good throughput.

9.2.2 A Case Simulation Study of Wireless Nodes in an Industrial Hall

Additional simulations in an industrial hall environment were made. These give insight about the efficiency of SDMA, while line-of-sight (LOS) operations are not guaranteed, and reflected non-line-of-sight (NLOS) signals are present.

The simulations were similar to those addressed in Subsection 9.2.1, with the following exceptions. The communication is taking place in a hall with four reflected components as shown in Fig. 9.2. The rest of the reflections were assumed to be negligible due to shadowing by machinery etc. Reflections were set to cause –

7-dB attenuation, and random shadowing caused –10-dB attenuation. The shadowing was added to LOS and NLOS paths with probability of 0.1 and 0.4, respectively. The model was chosen in order to obtain a simple ray-tracing-type model for this case study.

Simulations included two base station configurations (four- or six-element arrays) and three different PC-BF versions: MSBF with constant relative transmission power of –10 dB, MSBF with PC, and maximum gain beamforming (MGBF) with PC. The MGBF weight vector is the principal eigenvector of the signal covariance matrix $\mathbf{\Phi}_s$. MGBF was applied to obtain information about the SDMA efficiency, if gain nulls are not directed towards interferers.

In order to guarantee as great a support rate as possible in cases with PC, a simple admission control scheme was implemented also. The admission control denied transmissions from nodes experiencing too poor channel and interference conditions. If admission control was not implemented, transmission powers were high and support percentages were still small.

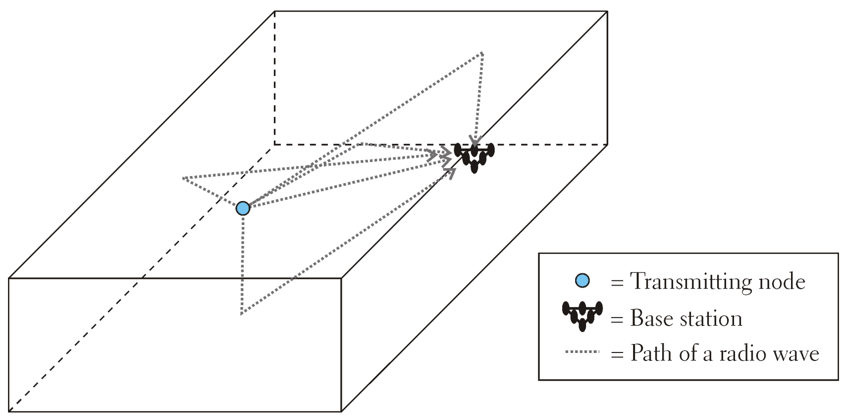

Fig. 9.2: A sketch of the multipath reflections in the industrial hall environment.

Support percentages of different four- and six-element antenna arrays and PC-BF configurations are shown in Fig. 9.3. The average transmission powers of these cases are collected in Table 9.1.

Fig. 9.3 shows that MGBF is not clearly good enough for the MA technique. MGBF does not direct its nulls as MSBF does. Additionally, as expected, PC and more antenna elements clearly increase the percentage of connections supported. If support probabilities are compared to those shown for LOS connections in Fig. 9.1, the decreased performance due to reflected signals and shadowing is evident. Multipath components and shadowing lead to a more scattered radio environment, and BF becomes a much harder task. The cure for severe multipath conditions is to increase the number of antenna elements n_a.

The average transmission powers in Table 9.1 indicate that PC combined with admission control can save transmission power. Table 9.1 reveals also that occasionally the situation is the opposite. Increases in transmission powers of some cases in Table 9.1 are the consequence of the admission control, and they should be interpreted in view of the support percentages in Fig. 9.3. Even though the system with MGBF and PC uses more power than the system without the PC in some cases, it has clear benefits in terms of the percentage of connections supported.

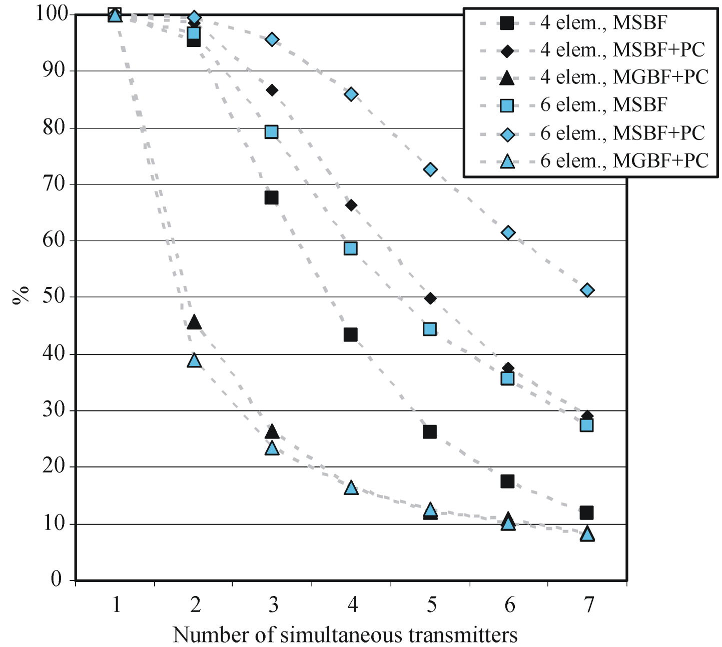

Fig. 9.3: Support probabilities over 100 cases with base station configurations and power control. The system included 15 randomly spread nodes.

Table 9.1: Transmission powers, in dB, of configurations, and different numbers of simultaneous transmitters.

Transmitters	4 elem., MSBF	4 elem., MSBF + PC	4 elem., MGBF + PC	6 elem., MSBF	6 elem., MSBF + PC	6 elem., MGBF + PC
2	-10	-17.1	-9.8	-10	-16.8	-12.2
3	-10	-8.7	-13.8	-10	-10.1	-14.6
4	-10	-10.3	-18.2	-10	-7.2	-19.4
5	-10	-11.8	-17.6	-10	-7.6	-18.1

All in all, SDMA is a promising technique for node access to the wired network. The greatest advantage can be achieved by an SDMA/TDMA combination. The possibility of supporting more connections to the wired network with a feedback channel is obvious from a survey of the literature [98], and it is also confirmed by the simulations in both line-of-sight and multipath environments.

Feedbackless communication between wireless and wired networks is possible using SDMA. This would make it possible to make smaller, cheaper, and simpler hardware for wireless sensor nodes. However, even though SDMA systems have much promise in lightening the configuration of sensor nodes, it must be taken into account that the effective use of BF and null steering is necessary. Moreover, the effect of many multipath signals on the performance must be considered properly in the system design. A well-planned application of control channel, non-moving nodes, and a fairly stable radio channel are required for transmissions without feedback.

9.3 Random Transmission Beamforming for Wireless Sensors

In designing wireless sensor networks, there are many contradictory requirements to be met, especially if the sensor nodes are deaf – *i.e.*, designed to be without a receiver and a feedback channel – the throughput and the fairness among the nodes are important.

The basic problem in deaf communication is the increased number of dropped packets. Additionally, some transmitting nodes may have serious trouble in getting any packets through to the receiving access point.

For improving the packet-loss ratio and the fairness among the wireless nodes, we propose that wireless sensors use transmission beamforming with randomly chosen predefined directions while transmitting to access points. The sensor itself selects one weight vector randomly for sending each packet. In other words, since the access point location is not known for the sensors, the sensors just select a random direction in which to send the packets.

This approach has several positive characteristics, especially when the system includes multiple access points. Firstly, transmitting in random directions gives spatial diversity to the transmissions. This means that the interference conditions vary even in a simple case with a few transmitting sensors. Secondly, the hardware/software combination is fairly simple, since there is no need for, *e.g.*, weight adaptation. Thirdly, if the access point is in the direction of the beamforming lobe, the transmitter gain is great than with an omnidirectional antenna.

This simulation demonstrates through an example how SINR levels of the transmitting wireless sensors are distributed in an access point. The case includes four wireless sensors with a four-element linear antenna array. The locations are drawn in Fig. 9.4. The free space path loss is assumed.

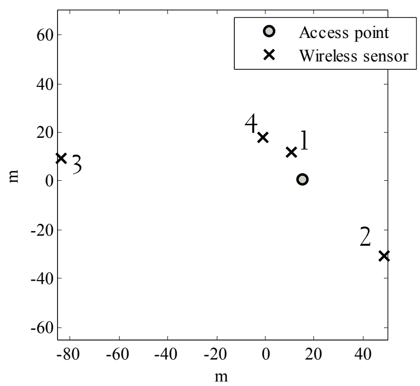

Fig. 9.4: Locations of the access point and wireless sensors.

The number of random transmission directions is four. The distributions are computed over all possible interfering transmitter and random transmission direction combinations. The random BF scenario is compared to a constant-power omnidirectional antenna case.

The SINR distributions of all wireless sensors are shown in Fig. 9.5. The results show that in all cases SINR levels of random beamforming are scattered more than in the omnidirectional antenna case. Depending on the SINR required in the transmission, random beamforming is more likely to guarantee successful transmission.

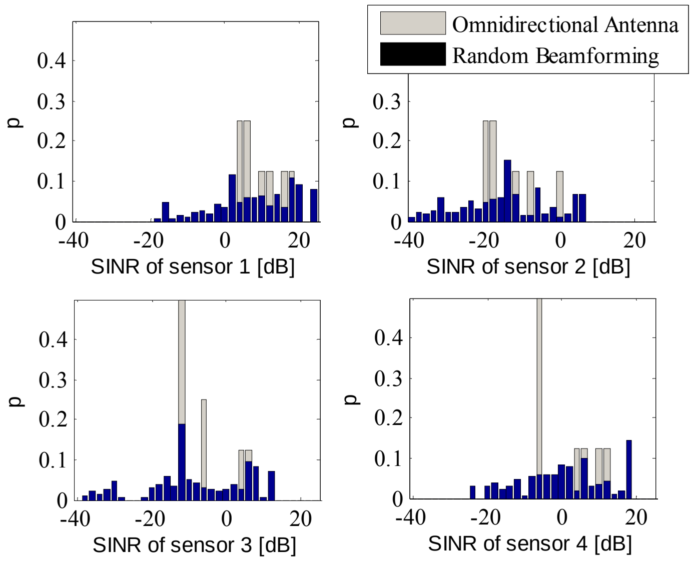

Fig. 9.5: SINR probability distributions of transmitting sensors over all possible combinations.

9.3.1 Simulation of Throughput Performance in a Multi-Access Point Scenario

The following simulations include a three-access-point system with 12 sensor nodes in the system. Wireless sensors are spread randomly throughout the system but no more than 100 m from the closest access point.

Sensor nodes transmit at random intervals. The transmission length is 5% of the expectation value of the interval between transmissions. That is, each sensor is expected to transmit 5% of the time. The intervals between transmissions of each sensor are taken from a beta distribution.

The system is assumed to include a CDMA system with a fixed processing gain. In the simulations, processing gains of 512, 256, 128, and 64 were studied. A transmission is considered lost if the SINR is below 5 dB. In each case, SINR levels are taken as the maximum of the SINRs experienced by the access points. The thermal noise is set to a constant level equal to the maximum power of a wireless transmitter transmitting at 100 m distance.

The random transmission beamforming is compared with omnidirectional antenna transmission schemes with a constant transmission power and a random transmission power [15]. All of the transmission schemes have the same average transmission power. The random powers are taken from negative binomial distribution. The random beamformer has four antenna elements, and it chooses its transmission direction from the four possible directions.

In addition to the transmission success ratio, fairness among the sensors is considered in the form of harmonic fairness [80]. Here the harmonic fairness is defined as a harmonic mean of the transmission success ratios of all sensors in each simulation.

The average transmission success ratios and harmonic fairness values over 100 simulations are shown in Fig. 9.6 and Fig. 9.7, respectively. The proposed random transmission beamforming scheme shows superior performance in both cases. The transmission rate success ratio of random BF is larger compared to the others in all except the constant power case with processing gain 512. Fig. 9.7 shows that the random BF scheme is more fair than the others – even though the difference is not that large while processing gain 64 is used.

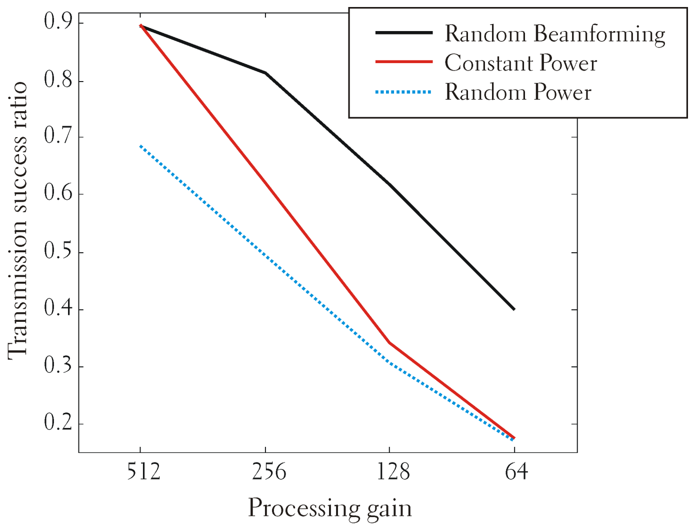

Fig. 9.6: Transmission success ratio over 100 simulations.

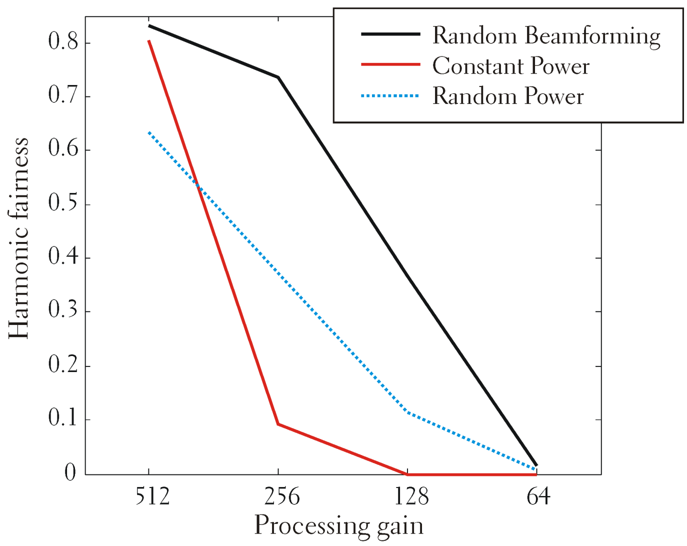

Fig. 9.7: Harmonic fairness over 100 simulations.

10. Conclusions

In this thesis, solutions for transmission power control and adaptive beamforming of wireless communication systems have been presented. The studies included separate treatment of the power control and beamforming problems in the form of a new block power control approach algorithm and a beamforming weight vector prediction algorithm, respectively, and joint treatment of the beamforming and power control problems in the uplink and downlink directions through signal-to-interference-and-noise-ratio estimation. All of the approaches were validated by simulations.

On the basis of the simulations presented, the block proportional–integral power control algorithm introduced here is seen to offer a performance advantage over the PIPC algorithm [81], especially in terms of the vector norm errors with respect to the optimal power vector. The down side of the algorithm is that it requires a great deal of signalling and measurement, including of the link gains inside the power control blocks, and the level of external interference. New ideas for tackling the difficult problem of tuning the control algorithm were presented.

Self-tuning prediction of the adaptive beamforming weight vector was presented with the help of three different prediction model formulations. The solution combines autoregressive-moving-average models with the recursive least squares technique. In the simulations, the self-tuning algorithms took about 1000 update points to converge. In addition, according to the simulations with one-step beamforming delay, the third prediction algorithm, BP3, with full utilisation of the beamforming vector history, was slightly superior to the other prediction algorithms and the normal delayed beamforming.

In the proposed practical solutions for the joint beamforming and power control, the common denominator is SINR estimation based on the covariance matrices of the desired signals. Solutions for uplink receiving beamforming and downlink transmission beamforming scenarios with antenna arrays in base stations were introduced.

In the uplink receiving beamforming and power control case, special attention was paid to the computational load, the practicality of the solution for the CDMA systems, and the fact that any power control based on the SINR level can be applied in the algorithm. The scheme for the joint downlink transmission beamforming and power control was based on estimating the SINR level at the receiver by using the covariance matrices utilised in the beamforming and the intercell interference estimated according to the regular power control command. The practicality of that approach is based on the absence of the requirement for extra measurements and signalling, and updating of transmission powers on the basis of knowledge of signal covariance matrices related to the latest channel variations. The proposed joint versions of adaptive beamforming and power control showed their superior performance with respect to the separate solutions in simulations.

For the transmission rate allocation, three algorithms aimed at better performance of multi-rate systems were presented. Of the transmission rate allocation algorithms proposed, the power control feasibility approach with a spectral radius estimation of the normalised link gain matrix seemed to be the most successful one with respect to fairness, outage probability, and consumption of transmission power.

According to the results in this thesis, beamforming makes it possible to use wireless sensors without a receiver and a feedback channel. The beamforming enables multiple access in the uplink case between wireless transmitters and a wired network access point. Switched random-transmission beamforming increases the performance of the connection, especially in cases involving congested networks. The use of random beamforming increases the fairness among the transmitters as well.

References

[1] A. Anttonen, T. Rautio, "Performance and complexity analysis for adaptive sample rate converters in GSM/UMTS/HIPERLAN2 mobile transceiver", Proceedings of IEEE International Symposium on Circuits and Systems, ISCAS, vol.4, pp. IV-489 - IV-492, 2002.

[2] S. Ariyavistakul, "SIR Based Power Control in a CDMA System", Proceedings of IEEE GLOBRCOM, Orlando, Florida, pp. 868-873, 1992.

[3] N. Bambos, "Toward Power-Sensitive Network Architectures in Wireless Communications: Concepts, Issues, and Design Aspects", IEEE Personal Communications, vol. 5, pp. 50–59, 1998.

[4] N.D. Bambos, S.C. Chen, G.J. Pottie, "Radio Link Admission Algorithms for Wireless Networks with Power Control and Active Link Quality Protection", Proceedings of INFOCOM '95, vol. 1, pp. 97-104, 1995.

[5] G. Barriac, R. Mudumbai, U. Madhow, "Distributed Beamforming for Information Transfer in Sensor Networks", Proceedings of 3rd International Symposium on Information Processing in Sensor Networks, IPSN'04, pp. 81-88, 2004.

[6] A. Bedekar, "Downlink Scheduling in CDMA Data Networks", Proceedings of IEEE GLOBECOM, vol.5, pp. 2653-2657, 1999.

[7] F. Berggren, R. Jäntti, S.-L. Kim, "A Generalized Algorithm for Constrained Power Control With Capability of Temporary Removal", IEEE Transactions on Vehicular Technology, vol. 50, no. 6, pp. 1604-1612, 2001.

[8] P.-R. Chang, B.-C. Wang, "Adaptive Fuzzy Power Control for CDMA Mobile Radio Systems", IEEE Transactions on Vehicular Technology, vol. 42, no. 2, pp. 225-236, 1996.

[9] K. Chawla, X. Qiu, "Throughput Performance of Adaptive Modulation in Cellular Systems", Proceedings of IEEE International Conference on Universal Personal Communications, pp. 945-950, 1998.

[10] S. Choi, J. Choi, H.-J. Im, B. Choi, "A Novel Adaptive Beamforming Algorithm for Antenna Array CDMA Systems With Strong Interferers", IEEE Transactions on Vehicular Technology, vol. 51, no. 5, pp. 808-816, 2002.

[11] C.-Y. Chong, S.P. Kumar, "Sensor Networks: Evolution, Opportunities and Challenges", Proceedings of the IEEE, vol. 91, no. 8, pp. 1247-1256, 2003.

[12] M.S. Elmusrati, "Power Control and MIMO Beamforming in CDMA Mobile Communications Systems", Licentiate Thesis, Helsinki University of Technology, Control Engineering Laboratory, Report 129, 2002.

[13] M.S. Elmusrati, "Radio Resource Scheduling and Smart Antennas in Cellular CDMA Communication Systems", Doctoral Thesis, Helsinki University of Technology, Control Engineering Laboratory, Report 142, 2004.

[14] M. Elmusrati, H. Koivo, "Multi-Objective Distributed Power and Rate Control for Wireless Communications", Proceedings of IEEE International Conference on Communications, vol. 3, pp. 1838-1842, 2003.

[15] M. Elmusrati, N. Tarhuni, R. Jäntti, "Transmitted Power Allocation for Wireless Deaf Sensors in Fading Channels", submitted to publication, 2006.

[16] M. El-Sayed, J. Jaffe, "A View of Telecommunications Network Evolution", IEEE Communications Magazine, vol. 40, no. 12, pp. 74-81, 2002.

[17] Encyclopædia Britannica Online, April 2003, <http://www.britannica.com/>.

[18] R.A. Fisher, "The Statistical Utilization of Multiple Measurements", Ann. Eugenics, vol. 8, pp. 376–386, 1938.

[19] G.J. Foschini, Z. Miljanic, "A Simple Distributed Autonomous Power Control Algorithm and Its Convergence", IEEE Transactions on Vehicular Technology, vol. 42, no. 4, 1993.

[20] R. Frenkiel, "A Brief History of Mobile Communications", IEEE Vehicular Technology Society News, vol. 49, no. 2, pp. 4-7, 2002.

[21] V.K. Garg, S.R. Laxpati, D. Wang, "Use of Smart Antenna System in Universal Mobile Communication Systems (UMTS)", IEEE Antennas and Wireless Propagation Letters, vol. 3, pp. 66-70, 2004.

[22] A.J. Goldsmith, "The capacity of Downlink Fading Channels with Variable Rate and Power", Transactions on Vehicular Technology, vol. 46, no. 3., pp. 569-580, 1997.

[23] A.J. Goldsmith, "Wireless Communications EE 359", course reader, 2001.

[24] D. Goodman, N. Mandayam, "Power Control for Wireless Data", IEEE Personal Communications, vol. 7, no. 2, pp. 48-54, 2000.

[25] J. Grandell, O. Salonaho, "Closed-Loop Power Control Algorithms in Soft Handover for WCDMA Systems", IEEE International Conference on Communications, vol. 3, pp. 791-795, 2001.

[26] S.A. Grandhi, R. Vijayan, D.J. Goodman, "Distributed Power Control in Cellular Radio Systems", IEEE Transactions on Communications, vol. 42, no. 2, 1994.

[27] S.A. Grandhi, J. Zander, R. Yates, "Constrained Power Control", Wireless Personal Communications, vol. 1, no. 4, pp. 257-270, 1995.

[28] M. Gudmundson, "Correlation Model for Shadow Fading in Mobile Radio Systems", IEE Electronic Letters, vol. 23, no. 27, pp. 2145-2146, 1991.

[29] F. Gunnarson, "Power Control in Cellular Radio Systems: Analysis, Design and Estimation", PhD thesis, Linköpings Universitet, Sweden, 2000.

[30] S.V. Hanly, D.N. Tse, “Power Control and Capacity of Spread Spectrum Wireless Networks”, Automatica, vol. 35, no. 12, pp. 1987-2012, 1999.

[31] S. Haykin, “Digital Communications”, Wiley, 2001.

[32] J. Holst, “Adaptive Prediction and Recursive Estimation”, Department of Automatic Control, Lund Institute of Technology, Sweden, 1977.

[33] C.-Y. Huang, R. Yates, “Rate of Convergence for Minimum Power Assignment Algorithms in Cellular Radio Systems”, ACM/Baltzer Wireless Networks Journal, vol. 4, no. 3, pp. 223-231, 1998.

[34] W.J. Huang, J.F. Doherty, “An Evaluation of Blocking Probability for Three-fold SDMA”, Proc. Military Comm. Conf., vol. 2, pp. 1248-1252, 2001.

[35] S.A. Jafar, A. Goldsmith, “Adaptive Multirate CDMA for Uplink Throughput maximization”, IEEE Transactions on Wireless Communications”, vol. 2, no.2, pp. 218-228, 2003.

[36] W.C. Jakes, “Microwave Mobile Communication”, John Wiley & Sons, NY, 1974.

[37] R. Jäntti, “Power Control and Transmission Rate Managemenet in Cellular Radio Systems – A snapshot approach”, Doctoral thesis, Helsinki University of Technology, Control Engineering Laboratory, Report 123, 2001.

[38] R. Jäntti, S.-L. Kim, ”Second-Order Power Control with Asymptotically Fast Convergence”, IEEE Selected Areas of Communications, vol. 18, no. 3, pp. 447-457, 2000.

[39] R. Jäntti, S.L. Kim, “Selective Power Control with Active Link Protection for Combined Rate and Power Control”, Proceedings of IEEE Vehicular Technology Conference, IEEE VTC 2000 – Spring, vol. 3, pp. 1960-1964, 2000.

[40] H. Kaaranen, A. Ahtiainen, L. Laitinen, S. Naghian, V. Niemi, “UMTS Networks – Architecture, Mobility and Services”, Wiley, 2nd ed., 2005.

[41] I.-M. Kim, H.-M. Kim, D.S. Kwon, “Optimum Rate Allocation for Two-Class Services in CDMA Smart Antenna Systems”, IEEE Transactions on Communications, vol. 51, no. 5, pp. 810-816, 2003.

[42] S.-L. Kim, Z. Rosberg, J. Zander, “Combined Power Control and Transmission Rate Selection in Cellular Networks”, Proceedings of IEEE Vehicular Technology Conference, IEEE VTC 1999 – Fall, vol. 3, pp. 1653-1657, 1999.

[43] H. Knutsson, M. Borga, T. Landelius, “Generalized Eigenproblem for Stochastic Process Covariances”, Report LiTH-ISY-R-1916, Computer Vision Laboratory, Linköping University, Sweden, 1996.

[44] H.N. Koivo, “A Multi-Variable Self-Tuning Control”, Automatica, vol. 16, pp. 351-366, 1980.

[45] S. Kwon, I. Oh, S. Choi, ”Adaptive Beamforming from the Generalized Eigenvalue Problem with a Linear Complexity for a Wideband CDMA System”, Proceedings of 50th IEEE Vehicular Technology Conference, VTC 1999 Fall, vol. 3, pp. 1890-1894, 1999.

[46] F.C.M. Lau, W.M. Tam, “Achievable-SIR-Based Predictive Closed-Loop Power Control in a CDMA Mobile System”, IEEE Transactions on Vehicular Technology, vol. 51, no. 4, pp. 720-728, 2002.

[47] L.C.Y. Lee, "Mobile Communications Engineering", McGraw-Hill, NY, 1982.

[48] J.-C. Lin, T.-H. Lee, Y.-T. Su, "Power Control Algorithm for Cellular Radio Systems", IEEE Electronic Letters, vol. 30, no. 3, pp. 195-197, 1994.

[49] X. Li, Z. Gajic, "An Improved SIR-based Power Control for CDMA Systems using Steffensen Iterations", Proceedings of Conference on Information Sciences and Systems, Princeton University, 2002.

[50] Y.-C. Liang, F.P.S. Chin, K.J.R. Liu, "Joint Downlink Beamforming, Power Control, and Data Rate Allocation for DS-CDMA Mobile Radio with Multimedia Services", Proceedings of IEEE International Conference on Multimedia and Expo, ICME 2000, vol. 3, 1455-1458, 2000.

[51] Y.-C. Liang, F. P. S. Chin, "Downlink Channel Covariance Matrix (DCCM) Estimation and its Applications in Wireless DS-CDMA Systems," IEEE Journal of Selected Areas in Communication, vol. 19, pp. 222–232, Feb. 2001.

[52] J.C. Liberti, T.S. Rappaport, "Smart Antennas for Wireless Communications", Prentice Hall PTR, 1999.

[53] L. Ljung, "System Identification: Theory for the User", Englewood Cliffs, Prentice Hall, 1987.

[54] J. Lunze, "Feedback Control of Large-Scale Systems", Prentice Hall, 1992.

[55] U. Martin, "Spatio-temporal Radio Channel Characteristics in Urban Macrocells", IEE Proceedings on Radar, Sonar and Navigation, vol. 145, no. 1, pp. 42-49, 1998.

[56] A. Mercado, K.J.R. Liu, "Adaptive QoS for Mobile Multimedia Applications Using Power Control and Smart Antennas", Proceedings of IEEE International Conference on Communications, ICC 2000, vol. 1, pp. 60-64, 2000.

[57] C.D. Meyer, "Matrix Analysis and Applied Linear Algebra", SIAM, 2000.

[58] D. Mitra, "An Asynchronous Distributed Algorithm for Power Control in Cellular Radio Systems", in J.M. Holtzman, D.J. Goodman, editors, "Wireless and Mobile Communications", Kluwer Academic Publisher, Boston, MA, USA, 1994.

[59] J. Mo, J. Walrand, "Fair End-to-End Window-Based Congestion Control", IEEE/ACM Transactions on Networking, vol. 8, no. 5, pp. 556-567, 2000.

[60] R.A. Monzingo, T.W. Miller, "Introduction to Adaptive Arrays", Wiley New York, 1980.

[61] S. Naghian, "Location-Sensitive Intelligent Radio Resource Management and its Application in WCDMA Mobile Systems", Doctoral thesis, Helsinki University of Technology, Applied Electronics Laboratory, Research report B8, 2001.

[62] A.F. Naguib, "Power Control in Wireless CDMA: Performance with Cell Site Antenna Arrays", Proceedings of IEEE Global Telecommunications Conference, GLOBECOM '95, vol. 1, pp. 225-229, 1995.

[63] D. Nicholson, C.M. Lloyd, S.J. Julier, J.K. Uhlmann, "Scalable Distributed Data Fusion", Proceedings of Fifth International Conference on Information Fusion, ISIF, vol. 1, pp. 630-635, 2002.

[64] S.-J. Oh, K.M. Wasserman, “Optimality of Greedy Power Control and Variable Spreading Gain in Multi-Class CDMA Mobile Networks”, Proceedings of ACM/IEEE MobiCom’99, pp. 102-112, 1999.

[65] S.U. Pillai, T. Suel, S. Cha, “The Perron-Frobenius Theorem: Some of its Applications”, IEEE Signal Processing Magazine, vol. 22, no. 2, pp. 62-75, 2005.

[66] L. Quian, Z. Gajic, “Variance Minimization Stochastic Power Control in CDMA Systems”, Proceedings of IEEE Conference on Communications 2002, vol. 3, pp. 1763-1767, 2002.

[67] R. Ramanathan, “On the Performance of Ad Hoc Networks with Beamforming Antennas”, Proceedings of the 2nd ACM International Symposium on Mobile Ad Hoc Networking & Computing, pp. 95-105, 2001.

[68] F. Rashid-Farrokhi, K.J.R. Liu, L. Tassiulas, “Transmit Beamforming and Power Control for Cellular Wireless Systems”, IEEE Selected Areas in Communications, vol. 16, no. 8, pp. 1437-1450, 1998.

[69] F. Rashid-Farrokhi, L. Tassiulas, K.J.R. Liu, “Joint Optimal Power Control and Beamforming in Wireless Networks Using Antenna Arrays”, IEEE Transactions on Communication, vol. 46, no. 10, pp. 1313-1324, 1998.

[70] M. Rintamäki, I. Virtej, H. Koivo, ”Two-Mode Fast Power Control for WCDMA Systems”, Proceedings of 53rd IEEE Vehicular Technology Conference, VTC 2001 Spring, vol. 4, pp. 2893-2897, 2001.

[71] M. Rintamäki, H. Koivo, I. Hartimo, “Application of the Generalized Predictive Control Method in Closed-Loop Power Control of CDMA Cellular Communication Systems”, Proceedings of Nordic Signal Processing Symposium, NORSIG, 2004.

[72] M. Rintamäki, “Adaptive Power Control in CDMA Cellular Communication Systems”, Doctoral Thesis, Helsinki University of Technology, Signal Processing Laboratory, Report 53, 2005.

[73] Z. Rosberg, J. Zander, “Toward a Framework for Power Control in Cellular Systems”, ACM/Baltzer Wireless Network Journal, vol. 4, pp. 215-222, 1998.

[74] L. Råde, B. Westergren, “Beta Mathematics Handbook”, Studentlitteratur Sweden, 2nd ed., 1990.

[75] A. Sampath, P.S. Kumar, J. Holtzman, “Power Control and Resource Management for a Multimedia CDMA Wireless System”, Proceedings of IEEE International Symposium on Personal, Indoor and Mobile Radio Communications, vol. 1, pp. 21-25, 1995.

[76] M. Schubert, H. Boche, “A Unifying Theory for Uplink and Downlink Multi-User Beamforming”, Proceedings of International Zürich Seminar on Broadband Communication, Switzerland, pp. 27-1 – 27-6, 2002.

[77] M. Schubert, H. Boche, “Solution of the Multiuser Downlink Beamforming Problem With Individual SINR Constraints”, IEEE Transactions on Vehicular Technology, vol. 53, no. 1, pp. 18-28, 2004.

[78] J. Sevenhans, Z.-Y. Chang, “A/D and D/A conversion for telecommunication”, IEEE Circuits Devic., 14(1): 32 – 42, 1998.

[79] G. Song, K. Gong, “Capacity and Power Allocation of CDMA Systems with Joint Power Control and Optimum Beamforming”, Proceedings of IEEE International Conference on Communication Technology, WCC – ICCT 2000, vol. 1, pp. 590-593, 2000.

[80] C. Touati, E. Altman, J. Galtier, “Fair Power and Transmission Rate Control in Wireless Networks”, Proceedings of Global Telecommunication Conference GLOBECOM 2002, vol. 2, pp. 1229-1233, 2002.

[81] Z. Uykan, R. Jäntti, H. Koivo, ”A PI-Power Control Algorithm for Cellular Radio Systems”, Proceedings of IEEE International Symposium on Spread Spectrum Techniques and Applications, ISSSTA 2000, vol. 2, pp. 782–785, 2000.

[82] B.D. Van Veen, K.M. Buckley, “Beamforming: a Versatile Approach to Spatial Filtering”, IEEE ASSP Magazine, vol. 5, no. 2, pp. 4–24, 1988

[83] M.A.M. Vieira, C.N. Coelho Jr., D.C. da Silva Jr., J.M. da Mata, “Survey on Wireless Sensor Devices”, Proceedings of IEEE Conference on Emerging Technologies and Factory Automation, ETFA '03, vol. 1, pp. 537–544, 2003.

[84] I. Virtej, O. Kansanen, H. Koivo, “Enhanced Predictive Fast Power Control for 3G Systems”, Proceedings of 53rd IEEE Vehicular Technology Conference, VTC 2001 Spring, vol. 4, pp. 2864–2868, 2001.

[85] E. Visotsky, U. Madhow, “Optimum Beamforming using Transmit Antenna Arrays”, Proceedings of 49th IEEE Vehicular Technology Conference 1999, vol. 1, pp. 851–856, 2001.

[86] P. Viswanath, D.N.C. Tse, R. Laroia, “Opportunistic Beamforming Using Dumb Antennas”, IEEE Transactions on Information Theory”, vol. 48, no. 6, 2002.

[87] A.J. Viterbi, “CDMA Principles of Spread Spectrum Communication”, Addison-Westley, Reading, MA, 1995.

[88] A.J. Viterbi, A.M. Viterbi, E. Zehavi, “Performance of Power-Controlled Wideband Terrestrial Digital Communication”, IEEE Transactions on Communication, vol. 41, no. 4, 1993.

[89] A. Wang, W. R. Heinzelman, A. P. Chandrakasan, “Energy-Scalable Protocols for Battery-Operated Microsensor Networks”, Proceedings of IEEE Signals Processing Workshop, pp. 483–492, 1999.

[90] C. Wang, K. Sohraby, B. Li, M. Daneshmand, Y. Hu, “A Survey of Transport Protocols for Wireless Sensor Networks”, IEEE Network, vol. 20, no. 3, pp. 34–40, 2006.

[91] L. Wang, Y. Xiao, “Energy Saving Mechanisms in Sensor Networks”, Proceedings of 2nd International Conference on Broadband Networks, vol. 1, pp. 724–732, 2005.

[92] Wikipedia.org, “Enhanced Data Rates for Global Evolution” July 2006, <http://en.wikipedia.org/wiki/Enhanced_Data_Rates_for_Global_Evolution>.

[93] R.J. Wood, M.J. O’Neill, “A New Method for Calculating the Spectral Radius of an Input-Output Matrix”, Technical Report rgai-01-01, Research Group for Complex Systems, Charles Stuart University, Bathurst, Australia.

[94] K. Yao, R. Hudson, C. Reed, D. Chen, F. Lorenzelli, “Blind Beamforming on a Randomly Distributed Sensor Array System”, IEEE Journal of Selected Areas in Communications, vol. 16, no. 8, pp. 1555–1567, 1998.

[95] R.D. Yates, “A Framework for Uplink Power Control in Cellular Radio Systems”, IEEE Journal of Selected Areas in Communications, vol. 13, no. 7, pp. 1341–1347, 1995.

[96] R.D. Yates, C.-Y. Huang, “Integrated Power Control and Base Station Assignment”, IEEE Transactions on Vehicular Technology, vol. 44, no. 3, 638–644, 1995.

[97] A. Yener, R.D. Yates, S. Ulukus, “Interference Management for CDMA Systems Through Power Control, Multiuser Detection and Beamforming”, IEEE Transactions on Communications, vol. 49, no. 7, pp. 1227–1239, 2001.

[98] J. Yunjian, S. Hara, Y. Hara, ”Impact of Closed-loop Power Control on SDMA/TDMA System Performance”, Proceedings of 56th Vehicular Tech. Conference, VTC Fall-2002, vol. 3, pp. 1825–1829, 2002.

[99] J. Zander, “Radio Resource Management in Future Wireless Networks – Requirements and Limitations”, IEEE Communications Magazine, vol. 5, no. 8, 1997.

[100] J. Zander, S.-L. Kim, ”Radio Resource Management for Wireless Networks”, Artech House, Boston, MA, 2001.

[101] J. Zander, “Performance of Optimum Transmitter Power Control in Cellular Radio Systems”, IEEE Transactions on Vehicular Technology, vol. 41, no. 1, pp. 57–62, 1992.

[102] J. Zander, “Distributed Cochannel Interference Control in Cellular Radio Systems”, IEEE Transactions on Vehicular Technology, vol. 41, no. 3, pp. 305–311, 1992

[103] W.R. Zhang, V.K. Bhargava, N. Guo, “Power Control by Measuring Intercell Interference”, IEEE Transactions on Vehicular Technology, vol. 52, no. 1, pp. 96–107, 2003.

[104] K.J. Åström, B. Wittenmark, “Computer-Controlled Systems, Theory and Design”, Prentice Hall, 3rd ed., 1997.

HELSINKI UNIVERSITY OF TECHNOLOGY CONTROL ENGINEERING LABORATORY

Editor: H. Koivo

Report 139	Halmevaara, K., Hyötyniemi, H. Process Performance Optimization Using Iterative Regression Tuning. April 2004.
Report 140	Viitamäki, P. Hybrid Modeling of Paper Machine Grade Changes. May 2004.
Report 141	Pöyhönen, S. Support Vector Machine Based Classification in Condition Monitoring of Induction Motors. June 2004.
Report 142	Elmusrati, M. S. Radio Resource Scheduling and Smart Antennas in Cellular CDMA Communication Systems. August 2004.
Report 143	Tenno, A. Modelling and Evaluation of Valve-Regulated Lead-Acid Batteries. September 2004.
Report 144	Hyötyniemi, H. Hebbian Neuron Grids: System Theoretic Approach. September 2004.
Report 145	Hyötyniemi, H. (ed.) Complex Systems: Science at the Edge of Chaos - Collected papers of the Spring 2003 postgraduate seminar. October 2004.
Report 146	Paanasalo, J. Modelling and Control of Printing Paper Surface Winding. June 2005.
Report 147	Mohamed, F. Microgrid Modelling and Simulation. March 2006.
Report 148	Mäenpää, T. Robust Model Predictive Control for Cross-Directional Processes. May 2006.
Report 149	Kantola, K. Modelling, Estimation and Control of Electroless Nickel Plating Process of Printed Circuit Board Manufacturing. March 2006.
Report 150	Virtanen, T. Fault Diagnostics and Vibration Control of Paper Winders. June 2006.
Report 151	Hyötyniemi, H. Neocybernetics in Biological Systems. August 2006.
Report 152	Hasu, V. Radio Resource Management in Wireless Communication: Beamforming, Transmission Power Control, and Rate Allocation. June 2007.

ISBN 978-951-22-8821-2

ISSN 0356-0872

Picaset Oy, Helsinki 2007